(R) evolution

PEQUEÑOS ANIMALES

Nº 6

SUMARIO

Nº 6

(R) evolution
PEQUEÑOS ANIMALES

EDITA:
IMPULSO VET
impulsovet@impulsovet.es

Instrument shank-assisted ovariohysterectomy: a randomized clinical trial of surgical and pain alleviation efficiency of a single-person modified technique

Ovariohisterectomía asistida por vástago instrumental

Keywords:
instrument shank-assisted, ovariohysterectomy, pain score, deep-chest, dog, OHE

Palabras clave:
instrumento asistido por vástago, ovariohisterectomía, puntuación de dolor, tórax profundo, perro, OHE

https://www.frontiersin.org/articles/10.3389/fvets.2023.1083376/full

Navid Ziaei Darounkolaei[1*], Seyed Mohamad Sadegh Mousavi Kiasary[2,3], Amirhoushang Behzadi[4], Niki Nabavi Mosavi[1], Shima Mahmoodi Ferdowsi[4]

1. Babol Branch, Department of Surgery and Radiology, Faculty of Veterinary Medicine, Islamic Azad University, Babol, Iran
2. Health Policy Research Center, Institute of Health, Shiraz University of Medical Sciences, Shiraz, Iran
3. Nano Bio Electronic Devices Lab, Cancer Electronics Research Group, School of Electrical and Computer Engineering, College of Engineering, University of Tehran, Tehran, Iran
4. Babol Branch, Faculty of Veterinary Medicine, Islamic Azad University, Babol, Iran

Tabla de contenido:

Objetivos: *Evaluar una técnica de ovariohisterectomía modificada (OHE) realizada por una sola persona y compararla con el método convencional en función de la eficiencia del tiempo, el trauma y el dolor postoperatorio.*

Métodos: *En un estudio prospectivo, aleatorizado y experimental, 18 perras sanas, grandes, de pecho profundo y mestizas intactas fueron asignadas aleatoriamente a los grupos convencionales (n = 9) y asistidos por vástagos instrumentales (n = 9). Sobre la base de grabaciones de vídeo, se analizaron las distintas duraciones de los pasos quirúrgicos: tiempo total de cirugía (TST), tiempo de intervención pedicular, tiempo de liberación suspensoria (SRT), tiempo de vástago (ShT), tiempo de pinzamiento (ClpT), tiempo de ligadura (LigT) y tiempo de cierre (TC). Para medir el dolor se utilizaron la escala de dolor compuesta de Glasgow (GCMPS-SF), la escala de dolor de la Universidad de Melbourne (UMPS) y las escalas analógicas visuales (EVA). También se investigó la fluctuación de la proteína C reactiva (PCR). Estas evaluaciones se realizaron antes y 6, 24, 48 y 72 h después de la operación.*

Objectives: To evaluate a modified ovariohysterectomy (OHE) technique performed by a single person and compare it with the conventional method based on time efficiency, trauma, and postoperative pain.

Methods: In a prospective, randomized, experimental study, 18 healthy, large, deep-chested, mixed-breed intact female dogs were randomly allocated to conventional (n = 9) and instrument shank-assisted (n = 9) groups. On the basis of video recordings, the various surgical step durations were analyzed: total surgery time (TST), pedicle intervention time (PIT), suspensory release time (SRT), shanking time (ShT), clamping time (ClpT), ligating time (LigT), and closure time (CT). The Glasgow composite pain scale short-form (GCMPS-SF), university of Melbourne pain scale (UMPS), and Visual Analogue Scales (VAS) were used to measure pain. C-reactive protein (CRP) fluctuation was also investigated. These evaluations were completed before and 6, 24, 48, and 72 h postoperatively.

Results: Instrument shank-assisted OHE was less time-consuming than conventional OHE ($p = 0.005$), improved PIT by 30.7% (6.44 min for both pedicles, $p = 0.014$), and correlated strongly with TST ($\rho = 0.862$, $p = 0.003$ and $\rho = 0.955$, $p = 0.000$, respectively). The two method's surgical step durations were also TST = 47.40 ± 9.9 vs. 34.70 ± 6.7 min, PIT = 20.96 ± 5.78 vs. 14.52 ± 3.73 min, SRT = 78.97 ± 69.10 vs. ShT = 20.39 ± 8.18 s ($p = 0.035$), ClpT = 50.66 ± 45.04 vs. 63.55 ± 37.15 s ($p = 0.662$), LigT = 12.82 ± 3.37 vs. 8.02 ± 3.11 min ($p = 0.005$), and CT = 16.40 ± 4.5 vs. 11.60 ± 2.5 min ($p = 0.013$), respectively. While both techniques inflicted pain on the animals, the novel approach resulted in a reduction of pain at T6 (GCMPS-SF, $p = 0.015$ and VAS, $p = 0.002$), T24 (UMPS, $p = 0.003$), and T48 (GCMPS-SF, $p = 0.015$ and UMPS, $p = 0.050$). Both methods exhibited a peak in CRP level after 24 h, which subsequently returned to baseline after 48 h. However, the shank-assisted method demonstrated a significantly lower reduction in CRP level at the 48-h compared to the other group ($p = 0.032$).

Conclusion: Instrument shank-assisted technique permitted ovarian removal without an assistant, less damage to animals and reducing its time when compared to a conventional technique, and resulting in an alternative that causes less surgical stress and fatigue. Further research with a larger population size is required to determine the serum CRP levels as an alternative pain biomarker.

Tabla de contenido:

1. Introduction

Elective ovariohysterectomy (OHE) is one of the most common surgeries done on dogs and cats (1). However, there are still problems with this technique, despite how common it is. Prior to the start of the operation, inexperienced graduates are anxious about how to do OHE on their own, and after the procedure is finished, they are concerned with the reliability of ligatures. As they consider how to do this procedure at an acceptable speed, their anxiety will increase. When a surgeon acquires experience, new issues develop, such as how to properly perform a high-risk, quick surgery with several implications, such as hemorrhage (2, 3), surgical trauma, organ manipulation, inflammation (4, 5), surgical stress (6), wound healing, and acute pain. The frequency of ovarian remnant syndrome was increasing mostly among young surgeons because of a concern about vascular rupture while breaking the suspensory ligament and exposing the ovaries inadequately, particularly in patients with obesity or other comorbidities (7–9). According to Berzon's study, 1% of bitches experienced recurrent estrus following OHE by fourth-year veterinary students (2). However, the overall frequency of complications by final-year veterinary students was found to be as high as 29 (20.6%) out of 141 bitches, with 1 (5%) out of 20 experiencing post-surgical pseudopregnancy (7). As experience grows, less consideration is given to this problem. To achieve the aforementioned results, the surgeon may be skilled in rupturing the suspensory ligament to expose the ovaries and make their pedicle accessible for ligature placement (10). The success of the operation hinges on the surgeon's willingness to pull, compress, strumming, tear, or sever the suspensory ligament (11), which is accompanied by extensive tissue damage. Drastic tissue damage and the time-consuming nature of its execution have made it the leader in painful surgeries in veterinary medicine, particularly for inexperienced surgeons. The experts, anesthesiologists, surgeons, and experienced researchers have adopted OHE as the acute surgical pain model because of the intensity of the pain caused by an experienced surgeon's OHE (12–14). Acute postoperative pain has long been a problem for surgeons. Inadequate management of postoperative pain can result in a number of undesirable outcomes, including (1) physiological changes comprising tachycardia, hypertension (due to peripheral vasoconstriction, increased myocardial contractility, and systemic vascular resistance), cardiac arrhythmias, tachypnea, superficial respiratory pattern, pale mucous membranes, mydriasis, sialorrhea, and hyperglycemia (2), behavioral changes comprising vocalization (such as cries, whimpers, and growls), looking and licking the affected area, alteration of the facial expression (submissive attitude), self-mutilation, muscle stiffness or weakness, restlessness and anxiety, apathy and inactivity, aggression, fear, and depression, stereotypes, anorexia or hyporexia, reduction of grooming, prayer posture, sleep disorders, and (3) changes in biochemical parameters by the decrease of PaO2, PaCO2, HCO3, and an increase of H+, cortisol, lactate, and glucose (15–20), prolonging the recovery of patients (17, 21, 22). Despite these hazards, OHE is considered to be a very straightforward procedure, and numerous dog owners visit a veterinary clinic every day to have their pets spayed. Hence, the incidence of problems justifies the adoption of procedures, such as instrument shank-assisted OHE, as well as the many theories pertaining to surgical duration, pain, and trauma.

The length of surgery is a primary factor of the severity of postoperative issues, and it is inversely related to the surgeon's skills and expertise (13). Skill is considered in two fields: non-technical skills (e.g., knowledge, situational awareness, decision-making, conscientiousness, intraoperative communication, teamwork, and leadership) (23–25) and technical skills (psychomotor actions). The latter would be

Tabla de contenido:

gained and empowered via an educational program known as Objective Structured Assessment of Technical Skills (OSATS), which has been thoroughly introduced and verified (26, 27). Besides these abilities, some surgical procedures, such as minimally invasive procedures, are time-consuming and instrument-dependent (28, 29), which may not be an option for some animals. Naturally, each operation consists of a succession of procedures with varying durations, since some are simpler than others, such as entering the abdominal cavity through the linea alba, while others, such as the anatomical access to the ovaries, provide challenges. Understanding the elements that determine the duration of surgical steps as well as the total duration makes it simpler and more objective to estimate its sufficiency and leads to a more trustworthy conclusion.

Animal pain is hard to judge because it depends on many things, such as the amount of pain, the type of injury, and the animal's own characteristics. As a result of the intricate nature of pain perception, several multidimensional questionnaires for qualitative pain assessment and validated behavioral scales have been developed to assess pain intensity in dogs (30, 31). Each of these methodologies assigns a different number of points to certain animal behavioral changes. The sum of the points indicates the observed pain level of the animal. Commonly used pain scales include the Glasgow composite measure pain scale (GCMPS-SF), the University of Melbourne pain scale (UMPS), and the Visual Analogue Scale (VAS), with corresponding ranges of 0–28, 0–24, and 0–10. Each of these solutions seems capable of filling some of the gaps left by the others, since they possess almost separate criteria with little overlap (32).

It is considered that the pain will always correspond to specific parameters that changed when the discomfort began or emerged. Clinical studies may describe a vast array of biomarker variations. Some parameters represent a range of events, but others may be directly triggered by the existing pain. The inflammatory response to surgical trauma or stress (33) activates the hypothalamus, causing it to release corticotropin-releasing hormone and arginine vasopressin, both of which stimulate anterior pituitary adrenocorticotropic hormone production, which in turn stimulates cortisol secretion by the adrenal cortex (19). Cortisol levels vary based on the severity or grade of surgery. The surgical interventions were categorized based on the modified Johns Hopkins surgical criteria, which delineate three levels of invasiveness: grade I, indicating minimally invasive procedures; grade II, indicating moderately invasive procedures; and grade III, indicating highly invasive procedures (34). When comparing grade 2 and grade 3 operations to grade 1, these differences may be identified, but they cannot be separated. Cortisol is a commonly utilized measurement for assessing stress levels and has demonstrated efficacy in evaluating intraoperative noxious stimuli. However, its sensitivity may be inadequate for capturing the variations that arise from repeated intraoperative noxious stimuli in a single animal (35). Cortisol levels seem to fluctuate with age, gender, disease, and the degree of surgical or anesthetic invasiveness. As a result, based on the research conducted so far, it is difficult to determine which is the primary cause of the alterations (36). Glucose is another biochemical parameter that surgery affects, and its clinical monitoring appears straightforward. Growth hormone (somatotrophin) levels increase in response to surgery and trauma; their release from the anterior pituitary is promoted by hypothalamic growth hormone-releasing factor (37, 38), which has an anti-insulin effect by inhibiting glucose uptake and utilization by cells. However, glucose utilization by cells is limited during surgery due to high cortisol levels (39). As a consequence, blood glucose levels rise. Furthermore, cortisol and catecholamines promote glucose production.

Tabla de contenido:

In addition, a hyperglycemic response may result from a drop in insulin concentration during induction of anesthesia and during surgery, resulting in insulin secretion failure. Ultimately, the surgical invasion causes an increase in blood glucose content (40). Regardless of the causes of elevated glucose levels, the amount of rise in simple operations is negligible (19). Immunological mediators such as cytokines or interleukins (ILs) such as IL-1, IL-6, and tumor necrosis factor-alpha (TNF-α) mediate the rapid activation of the immune system following surgery. The presence of IL-6 depends on the extent of the surgical tissue damage (20). Despite the fact that the plasma level of IL-6 molecules with a short half-life increases within 30–60 min and becomes substantial after 2–4 h with quick returns to baseline, the maximum level may be attained 24 h after major operations, which may be prolonged 48–72 h postoperatively (19, 41). IL-6 stimulates the release of proteins, especially C-reactive protein (CRP), from the liver to commence the "acute phase response," which comprises a variety of changes (19, 42). Based on a comparable study design (42), the postoperative CRP concentration increased more slowly and reached its peak after 48 h. After that, it went down at a slower rate, with a mean half-life of 62 h compared to 15 h for IL-6 (43). This might make it a valuable and accurate marker for regular diagnostics of systemic inflammation in dogs (44, 45) and a predictor of surgical trauma severity (46).

Therefore, one of the most difficult things for surgeons to do is choose a technique that will cause the least amount of damage, cause the least amount of pain after the surgery, and take the least amount of time. These are a trio of the key challenges for surgeons. The development or modification of minimally invasive techniques has only been able to improve the first two of these aspects, but with significant limitations (47). The aim of this study is to compare a modified OHE procedure that only needs one person to do it with the standard procedure in terms of time, trauma, and pain after the surgery. This will help researchers come up with a way to reduce the length of surgery, the amount of trauma, and immediate postoperative pain.

2. Materials and methods

2.1. Animals and study design

This research was authorized by the Iranian biomedical research ethics committee [IR.IAU.BABOL.REC.1399.004 (48), IR.IAU.BABOL.REC.1399.015 (49) and IR.IAU.BABOL.REC.1399.093 (50)] and conducted at the Babol branch of Azad University.

In a randomized controlled trial, 18 healthy, large, deep-chested intact female mixed-breed dogs were included. Animals were divided into two equal groups randomly by coin flipping, using a sterile suture sachet (51–53) (NZD) after inducing anesthesia and draping the surgical area. The sample size was evaluated using the software GPower 3.1.9.7. The presence of 9 dogs in each group resulted in a power of 0.9 (Power = 1 − β = 0.9) for TST with effect size $d > 1.50$ at a significance level of = 0.05.

Shelter dogs with ASA I (the American Society of Anesthesiologists) physical status enrolled in the study (54). The physical exam checked the patient's heart rate (HR), breathing rate (RR), and rectal temperature (RT). It also checked for internal and external parasites, did a complete blood count, and looked at the Hb, PCV, CRP, and glucose levels in the blood. The study was conducted on bitches in diestrus, based on vaginal smear cytology. Animals with a body condition score between 4 and 6 out of 9 were chosen. Animals under 1 year old, in estrus, pregnant, or lactating, with a weak or no response to painful stimuli (a needlestick in the lower abdomen), with a history of physical or behavioral issues, or with abnormal vaginal secretions were excluded.

Each dog scheduled for surgery on a particular day spent 3 days before and 3 days after the surgery in a separate

cage with free access to food and water. Ten days after surgery, the sutures were removed.

2.2. Anesthesia

The animal's resting vital parameters (HR, RR, and RT) were recorded before anesthesia. Anesthesia and analgesia were provided by acepromazine (10 mg mL−1, Neurotranq; Alfasan, Woerden, Holland), midazolam (5 mg mL−1, Midazolam; Caspian, Rasht, Iran), pethidine (100 mg 2 mL−1, Petholan; Adeka, İstanbul, Turkey), medetomidine (1,000 mcg mL−1, Dorbene Vet; Syva, León, Spain) and ketamine (50 mg mL−1, Ketamine HCl Inj.; Rotexmedica GmbH, Trittau, Germany), and ketorolac (30 mg mL−1, Ketorolac; Alborz Darou, Tehran, Iran). A 19G catheter was placed aseptically in the cephalic vein for a given lactated Ringer's solution (250 mL, lactated Ringer's solution; Shahid Ghazi, Tabriz, Iran) at a rate of 5 mL kg−1 h−1.

The animals were premedicated by acepromazine at 0.02 mg kg−1, midazolam at 0.5 mg kg−1, meperidine at 2 mg kg−1, medetomidine at 20 mcg kg−1, and ketamine at 4 mg kg−1 IM. They received ketorolac at 1 mg kg−1 immediately before surgical asepsis. The maintenance of anesthesia was achieved by administering a consistent anesthetic mixture (ketamine at 4 mg kg−1 and midazolam at 0.27 mg kg−1) at a variable rate of 0.2–0.5 mg kg−1, depending on the ketamine levels present in the mixture. The administration of the anesthetic was monitored through the use of several parameters, including SpO2, ECG, non-invasive blood pressure measured through a blood pressure cuff (size #4) placed proximal to the carpus over the radial artery at five-minute intervals, and respiration. The surgical procedure and manipulation were also taken into account during the administration of anesthesia. The Pm-7000vet, manufactured by Wuhan Zoncare Bio-medical Electronics Co., Ltd., was used to monitor animals. The animals' cardiorespiratory parameters were monitored until they demonstrated full recovery.

A nociceptive response was defined as a 20% or more rise in heart rate over the base rate, accompanied with an increase in breathing frequency and blood pressure proportionate to a painful surgical procedure (20, 55, 56). Ketamine at 0.5 mg kg−1 was used for rescue analgesia during surgery. The timeline details of measures were provided in **Table 1**.

2.3. Surgery

2.3.1. The surgeon and surgical team

Two months after graduation, a female doctor of veterinary medicine (DVM) with minimum experience (according to the veterinary training course) in the conventional approach and no expertise with the new methodology has been selected as the surgeon (NNM). The selected surgeon and surgical team underwent a one-week training course for each surgery 10 days prior to the start of the study. During the training course, one surgery was done on each technique by the advisor, and then the techniques were randomly performed on 12 dogs (6 dogs each technique) by the surgeon conducting the study. The random approach has been a coin toss (51–53); thus, the first-day method was determined by tossing a coin, and the next day the opposite technique must be followed. The study surgeries were performed by the same team under the supervision of the dissertation adviser (NZD).

2.3.2. Aseptic surgical preparation

In dorsal recumbency, the ventral abdomen was aseptically prepped after hair removal from mid-chest to the end of the pelvic symphysis and the inner thigh. During pre-surgical aseptic preparation, the skin was alternately scrubbed three times with 7.5% povidone-iodine and 70% ethyl alcohol. After the final povidone-iodine scrub is complete, a 10% povidone-iodine solution is applied to the surgical field (1).

Steps	Time (min)	Medicines/Dose/Application	Rout/Location/Area
Anesthesia, Premedication[1st]	0 (Start)	Acepromazine (10 mg mL^{-1}), 0.02 mg kg^{-1}	IM
		Midazolam (5 mg mL^{-1}), 0.5 mg kg^{-1}	
		Meperidine (50 mg mL^{-1}), 2 mg kg^{-1}	
Vital parameters monitor			
– Electrocardiograph	1–2 min after laying down	Lead II	On the elbows and knees
– Blood pressure		Neo #4	On the carpus over radial artery
– Pulse oximeter		Veterinary SPO2 transducer	On the ear until induction, then on the tongue
IV catheterization	10	19G	Cephalic vein
Preventive antibiotic		Cefazolin (1 g vial^{-1}), 22 mg kg^{-1}	IV
Fluid therapy		Lactated Ringer's solution, 5 mL kg^{-1} h^{-1}	IV
Hair clip		No 40	Mid-chest to mid-thigh
Anesthesia, Premedication[2nd]	15	Medetomidine (1,000 mcg mL^{-1}), 20 mcg kg^{-1}	IM
		Ketorolac (30 mg mL^{-1}), 1 mg kg^{-1}	SC
Aseptic preparation	17	Povidone Iodine scrub (7.5%) and 70° ethyl alcohol, three times consecutively; then Povidone Iodine solution (10%) was applied	
Anesthesia, Induction	20–25	Ketamine (50 mg mL^{-1}), 4 mg kg^{-1}	IV, Anesthetic mixture
		Midazolam (5 mg mL^{-1}), 0.27 mg kg^{-1}	
Endotracheal intubation	Immediately after induction	A maximum size based on the rough estimation using the $\sqrt{}$ (Body weight×5)	Intraoral, mid-trachea
Anesthesia, Maintenance	As needed	Induction anesthetic mixture, 0.2–0.5 mg kg^{-1} based on the ketamine	IV, Anesthetic mixture
Intraoperative rescue analgesia	As needed	Ketamine, 0.5 mg kg^{-1}	during surgery based on HR and RR and surgical manipulation
End of surgery (the last skin suture)			
– Conventional – Instrument Shank-assisted	67–72 55–60		
Postoperative antibiotic	Every 8 h	Cefazolin (1 g vial^{-1}), 22 mg kg^{-1}	IM, for 3 days
Postoperative rescue analgesia	Every day	Ketoprofen, 2 mg kg^{-1}	IM, as needed, at cefazolin injection time evaluation as needed

IM, intramuscular; IV, intravenous; SC, subcutaneous; HR, heart rate; RR, respiratory rate.
1st: administration of the first part of pre-anesthetic drugs, which included Acepromazine, Midazolam, and Meperidine; 2nd: Administration of the second part of pre-anesthetic drugs which included Medetomidine and Ketorolac.

TABLE 1. *The measures carried out during the conventional (n = 9) and Instrument Shank-assisted ovariohysterectomy (n = 9).*

2.3.3. Approach and incision length

A ventral midline celiotomy was performed immediately caudal to the umbilicus and extending one-third of the way to the pubic rim (11) for both methods, in order to achieve the same incision length (57, 58).

2.3.4. Surgical methods

2.3.4.1. Conventional (triple hemostatic) OHE

In the control group, the triple-clamp OHE (1) was done after entrance into the abdominal cavity and control of the uterine horn without a spay hook. During this method, the surgeon's dominant index finger is used to grab the left horn of the uterus. For organ manipulation, rat-toothed Crile forceps secured to the proper ligament were utilized. The suspensory ligament was strummed and released manually in the caudomedial direction. After creating a mesovarium window, two simple ligatures were placed on top of one another in the first clamp crush near the kidney. One transfixation ligature was then tightened in lieu of the middle clamp near the ovary [Polydioxanone (PDS II), 2–0]. The pedicle was transected and inspected for hemorrhage. The same techniques were then conducted on the contralateral pedicle. Separately, the cervix and uterine arteries were ligated (PDS II 2–0). Linea alba (PDS II 0),

subcutaneous tissue (PDS II 2–0), and skin (monofilament Polyamide 0) were routinely closed. A stent bandage was then placed over the suture line.

2.3.4.2. Modified instrument shank-assisted OHE

After accessing the visceral organs, first the left uterine horn and ovary were seized. A hemostat forceps was placed on the proper ligament to manipulate the ovary and its pedicle (**Figure 1A**). Then a window was created in the broad ligament (**Figure 1B**), and one of the handles of a Mayo-Hegar needle holder was passed through this window **(Figure 1C**), then secured (**Figure 1D**). After securing the ratchets, the needle holder was positioned over the surgical incision on the abdomen (**Figure 1D**). While pulling the first hemostat (on the proper ligament), the second hemostat was put on the ovarian pedicle, as far away from the ovary as possible (between the ovary and the needle holder's locked handles) (**Figure 1E**). While doing this, with the second hemostat, the needle holder shanks were pushed along the suspensory ligament toward the viscera to attain the appropriate distance. After securing the second hemostat, it was placed crosswise on the needle holder's shanks so that it would not be dragged into the abdominal cavity and would stay visible to the surgeon outside the abdomen at all times (**Figure 1F**). The third and fourth hemostats were then inserted between the ovary and the second forceps (**Figure 1F**). These forceps have crushed the tissues in preparation for the installation of the ligature. After crushing the pedicle, the forceps were removed, and circumferential and transfixation ligatures were applied to the pedicle in the formed groove. The ovarian pedicle was sharply transected using a scalpel immediately after the transfixation ligature, while it was protected by a hemostat. Throughout the application of these steps, the second forceps remained firmly on the ovarian pedicle, preventing it from being dragged within. The needle holder was put down after being released (**Figure 1G**). After gently grasping the corner of the ovarian pedicle with tissue forceps, the second forceps was released. The ovarian pedicle was inspected for hemorrhage and then released. The procedures were repeated for the contralateral ovary. The remainder of the procedure up to the final skin gap suture was routinely performed (same as the triple hemostatic method).

2.3.5. Surgical time intervals

All surgeries were video captured, and the time intervals between each step were retrieved. The initiation of the incision and the final abdominal closure suture were considered the beginning and finish of the surgical procedure, respectively. These are the defined time intervals:

Total surgery time (TST): From the initial skin incision to the last skin suture of an abdominal incision.

Pedicle intervention time (PIT): From placing a hemostat on the proper ligament of the left ovary through cutting the right pedicle following the installation of its ligature; incorporating SRT, ShT, ClpT, and LigT for the left and right pedicles.

Suspensory release time (SRT): Digital strumming of the suspensory ligament.

Shanking time (ShT): From the end of windowing (the process of creating a window in the broad ligament) until the start of anchoring clamp placement. An anchoring clamp is a hemostatic clamp placed on the ovarian pedicle as far away from the ovary as possible to prevent dragging into the abdominal cavity.

Clamping time (ClpT): From the placement of the anchoring clamp to the completion of the last ligating clamp, near the ovary. The ligating clamp is a hemostatic forceps that is used to crush the ovarian pedicle and create a groove for the installation of the ligature. After the anchoring clamp, these forceps are secured to the pedicle on the ovary side.

Ligating time (LigT): From the beginning of the first simple ligature until the finish of the trans-fixing ligature of both pedicles.

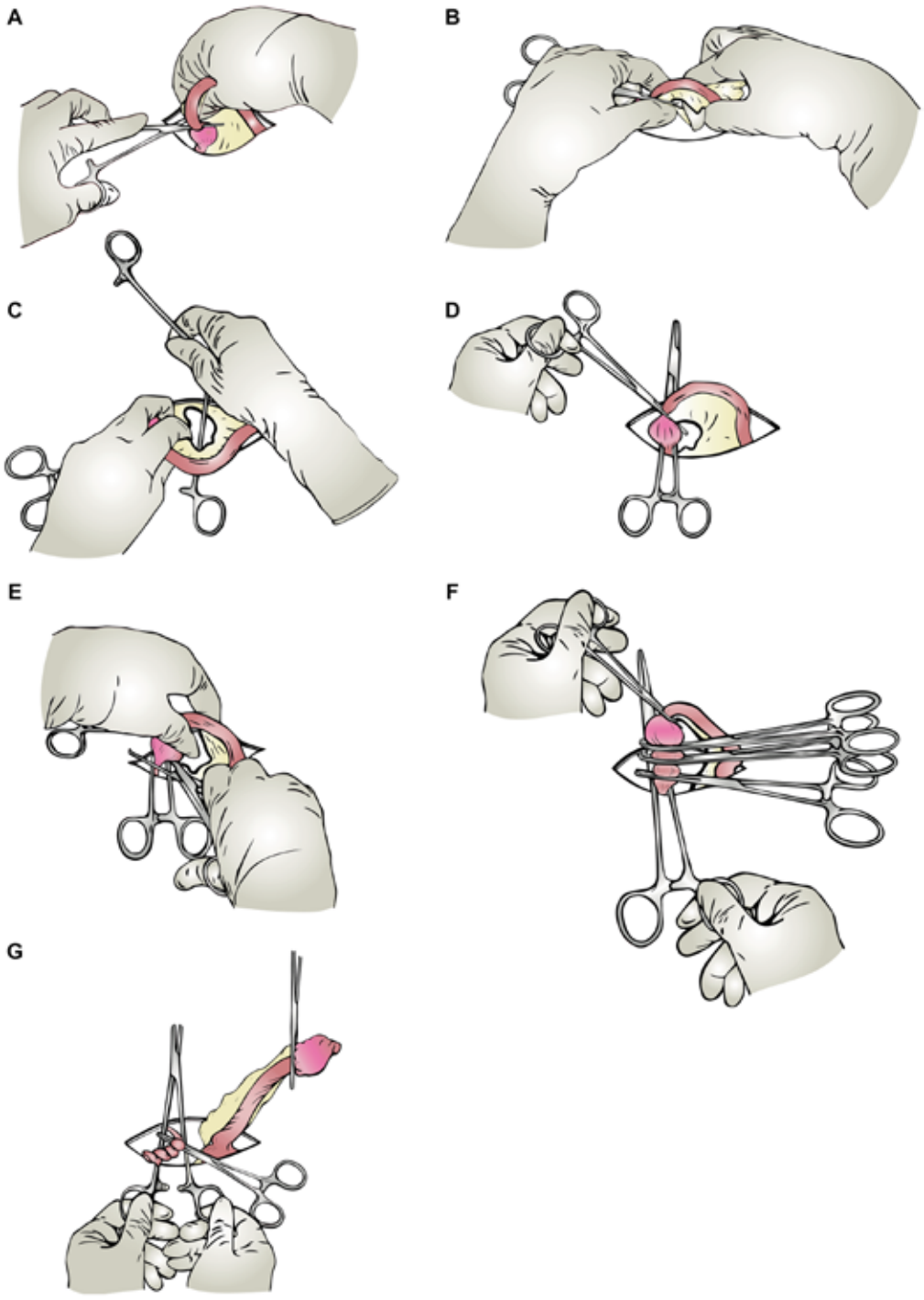

Figure 1. *Schematic steps of the modified Instrument shank-assisted ovariohysterectomy. Most steps in this method are similar to the triple-clamp technique. Wherein the pedicle is retained outside the abdomen by a straight Ochsner hemostat placed on the shanks of a needle-holder crossly. (**A**) Proper ligament clamping: After identifying the uterine horn, the rat-toothed Crile forceps are placed on the proper ligament to manipulate the ovary and its pedicle. (**B**) Windowing: A window is created in the mesovarium with an index finger. (**C**) Shanking (needle holder's shank insertion): The needle holder's shank is passed through the created window in the previous step, and the ratchets are locked, so the ovarian pedicle locates between the shanks. (**D**) Shank-IN: The shanks are oriented crossly to the incision on the abdomen. (**E**) Applying the "Anchoring clamp" (The ovarian pedicle's 1st clamp): Holding the proper ligament forceps with one hand, push the anchoring clamp (first clamp), which is on the needle holder's shank, toward the viscera, and lock it on a suitable level of the ovarian pedicle. (**F**) Triple hemostatic: The "ligating clamps" were secured between the Anchoring clamp and the ovary out of the abdominal cavity to crush the tissue for ligature placement. (**G**) Ligation and shank-OUT: Apply two simple ligatures and one transfixing ligature close to the ovary in the crushed groove created in the previous step.*

Tabla de contenido:

Other surgical procedures time (OSPT): All surgical procedures, except PIT and CT.

Closure time (CT): Closure time starts from the linea alba to the last skin suture tying.

2.4. Pain assessments

There are many different kinds of subjective scoring systems, and some of them have been used in veterinary medicine (59). In this study, postoperative pain was measured using the Glasgow composite pain scale short form (GCMPS-SF) (60), the University of Melbourne pain scale (UMPS) (61), and visual analogue scales (VAS) (62). A trained, male examiner (AB) who was single-blinded measured the post-surgical pain (30, 31). He became acquainted with the dogs the day before surgery. Moreover, the similar abdominal closure and the bandage have prevented the procedure from being identified. Multidimensional pain assessments were carried out 1 h before surgery (0) and 6-, 24-, 48-, and 72-h following skin suturing.

2.5. CRP

Five milliliters of blood were drawn from the lateral saphenous vein after the same pain evaluation times. The samples were kept at the temperature of the operation room for 20–25 min before being transported to the laboratory. The serum separated by centrifuging at 3,000 rpm for 15 min was stored in a microtube at −20°C until the research ended. CRP levels (mg L−1) were determined using the CRP latex agglutination technique using the CRP-LIA kit, Bionik in the laboratory of the faculty (4, 33).

2.6. Postoperative medications

Antimicrobial therapy (63) was started intravenously (IV) during premedication and maintained intramuscularly (IM) every 8 h for 3 days following surgery at 22 mg kg−1 of cefazolin (Exir, Tehran, Iran) in both groups. Ketoprofen (Ketomax; Rooyandarou, Tehran, Iran) at 2 mg kg−1 IM was given to animals having a GCMPS-SF score of 6 or higher out of 24 (45); throughout the examination, the UMPS and VAS ratings were also examined as supplementary criteria for determining a ketoprofen prescription.

2.7. Statistical analysis

The SPSS program (IBM SPSS Statistics for Windows, version 26, IBM Corp., Armonk, NY, United States) was used to look at the data. Along with normality confirmation using the Shapiro–Wilk test (except LigT), the study recruited the suspicious non-normal parametric data (PID, SRT, ShT, ClpT, LigT, and OSPT) after normalization based on the concordance of skewness and kurtosis coupled with stem-and-leaf plots. The duration of surgical steps was analyzed using a T-test. The Pearson correlation coefficient was used to determine the relationship between PIT and TST.

The Friedman test analyzes the progression of pain changes. Using Related-Samples Friedman's Two-Way ANOVA by Ranks, we compared pain levels between evaluating time intervals throughout each surgical process. Using Kruskal-Wallis H tests on mean, a comparison of pain levels at assessing time intervals between two surgical techniques has been conducted. On the median, Independent-Samples Kruskal-Wallis H followed by Independent-Samples Fisher Exact Sig. (2-sided test, for samples less than 10) has been implemented on the information obtained from three behavioral pain assessment methods.

Variations in CRP were evaluated using repeated measures ANOVA, independent samples t-test, and general linear model-univariate tests.

The correlation between CRP and age, weight, HR, RR, and RT was shown using Pearson's correlation coefficient. The partial eta squared was used to figure out how CRP and the body condition score (BCS) are related. Spearman's rho correlation coefficient was used to determine the relation between surgical time intervals and pain (based on GCMPS-SF). The statistical significance level was set at $p < 0.05$.

2.7.1. Data availability statement

All relevant data is contained within the article: The original contributions presented in the study are included in the article, further inquiries can be directed to the corresponding author.

3. Results

3.1. Participants' signalment and vital sign

There were no significant differences in the distribution of dogs by weight ($p = 0.726$) or age ($p = 0.598$) between the two groups. The mean and SD of age, weight, vital parameters (HR, RR, and RT), and BCS are shown in **Table 2**.

3.2. Surgical time analysis

Instrument shank-assisted OHE displayed shorter TSTs than the conventional method (34.70 ± 6.7 and 47.40 ± 9.9 min respectively, $p = 0.005$). Table 3 provides a comparison of the methods' time intervals. According to the new method, SRT is identical to ShT. ShT required 74% less time than SRT ($p = 0.009$), and moreover, LigT improved by 37% ($p = 0.005$) with the novel approach. Additionally, the OSPT and CT got 26 and 29% shorter, respectively.

Figure 2 shows how time intervals have changed, and Table 3 gives a statistical analysis of the changes. In each compartment of this figure, the difference favors the Instrument shank-assisted method.

Parameters	Conventional	Shank-assisted	*p*-value
Age	3.0 ± 1.9	2.6 ± 1.0	0.821
Weight	22.6 ± 4.3	21.8 ± 4.5	0.798
RT	38.7 ± 0.6	38.7 ± 0.3	0.877
HR	103.2 ± 25.0	106.0 ± 34.1	0.948
RR	29.3 ± 9.4	25.6 ± 5.0	0.622
BCS	4.7 ± 0.9	4.6 ± 0.9	0.422

Table 2. *Mean ± SD of age, weight, BCS, and preoperative vital parameters before anesthesia for the conventional (n = 9) and Instrument Shank-assisted ovariohysterectomy (n = 9).*

According to the comparable correlation pattern (64) between TST and PIT based on $\rho = 0.952$, $p = 0.0001$ and $\rho = 0.862$, $p = 0.003$ for conventional and instrument shank-assisted OHE, respectively, PIT plays a crucial role in TST during ovariohysterectomy. The correlation analysis of TST and ShT revealed that, from a temporal perspective, ShT alone did not significantly reduce TST ($\rho = 0.097$, $p = 0.804$).

During the conventional OHE, a single intraoperative hemorrhage in the ovarian pedicle was managed. The dog was excluded from the study. None of the dogs in either group had problems after surgery.

3.3. Pain

Using the Friedman test, pain score changes (Δ Pain in GCMPS-SF, UMPS, and VAS; Table 3) were statistically significant in both groups. The majority of the time, the data showed that the new method was associated with much less pain (**Table 4** and **Figures 3–5**).

Data	Units	Conventional	Shank-assisted	*p*-value
Time intervals				
TST	min	47.40 ± 9.9	34.70 ± 6.7	0.005
PIT	min	20.96 ± 5.78	14.52 ± 3.73	0.014
SRT	s	78.97 ± 69.10		}0.035
ShT	s		20.39 ± 8.18	
ClpT	s	50.66 ± 45.04	63.55 ± 37.15	0.662
LigT	min	12.82 ± 3.37	8.02 ± 3.11	0.005
OSPT	min	31.00 ± 7.0	23.00 ± 4.8	0.013
CT	min	16.40 ± 4.5	11.60 ± 2.5	0.013

Correlation*				
	ρ	*p*-value	*ρ*	*p*-value
TST vs. PIT	0.952****	0.000	0.862***	0.003
SRT	0.494	0.176		
ShT			0.097	0.804
ClpT	0.683**	0.043	0.754***	0.019
LigT	0.836***	0.010	0.618	0.076
TST vs. CT	0.768***	0.016	0.818***	0.007

TST, total surgery time; PIT, pedicle intervention time; SRT, suspensory release time; ShT, shanking time; ClpT, clamping time; LigT, ligating time; OSPT, other surgical procedures time; CT, closure time. *Pearson correlation stratification (very strong, strong, moderate, weak, and negligible): ****very strong, ***strong, **moderate. The significance level was set at 0.05.

Table 3. *Mean ± SD of different surgical steps time intervals recorded in the conventional (n = 9) and Instrument Shank-assisted ovariohysterectomy (n = 9) and correlation of surgical time intervals with total surgery time in deep-chested dogs.*

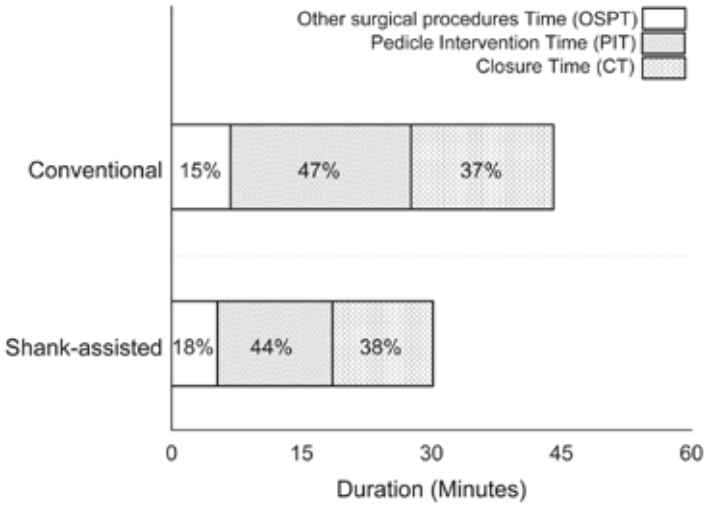

Figure 2. *Comparison of the time spent performing different steps in the conventional method (n = 9) and new modified Instrument shank-assisted method of ovariohysterectomy (n = 9) in deep chested-dogs. OSPT, Other surgical procedures time, which consist of all surgical steps, except PIT and CT; PIT, Pedicle intervention time, which is from placing a hemostat on the proper ligament of the left ovary to cutting the right pedicle after placement of its ligatures; CT, Closure time, from the linea alba to the last skin suture tying.*

Tabla de contenido:

			T0	T6	T24	T48	T72	*p*-value† (Δ Pain$^{0-72}$)
GCMPS-SF								
		Conventional	0 (0–0) (9)	**6 (2–14) (9)**	5 (3–10) (8)	**5 (2–8) (9)**	3 (1–12) (6)	0.002
		Shank-assisted	0 (0–0) (9)	**3 (2–5) (9)**	2 (0–6) (9)	**2 (0–4) (9)**	1 (0–7) (9)	0.000
p-value	Mean	K-W*	1.000	0.012	0.037	0.006	0.167	
	Median	K-W**		0.004	0.486	0.004	0.264	
		Fisher#		**0.015**	0.637	**0.015**	0.329	
UMPS								
		Conventional	0 (0–0) (9)	5 (2–8) (9)	**5 (3–10) (8)**	**5 (0–7) (9)**	3 (1–10) (6)	0.003
		Shank-assisted	0 (0–0) (9)	4 (1–6) (9)	**2 (1–4) (9)**	**1 (0–4) (9)**	2 (0–5) (9)	0.000
p-value	Mean	K-W*	1.000	0.099	0.002	0.018	1.000	
	Median	K-W**		0.058	0.002	0.016	0.264	
		Fisher		0.153	**0.003**	**0.050**	0.329	
VAS								
		Conventional	0 (0–0) (9)	**3 (1–5) (9)**	3 (1–6) (9)	2 (0–3) (9)	1 (0–6) (6)	0.002
		Shank-assisted	0 (0–0) (9)	**1 (1–2) (9)**	1 (0–4) (9)	1 (0–2) (9)	0 (0–5) (9)	0.001
p-value	Mean	K-W*	1.000	0.003	0.074	0.024	1.000	
	Median	K-W**		0.001	0.147	0.018	1.000	
		Fisher		**0.002**	0.335	0.057	1.000	

T0, before surgery; T6, 6 h after surgery; T24, 24 h after surgery; T48, 48 h after surgery; T72, 72 h after surgery; eGCMPS-SF, the short form of the Glasgow composite measure pain scale; UMPS, university of Melbourne pain scale; VAS, visual analogue scale. The bolded items show a statistically significant difference in a pain score between the two surgical procedures in each evaluating time intervals using the Kruskal-Wallis H analysis; Lowercase letters indicate statistical comparison of pain recorded at different assessment times in the same group using Related-Samples Friedman's Two-Way ANOVA by Ranks. †Friedman Test. *Independent-Samples Kruskal-Wallis H on mean. **Independent-Samples Kruskal-Wallis H on median. #Independent-Samples Fisher Exact Sig. (2-sided test) on Median (for samples less than 10). The significance level was set at 0.05.

Table 4. *Median (Min–Max) of pain scores and Δ Pain0–72 based on Glasgow composite pain scale short-form (GCMPS-SF), university of Melbourne pain scale (UMPS), and visual analogue scales (VAS) scales in the conventional (n = 9) and Instrument Shank-assisted ovariohysterectomy (n = 9) in deep-chested dogs.*

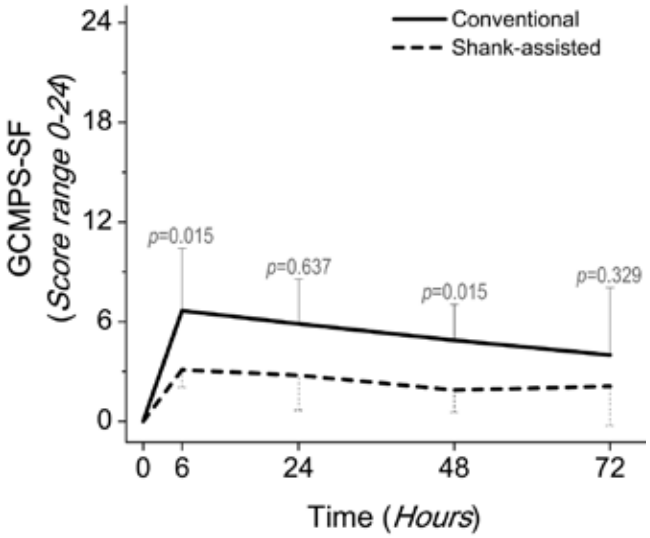

Figure 3. *Comparing postoperative pain scores using the Glasgow composite pain scale short-form (GCMPS-SF) in the conventional method (n = 9) and new modified Instrument shank-assisted method (n = 9) of ovariohysterectomy in deep chested-dogs. The p-value was calculated using an Independent-Samples Kruskal-Wallis H on median followed by Independent-Samples Fisher Exact Sig. (2-sided test) on Median shows the statistical difference in sampling times between two groups.*

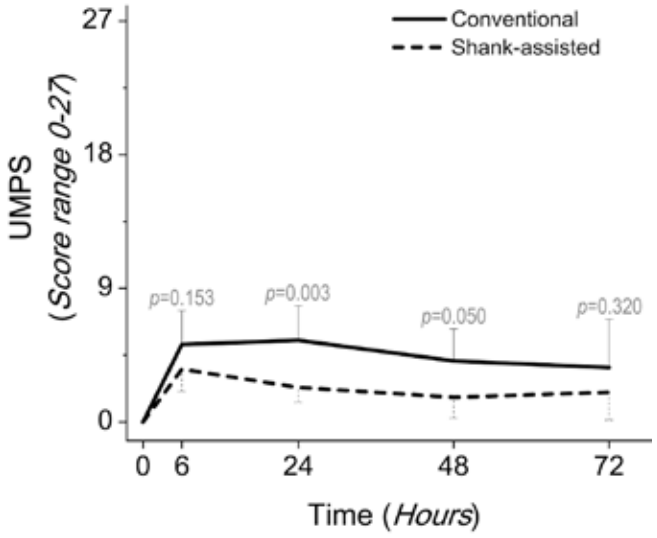

Figure 4. *Comparing postoperative pain scores using the university of Melbourne pain scale (UMPS) in the conventional method (n = 9) and new modified Instrument shank-assisted method (n = 9) of ovariohysterectomy in deep chested-dogs. The p-value was calculated using an Independent-Samples Kruskal-Wallis H on median followed by Independent-Samples Fisher Exact Sig. (2-sided test) on Median shows the statistical difference in sampling times between two groups.*

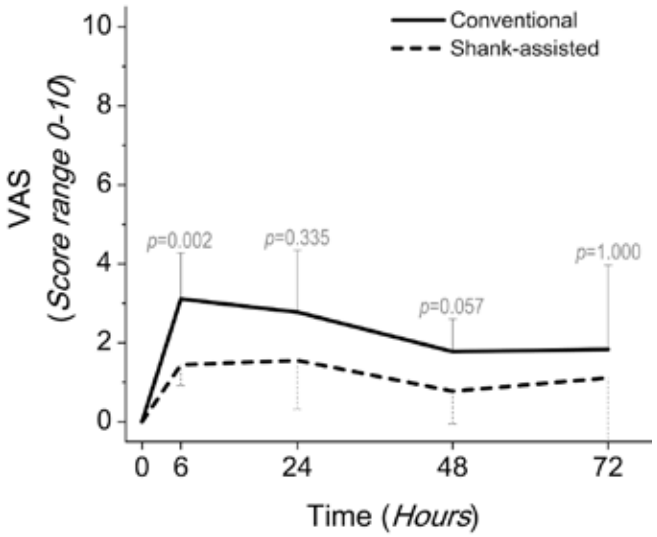

Figure 5. *Comparing postoperative pain scores using the visual analogue scales (VAS) in the conventional method (n = 9) and new modified Instrument shank-assisted method (n = 9) of ovariohysterectomy in deep chested-dogs. The p-value was calculated using an Independent-Samples Kruskal-Wallis H on median followed by Independent-Samples Fisher Exact Sig. (2-sided test) on Median shows the statistical difference in sampling times between two groups.*

(R) evolution

PEQUEÑOS ANIMALES

Tabla de contenido:

3.3.1. Rescue analgesia

After the surgery, 36 pain assessments have been done in each group, ranging from T6 to T72. These pain assessments have been carried out at 6-, 24-, 48-, and 72-h following surgery on nine animals in each group. The animals were injected with rescue analgesics 13 times (T6: 6, T24: 3, T48: 3, and T72: 1 dog) in the conventional group and twice (T24: 1 and T72: 1, both for one dog) in the novel group. Using the conventional methods, 8 dogs were injected with rescue analgesic, whereas just 1 dog received it using the alternative method.

3.4. CRP

After 24 h, the highest serum CRP levels were observed in both groups. **Figure 6** demonstrates that the conventional group's rate of rise accelerated more rapidly during the initial 6 h following surgery. The slope of the graph is determined to be y = 24.328x – 18.072 for traditional OHE and y = 4.9556x – 1.5667 for instrument shank-assisted OHE within the first 6 h. The traditional group observed a 4.9-fold increase in CRP acceleration on this basis. After 48 h, the Instrument shank-assisted OHE showed a significant decrease to baseline levels (p = 0.032; see **Tables 5, 6**). In contrast, although CRP levels decreased in the conventional group, they were not significantly different from their peak levels.

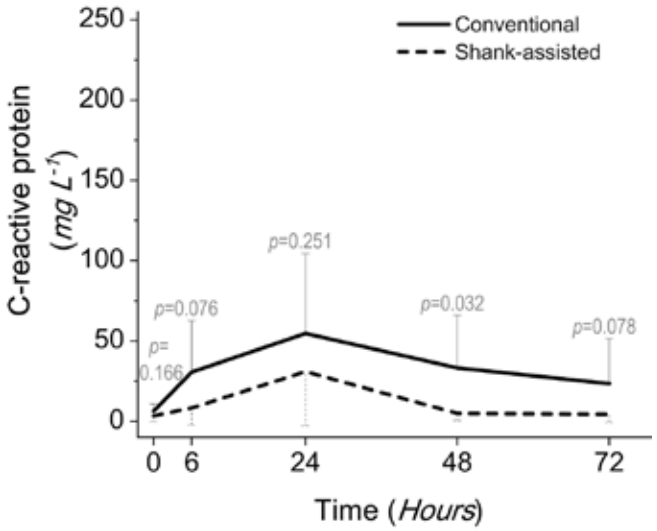

Figure 6. *Comparing postoperative serum C-reactive protein levels following the conventional method (n = 9) and new modified Instrument shank-assisted method (n = 9) of ovariohysterectomy in deep chested-dogs. The p-value was calculated using an independent samples T-test shows the statistical difference in sampling times between two groups.*

Sampling time	Groups		*p*-value
	Conventional	Instrument shank-assisted	
T 0	6.3 ± 4.6^{b}	3.4 ± 3.8^{b}	0.166
T 6	30.6 ± 31.9^{ab}	8.3 ± 10.7^{b}	0.076
T 24	54.7 ± 49.6^{a}	30.9 ± 33.7^{a}	0.251
T 48	33.2 ± 32.7^{ab}	5.0 ± 4.4^{b}	**0.032**
T 72	23.4 ± 28.2^{ab}	4.4 ± 5.0^{b}	0.078

Small letters indicate statistical comparisons in a group between different sampling times. The *p*-value shows the comparison of two groups at each sampling time. T 0, before surgery; T 6, 6 h after surgery; T 24, 24 h after surgery; T 48, 48 h after surgery; T 72, 72 h after surgery. The significance level was set at 0.05. *p*, *p*-value, the bolded text shows a significant correlation.

Table 5. *Mean ± SD of the serum CRP concentration (mg L–1) following the conventional (n = 9) and Instrument Shank-assisted ovariohysterectomy (n = 9) in deep-chested dogs.*

3.5. Correlations

The relationship between pain (as measured by GCMPS-SF, UMPS, and VAS), surgical time parameters, CRP, vital signs, age, weight, and BCS has been studied.

3.5.1. Surgical time intervals with pain

Spearman's rho correlation coefficient has studied the relationship between the overall surgical duration and the duration of the distinct phases. The analysis is described in full in Table 6, which is stated separately below.

Only pain in the conventional OHE exhibits a significant positive correlation with LigT at T72, according to GCMPS-SF.

Using the novel method, UMPS found significant negative relationships between pain and TST at T24 and T48. This study indicated that PIT has a vital function in lowering pain in T24.

The VAS has found a greater correlation between specific surgical stages and pain. GCMPS-SF, UMPS, and VAS were able to identify 1, 3, and 7 correlations, respectively, in this regard. In the new method, VAS identified an association between ClpT and less pain at T6 and T24, and between ClpT and OSPT at T48. This assessment method revealed that PIT, LigT, and most notably OSPT have a substantial effect on the incidence of pain on the third day following surgery in the conventional group (see **Table 6**).

3.5.2. CRP with pain

Using Spearman's rho correlation coefficient, CRP levels and pain were only shown to have significant moderate-to-strong negative relationships in five measurement points of total samples (two groups in total). These associations were detected at T24 (UMPS) and T72 (GCMPS-SF) in the conventional group and at T6 (VAS) and T48 (GCMPS-SF and VAS) in the instrument shank-assisted group, as shown in **Table 7**.

3.5.3. CRP with age, weight, vital signs, and BCS

Pearson's correlation coefficient indicated that there was no association between CRP changes and age, weight, HR, RR, and RT in both groups ($p > 0.05$). Partial eta squared (η P 2) was unable to identify a significant association between CRP and BCS using any of the two techniques.

4. Discussion

According to the present results, when implementing OHE with instrumental shank assisted technique, the surgery can be performed by one person with lesser surgical trauma. With the current solutions, digital strumming or sharp tearing of the suspensory ligament in deep-chested dogs has not only been a time-consuming process, but it has also failed to shorten the length of surgery and pain afterward (11). According to current research, a decrease of over 12 min in an alumnus surgeon's overall surgery length is a positive improvement (57). The reduction in surgical trauma has resulted in a slower increase in CRP levels and a shorter peak. These gains were made using the same equipment and facilities at no additional expense due to a modest modification in the surgical approach.

4.1. Surgical perspectives

OHE, like many other surgical procedures, seems to get more challenging as the size and weight of the animal increase. As body mass increases, the chest sinks deeper, and it becomes more difficult to reach and release the suspensory ligament (11). In the present study, the same higher body weight range enhanced the ovarian exposure challenge, allowing the method to be generalized to various sizes of dogs and cats; however, it may be accompanied by fewer problems in smaller animals.

Insufficient exposure during OHE leads to incorrect technique execution and raises the risk of ovarian remnant syndrome (2). The instrument shank-assisted OHE keeps the ovary outside of the abdomen without an assistant while maintaining the suspensory ligament. In obese and deep-chested dogs, as well as for unskilled surgeons who

Pain scales	Surgical time intervals	Methods															
		Conventional								Instrument shank-assisted							
		Pain 6		Pain 24		Pain 48		Pain 72		Pain 6		Pain 24		Pain 48		Pain 72	
		ρ	*p*	ρ	*p*	ρ	*p*	ρ	*p*	ρ	*p*	ρ	*p*	ρ	*p*	ρ	*p*
GCMPS-SF	TST	0.254	0.509	0.268	0.520	0.246	0.524	0.754	0.084	0.039	0.920	−0.343	0.366	−0.489	0.181	−0.309	0.418
	PIT	0.085	0.828	0.024	0.954	0.246	0.524	0.638	0.173	−0.208	0.591	−0.270	0.482	−0.282	0.462	−0.162	0.676
	SRT/ShT	0.356	0.347	0.098	0.818	0.042	0.914	0.116	0.827	0.321	0.400	0.405	0.279	0.068	0.861	0.359	0.343
	ClpT	−0.254	0.509	−0.073	0.863	0.314	0.411	0.493	0.321	−0.009	0.982	−0.555	0.121	−0.622	0.073	−0.373	0.322
	LigT	−0.034	0.931	0.073	0.863	0.610	0.081	0.899*	**0.015**	−0.303	0.428	−0.523	0.148	−0.316	0.407	−0.368	0.330
	CT	0.237	0.539	0.464	0.247	0.398	0.288	0.725	0.103	0.390	0.300	−0.093	0.812	−0.385	0.307	−0.111	0.776
	OSPT	0.254	0.509	0.293	0.482	0.271	0.480	0.754	0.084	−0.091	0.815	−0.449	0.225	−0.541	0.133	−0.352	0.353
UMPS	TST	0.118	0.762	0.393	0.336	0.220	0.569	0.348	0.499	−0.521	0.150	−0.705*	**0.034**	−0.670*	**0.048**	−0.336	0.376
	PIT	−0.068	0.863	0.417	0.304	0.458	0.215	0.522	0.288	−0.434	0.243	−0.685*	**0.042**	−0.385	0.307	−0.180	0.642
	SRT/ShT	0.135	0.729	0.528	0.179	0.441	0.235	0.319	0.538	−0.230	0.552	0.035	0.929	0.034	0.930	0.395	0.293
	ClpT	−0.051	0.897	0.246	0.558	0.186	0.631	0.319	0.538	−0.427	0.251	−0.557	0.119	−0.588	0.096	−0.220	0.570
	LigT	0.152	0.696	0.442	0.273	0.576	0.104	0.696	0.125	−0.085	0.828	−0.416	0.266	−0.299	0.434	−0.335	0.378
	CT	0.397	0.291	0.466	0.244	0.203	0.600	0.377	0.461	−0.655	0.055	−0.503	0.168	−0.590	0.094	−0.129	0.741
	OSPT	−0.034	0.931	0.405	0.319	0.407	0.277	0.638	0.173	−0.402	0.284	−0.613	0.079	−0.644	0.061	−0.323	0.396
VAS	TST	0.254	0.510	0.368	0.330	−0.059	0.879	0.638	0.173	−0.522	0.150	−0.422	0.258	−0.622	0.074	−0.193	0.618
	PIT	−0.009	0.982	0.368	0.330	0.218	0.573	0.880*	**0.021**	−0.433	0.244	−0.329	0.388	−0.472	0.199	−0.110	0.778
	SRT/ShT	0.289	0.451	0.564	0.113	0.564	0.113	0.698	0.123	−0.173	0.656	0.310	0.416	−0.027	0.946	0.578	0.103
	ClpT	0.149	0.703	0.197	0.612	0.149	0.703	0.395	0.439	−0.696*	**0.037**	−0.688*	**0.041**	−0.751*	**0.020**	−0.484	0.187
	LigT	0.035	0.929	0.291	0.448	0.287	0.454	0.820*	**0.046**	−0.346	0.361	−0.566	0.112	−0.330	0.386	−0.523	0.149
	CT	0.455	0.219	0.197	0.612	0.010	0.980	0.577	0.231	−0.520	0.152	−0.402	0.284	−0.508	0.163	0.000	1.000
	OSPT	0.009	0.982	0.616	0.078	0.149	0.703	0.941**	**0.005**	−0.435	0.242	−0.394	0.294	−0.720*	**0.029**	−0.304	0.426

ρ, Spearman's rho correlation coefficient; *p*, *p*-value, the bolded text shows a significant correlation; Pain 6, pain assessment 6 h after surgery; Pain 24, pain assessment 24 h after surgery; Pain 48, pain assessment 48 h after surgery; Pain 72, pain assessment 72 h after surgery; GCMPS-SF, the short form of the Glasgow composite measure pain scale; UMPS, university of Melbourne pain scale; VAS, visual analogue scale; TST, total surgery time; PIT, pedicle intervention time; SRT, suspensory release time; ShT, shanking time; ClpT, clamping time; LigT, ligating time; OSPT, other surgical procedures time; CT, closure time. *Correlation is significant at the 0.01 level (2-tailed). * Correlation is significant at the 0.05 level (2-tailed).

Table 6. *The correlation of surgical time intervals with post-surgical pain, which was evaluated using GCMPS-SF, UMPS, and VAS behavioral pain scales, after the conventional (n = 9) and Instrument Shank-assisted ovariohysterectomy (n = 9) in deep-chested mixed-breed dogs.*

Pain scales	CRP sampling times	Methods															
		Conventional								Instrument shank-assisted							
		Pain 6		Pain 24		Pain 48		Pain 72		Pain 6		Pain 24		Pain 48		Pain 72	
		ρ	*p*	ρ	*p*	ρ	*p*	ρ	*p*	ρ	*p*	ρ	*p*	ρ	*p*	ρ	*p*
GCMPS-SF	CRP 6	0.593	0.092	0.475	0.197	0.458	0.215	0.407	0.277	−0.182	0.639	−0.459	0.214	−0.130	0.739	−0.303	0.428
	CRP 24	−0.049	0.909	0.146	0.729	−0.195	0.643	−0.122	0.774	−0.498	0.173	−0.034	0.931	0.143	0.713	0.143	0.713
	CRP 48	−0.576	0.104	−0.280	0.466	−0.509	0.162	−0.492	0.179	−0.718*	**0.029**	−0.085	0.827	−0.051	0.896	0.043	0.913
	CRP 72	−0.551	0.257	−0.493	0.321	−0.638	0.173	−0.812*	**0.050**	−0.462	0.211	0.000	1.000	0.188	0.628	0.248	0.520
UMPS	CRP 6	0.245	0.526	0.304	0.427	0.321	0.400	0.152	0.696	−0.511	0.160	−0.034	0.931	−0.085	0.828	−0.111	0.777
	CRP 24	−0.626	0.097	−0.356	0.387	−0.638	0.089	−0.724*	**0.042**	−0.373	0.323	0.121	0.756	−0.243	0.529	−0.225	0.560
	CRP 48	−0.441	0.235	−0.153	0.695	−0.356	0.347	−0.356	0.347	−0.616	0.078	−0.068	0.861	−0.103	0.793	0.009	0.983
	CRP 72	−0.522	0.288	0.145	0.784	0.029	0.957	−0.058	0.913	−0.326	0.391	−0.034	0.930	0.198	0.610	0.240	0.533
VAS	CRP 6	0.140	0.720	0.009	0.982	0.114	0.771	−0.035	0.929	−0.779*	**0.013**	0.000	1.000	−0.087	0.825	−0.087	0.825
	CRP 24	−0.231	0.550	−0.043	0.913	−0.316	0.407	−0.162	0.676	−0.256	0.507	0.402	0.284	0.383	0.308	0.347	0.360
	CRP 48	−0.337	0.376	0.050	0.899	−0.069	0.859	−0.139	0.722	−0.713*	**0.031**	−0.160	0.680	−0.267	0.487	−0.205	0.597
	CRP 72	−0.577	0.231	−0.152	0.774	−0.213	0.686	−0.334	0.518	−0.220	0.569	0.303	0.428	0.440	0.235	0.468	0.204

ρ, Spearman's rho correlation coefficient; *p*, *p*-value, the bolded text shows a significant correlation; CRP, c-reactive protein; CRP 6, CRP sampling 6 h after surgery; CRP 24, CRP sampling 24 h after surgery; CRP 48, CRP sampling 48 h after surgery; CRP 72, CRP sampling 72 h after surgery; Pain 6, pain assessment 6 h after surgery; Pain 24, pain assessment 24 h after surgery; Pain 48, pain assessment 48 h after surgery; Pain 72, pain assessment 72 h after surgery; GCMPS-SF, the short form of the Glasgow composite measure pain scale; UMPS, university of Melbourne pain scale; VAS, visual analogue scale. *Correlation is significant at the 0.05 level (2-tailed).

Table 7. *The correlation of serum c-reactive protein levels with post-surgical pain, which was evaluated using GCMPS-SF, UMPS, and VAS behavioral pain scales, after the conventional (n = 9) and Instrument Shank-assisted ovariohysterectomy (n = 9) in deep-chested mixed-breed dogs.*

require a longer incision, the surgical assistant is essential (1, 2). So, a small incision without tearing the ligament is another achievement of the modified method, which led to limited surgical complications including incisional swelling, seroma, infection, delayed healing, ventral body wall dehiscence, self-inflicted trauma, pain (65), and hemorrhaging (66).

During a suspensory ligament release (66), an inexperienced surgeon is more likely to break the blood vessel and induce hemorrhage, which prompts the hurried application of surgical sponges. Stress has a negative impact on the non-technical skills of surgeons (67), leading Rodriguez et al. to conclude that intraoperative hemorrhage from an ovarian pedicle probably increased the retention of surgical sponges in veterinary patients (68). Therefore, removing ligament release from the surgical steps would likely reduce the frequency of hemorrhage and sponge retention; however, more research is required before a conclusion can be reached.

Hilgard's learning theory suggests that experience is a crucial component of the learning process (69). For unbiased comparisons, the study surgeries must be performed by a surgeon with no or equivalent prior experience in both methods. A minimum of surgeon experience in our study to the level of the veterinary training program according to conventional method seems to impose an inevitable minimal bias. However, the presence of an inexperienced surgeon could be a limitation of the present study. Given the possibility that a surgeon's lack of expertise might exacerbate surgical stress to the point where the impact of the technique is nullified, a week of training for each

method prior to the research allowed the current study to reveal the smallest difference between the procedures. TST has been reported to take between 55 and 130 min for inexperienced surgeons (70, 71). Freeman et al. established an optimal duration of 45 min for inexperienced surgeons after six surgeries (70). In this study, an average of almost 40 min TST demonstrated that the surgeon's skill is enhanced by training before to the start of main operations, and demonstrating our surgeons' experience (71) made the findings more realistic (11, 13, 70). Alternatively, previous research on pilots has yielded five levels of skill acquisition, including novice, advanced beginner, competent, proficient, and expert (25); If each 10-min improvement for OHE corresponded to one level of improvement for the surgeon's expert, then our surgeon's 12.7 min reduction in surgical duration using the instrument shank-assisted technique would theoretically qualify her as "competent."

Surgical experience makes sick animals healthier (72). Sir Francis Galton thought that talent was completely innate (73), but experience is a learning growth (25). Yet, from a different perspective, the surgeon's experience may provide no more than a 25% health improvement (72). On the other hand, OHE is still known as a model of acute pain in research studies. So, when animal pain after a technique is still a problem even after experienced surgeons have used it, it is important to look at the technique itself instead of just how it is taught. Consequently, both correct training and the training of correct techniques are emphasized in the surgical training curriculum, and the new method may contribute to the promotion of the latter, as indicated by the high effect sizes reported in the present study.

The type of operation is a stressor for the surgeon (74). Mental (75) and muscle (76) fatigue can delay an operation. Aside from the fact that the stress was not directly evaluated in our study, time as a major component in calculating surgical stress (74, 77) has been meticulously recorded and analyzed. Controversial is the scenario in which the total surgery time is reduced beyond the time spent on the ovarian pedicle. The technical difference between the two methods was SRT and ShT only had a time difference of 58.58 s in favor of the modified method, but TST was improved by 12.7 min. Non-correlation of these variables with TST indicates they did not directly contribute to the difference in TST, while ovarian exposure caused roughly 63% quicker application of ligatures (4.8 min improvement). The remainder of the improved duration was divided into two parts: (1) 3.1 min from the major procedures in OSPT, which include the separation of the broad ligament on both sides, the second ovary access, uterine arteries ligature placement, and uterine body close and cut; and (2) 4.8 min from CT. The procedures conducted in OSPT and CT were comparable among techniques, although the Instrument shank-assisted OHE required significantly less time. When we were nearing the end of the surgery, or, in other words, when the surgeon had reached extreme fatigue, 4.8 min more time was required to close the abdominal wall using the conventional technique. Therefore, significant time reduction in the mentioned two parts could be related to less fatigue and stress, which was paved through the shorter LigT in the new method. Peeters and Kirpensteijn's unsuccessful attempt to reduce surgical time by utilizing ovariectomy (OVE) instead of OHE (58) is another example of the surgeon's mental and physical strain at this time, as they did not eliminate digital strumming. Due to the strong correlation between TST and LigT in the present study, it is evident that the modified instrument shank-assisted technique can reduce the impact of the time required to install the ligatures, which was the primary factor in the significantly longer surgical time when the previous technique was used. Additionally, the small standard deviation (78) in these two portions may indicate the surgeon's optimal state of stability and fewer technical obstacles

Tabla de contenido:

during instrument shank-assisted OHE, which may require further investigation.

According to research findings, the surgeon's stress level may be enhanced due to a lack of familiarity with the members of the surgical team (67). While the present study did not measure the stress level of the surgeon, efforts were made to mitigate concerns regarding the presence of new team members. This was achieved through measures such as facilitating familiarity and collaboration among team members during the pre-study training course as well as maintaining a consistent surgical team.

Surgical supervisor changes complicate student-led surgical procedures (57). This study's experienced academic surgeon continuously supervised the surgical procedures, eliminating the possibility of this error, as observed in Harris's study due to a change in supervisor.

The time interval proportion found in this study could be used in general, even though an experienced surgeon could cut the total time needed for surgery. Hence, based on Shivley's yearly savings of 73.3 h (11), a 26.7% decrease in TST in instrument shank-assisted OHE could save 195.7 h (>2.5 times).

In concluding, as ovarian manipulation and pedicle ligatures were identified as the most essential procedures of OHE in a previous study (79), these findings have been meticulously confirmed in the present study. In the instrument shank-assisted OHE, a more accessible ovarian pedicle facilitated all subsequent steps of the surgery.

Due to the surgical discussion's focus on inexperienced surgeons, it is reasonable to assume that the significance of this technique will change as the surgeon's experience grows, whereas the pain-related advantages of this surgical technique will be discussed in a separate chapter, considering all surgeons to be subject to the implementation of this technique.

4.2. Pain perspective

The current study confirmed that, compared to instrument shank-assisted OHE, digital strumming of the ovarian pedicle during conventional OHE makes ligature placement more challenging, possibly due to unwanted visceral interferences or manipulations, prolongs the duration of surgery, and increases pain. Digital strumming is an unpleasant surgical procedure followed by considerable surgical trauma. Thereby, it is anticipated that modifying traditionally invasive procedures would improve patients' recoveries and well-being.

Subjective pain scales (44, 80) and, controversially, CRP have been used to measure pain since vital signs are not sensitive enough (81) and animals cannot communicate verbally (47). Several multidimensional structured behavior scales have been adapted for use in veterinary medicine (59), and the multidimensional GCMPS-SF for acute pain has been authorized for use in dogs (45, 60) with more sensitive and consistent results (82). The UMPS (which comprises six categories of physiological data) and VAS (with more flexibility) were used to compensate for the insufficiency of the GCMPS-SF and reduce the secrecy of the pain.

The results of pain assessments vary based on the experience and knowledge of the veterinarians, which are affected by age, gender, and time since graduation (31, 83). It was anticipated that using a trained, blinded assessor (30), a wound dressing, and three distinct pain scales would reduce the influence of qualitative variable bias in the current study. On the other hand, demographic data and dog acclimation before surgery suggest that individual pain tolerance, species, age, body condition, and environmental factors that can change or mask pain intensity are not confounding variables.

Since severe pain after surgery is often underestimated (84), it needs to be measured in a new surgical procedure (85). The perception of postoperative pain is dependent not only on surgical duration and technique (86), but also on

Tabla de contenido:

analgesic type (87), dose, multimodality (88–90), the use of preventative analgesia (91), route of administration, and the pharmacokinetics of medications (92). Pain can result in delayed wound healing and surgical site infection (93), and bandages may not be adequate for preventing suture line contamination (94). So, surgeons prefer to modify surgical procedures to reduce postoperative pain (47). This was one of the most important goals of instrument shank-assisted OHE, which had an effect size d of >1.27, > 1.32, and > 1.77 and a power of 0.811, 0.836, and 0.968 at T6, T24, and T48, respectively, based on provided GCMPS-SF pain measurements.

Sampling time is essential for accurately determining pain on time. In this study, sampling times were adjusted according to four theoretical elements: (1) the clinical duration of action of the analgesic agent (meperidine, medetomidine, and ketorolac), which may provide enough pain relief; (2) the plasma half-life of the anesthetic selected for premedication, induction, and maintenance of anesthesia (acepromazine, midazolam, and ketamine), which may change the responses given for pain evaluation; (3) the minimum estimated duration for pain onset, peak, and subsidence; and (4) the pathophysiology of CRP turnover. By giving dogs nonsteroidal anti-inflammatory drugs (NSAIDs) before surgery to help with pain after surgery (95, 96), it was thought that ketorolac might be enough for the first few hours after surgery. However, the results have only shown that this is true for the new technique. It was anticipated that the pharmacologic effects of the long-half-life (t½) drugs acepromazine (97), ketorolac (98, 99), and ketamine (nor-ketamine) (100) with residual effects of 7.1, 4.5 (or 10 based on relevant reference), and 6.2 h, respectively, would be felt from premedication until endotracheal extubation. Because sedatives, analgesics, and injectable dissociative anesthetics can change responses like facial expression, salivation, mydriasis, and cardiorespiratory parameters, which were evaluated in the GCMPS-SF, UMPS, and VAS, early pain assessment (<6 h) was not considered in this study.

The requirement of rescue analgesia may be regarded as a reliable indicator of the surgical technique's incompetence. According to a previous report in humans (101), after hip and knee arthroplasty, ketoprofen had the same analgesic effect as extradural morphine. Mathews et al. find that ketoprofen has a comparable impact to meloxicam and conclude that it could be a useful way for controlling postoperative pain (102). Similar to carprofen, meloxicam, and tolfenamic acid, ketoprofen produced excellent postoperative analgesia in cats, but with a lesser effect on tenderness (103). In the meantime, more recent studies indicate the administration of NSAIDs is superior to opioids due to faster recovery of normal functions and greater satisfaction with postoperative well-being (104). Nevertheless, these findings should be taken with care when applied to OHE in veterinary medicine. In the present study, animals that got rescue analgesia were not excluded, and 8 dogs in the conventional group who received rescue analgesia at 13 evaluation times were included for analysis. If getting rescue analgesics improved outcomes, the dogs in the first group were unable to demonstrate superior outcomes despite receiving frequent pain treatment. The number of animals administered rescue analgesics may be a reflection of the severity of surgical trauma and the invasiveness of the conventional technique. Receiving rescue analgesics in 1 dog out of 2 evaluation times can be attributed to greater well-being using the modified method and can be interpreted in two aspects: first, a standard protocol of analgesics is still recommended after surgery, and second, it may be useful in shelter or stray dogs that may not receive proper follow-up treatment, for example.

At 6 h postoperatively, eight out of nine dogs treated with the conventional method received rescue analgesia. This demonstrates at least two important

points: (1) ketorolac provides inadequate postoperative analgesia for the conventional OHE performed by an inexperienced surgeon, although it has been used in humans to control moderate to severe post-operative pain, and it may be effective in dogs (105), as effective as flunixin, and more effective than butorphanol or a low dose of oxymorphone (106), by affecting opioid receptors centrally with comparable efficacy to morphine (99), and (2) the current modification has decreased postoperative pain to the point that ketorolac could control it, so that none of the dogs in the second group required T6 rescue analgesia.

Our "competent" surgeon has made the surgery quick and competitive in terms of time (see "Surgical perspective"). Since the new method causes less pain and this surgery is still done to create a model of acute pain for research, it is safe to assume that this surgical method is not limited to a certain group of surgeons, no matter how much experience they have, and that it is better to make it more general.

In addition to the psychological burden experienced by the surgeon, contemporary approaches have been developed to assess the degree of pain and surgical stress imposed on the patient. While certain methods, including pupillometry, surgical pleth index (SPI), skin conductance, cardiovascular, and cardiorespiratory indices, require further advancements in sensor technology and interpretation algorithms to investigate animal responses to anesthesia and surgery, their applicability has not yet been confirmed. In the field of veterinary medicine, additional quantitative techniques have been introduced for animal assessment. These include the parasympathetic tone activity index (PTA index), which analyzes heart rate variability, and the bispectral index (BIS), which analyzes electroencephalography, with the potential for animal interpretation. Despite ongoing debates regarding the universal implementation of their use in all treatment procedures and drug protocols (107), the accessibility of these remedies may not always be assured. It is worth noting that the application of PTA as a means of assessing pain in conscious animals within the field of veterinary medicine is challenging. This is primarily due to the presence of unwanted movements by the animal, which directly impact heart rate variability. Consequently, alternative models capable of detecting these fluctuations should be employed (20, 32, 107, 108). The use of more recent medications, and therefore the recording of the quantity of anesthetics used (55) and the vital parameters throughout the operation, seems to be a large issue that would need review in separate research, other than that this technology was not available for the current study.

A number of different physiological parameters, such as plasma vasopressin, urine noradrenaline, and creatinine concentrations, have been suggested to assess the degree of irritation and pain caused by a surgical method. It appears that documenting additional facts and aiding in the final assessment of the effectiveness of the presented technique may be accomplished by comparing the changes in these parameters during anesthesia between the two methods. The conventional OHE involves applying extremely stretching stress to digitally strumming the suspensory ligament, while the new method involves keeping this ligament under tension all the way through the ligature placement process. Further research is warranted to compare the two methods from this perspective, as acute noxious stimuli during stretching of the pedicles can increase systolic blood pressure, heart rate, plasma vasopressin concentration, and urinary noradrenaline/creatinine ratio (55).

One of the initial observable events following surgery is the elevation in temperature and inflammation of the surgical site, attributed to enhanced blood circulation to the area where surgery was performed. Infrared thermography (IRT) is a proficient technique for assessing thermal variations in problematic areas, as it measures the surface temperature of the skin through ther-

Tabla de contenido:

mographic maps. This technique may be used to recognize the localized changes in blood supply and localized increases in temperature that occur in response to stress. The assessment of the efficacy of local anesthesia through the analysis of alterations in surface blood circulation linked to sympathetic activity is among the additional functionalities of IRT (109). However, it has been observed that this technique has not demonstrated sufficient effectiveness in dogs (110). The present study suggests that while the implementation of IRT for evaluating pain and inflammation in the surgical approach area was effective, practical limitations arose due to the bandage covering the surgical site. Conversely, the thermographic assessment of regions where the suspensory ligament has been torn, situated on the roof of the abdominal cavity, may not be deemed reliable in theory. This is due to the fact that the heating of the dermis surface is directly linked to the local dermal microcirculation, which is under the control of the ANS. Nevertheless, the non-invasive nature of this method of evaluation may be an appealing subject for further research.

Pupil shape has been a key indicator for neurological assessment for over a century (111), and automated pupillometers have become increasingly important due to the difficulty of detecting the "reactive pupil" characteristic (112). In addition, assessing pupil reactivity using a pupillometer offers an objective, rather than subjective, evaluation of the neurological examination. Automated pupillometers can distinguish between canine conscious and anesthetic pupillary light reflex (PLR) and continuously assess an animal before, during, and after anesthesia (113). It seems that PLR devices could be useful in research like the current one, provided that the assessments are standardized.

Evaluation of a novel surgical procedure extends beyond surgical parameters and postoperative discomfort. Surgical invasiveness may be assessed separately. Based on past research, the invasiveness of the surgical procedure may be related to postoperative pain. Consequently, the question of surgical trauma severity is a separate topic that will be addressed further in "CRP perspective."

4.3. CRP perspective

In this study, the traditional OHE method was changed in a way that reduced the amount of trauma. With the new technique, the amount of surgery-related trauma had a smoother pattern and went back to normal almost 30% faster. These results predicted a shorter period of recovery time subsequent to instrument shank-assisted OHE.

The postoperative acute-phase response develops faster in dogs compared to humans. Tissue damage and pain after invasive surgery are associated with a rise in blood acute-phase proteins, primarily CRP, which may be a valuable diagnostic biological marker of early postoperative complications (114, 115). The CRP, a sensitive biomarker of infection (116), inflammation, and tissue damage (46), is more sensitive than serum cortisol (81) in detecting surgical trauma (13) and can assess various surgical procedures in dogs (33, 117), peaking 24 h postoperatively (42). The short half-life of canine CRP (19 h) makes it a useful marker for identifying the intensity of mild clinical stressors (33, 118, 119) whose effects dissipate more rapidly.

It has been stated earlier that the slope of changes is a reliable predictor variable for the expected peak (13). A five-fold smoother slope in the elevation of CRP concentration generated a milder peak after instrument shank-assisted ovariohysterectomy, so its return level to the base value showed a significant reduction at T48 compared to that of the animals in the opposite group. Thus, it is suggested that future research on the slope of the post-OHE CRP increase would also be planned to reduce study duration and be used for designing and scheduling postoperative analgesia protocols and lengths. As CRP is ele-

Tabla de contenido:

vated approximately 6 h after a single stimulation (119), the present data revealed that there is no clinical necessity for sampling before 6 h after surgery. Moreover, because serum concentration peaks between 24 and 48 h in dogs (42, 115, 119), and CRP has a short half-life (33, 118, 119), the last measurement time of 72 h after surgery was appropriate for CRP return.

It has been imagined that OVE can satisfy surgeons' hopes by reducing the consequences of OHE. Moldal et al. did not find any differences in the levels of CRP, glucose, or iron in the blood between them. Therefore, the greatest trauma in OHE occurs during the surgeon's manipulation of the ovarian pedicle (86). Thereby, the instrument shank-assisted method's unique characteristic can be considered an advantage. By reducing manipulation of the ovarian pedicle through eliminating digital strumming, the surgical trauma has also been reduced to a level close to the lowest expected minimum. Experienced surgeons have the advantage of avoiding unnecessary organ manipulation (26, 27), which causes minimal surgical trauma and postoperative serum CRP concentration. Hence, the present modified technique, which entails less organ touch, presents surgical quality closer to that of an experienced surgeon.

It is not without merit to state that CRP concentrations seem to be a decent predictor of how invasive an operation is (120), despite some contradictory reports, such as that there is no correlation between the length of surgery and CRP, despite its rise (121), or that CRP concentrations may not be significant in the diagnosis of a disease (118). In the present study, the return to baseline after a moderate rise in CRP levels utilizing the instrument shank-assisted OHE, as contrasted to the conventional group's high CRP levels, suggests that the instrument shank-assisted OHE could be concluded as having a minor invasive nature.

The risk of infection is increased when abnormal CRP responses are seen 5 or 7 days following surgery (116). A progressive decrease in serum CRP content in both groups could indicate the absence of infection. It is not unlikely that a procedure requiring fundamentally less organ manipulation would result in improved recovery, but ultimate healing was not the focus of this study.

Finally, the pattern of CRP changes followed the pain charts without correlation, according to the data. So, at least when the surgery is minor, there may not be a statistical correlation between changes in the CRP and pain. This may be because of the wide range of its reported changes. In this instance, the CRP profile may be able to anticipate pain patterns, but it cannot be used to make statistical conclusions.

The CRP changes showed that OVE and other similar procedures cannot be the final solution to animal comfort, and modification of the surgical technique on the more severe parts of the surgery is necessary, whether it is the method proposed in the current study or other solutions that may be introduced later. Although the graphs of CRP and pain changes appear similar, establishing a definitive relationship or statistically significant correlation between them requires further research.

5. Conclusion

The current study supported the practicability of a single-person ovariohysterectomy in deep-chested adult mixed-breed dogs without tearing the suspensory ligament, along with a reduction in surgical length, CRP, and pain. On the basis of the results, there are still questions regarding the efficiency of using serum CRP concentration as an alternative pain assessment indicator.

6. Limitations and future research

Future studies evaluating physiological values, pain, the amounts of analgesics and anesthetics consumed during the operation, hemorrhage, heat loss, instrument handling errors, wound size, and more tissue handling can help de-

termine the surgical technique more precisely. Intraoperative evaluations need an up-to-date drug anesthesia protocol, which was not available in this study because certain nonsteroidal anti-inflammatory drugs were not available in the area and veterinarians were not allowed to use opioids or isoflurane. Further research will be needed to compare the performance of surgeons with varying degrees of expertise and animals of varying ages, making it more difficult to generalize the findings.

Data availability statement

The original contributions presented in the study are included in the article/Supplementary material, further inquiries can be directed to the corresponding author.

Ethics statement

The animal study was approved by Iranian biomedical research ethics committee IR.IAU.BABOL.REC.1399.004, IR.IAU.BABOL.REC.1399.015, and IR.IAU.BABOL.REC.1399.093. The study was conducted in accordance with the local legislation and institutional requirements.

Author contributions

NZ: idea, project design, project implementation, statistical analysis, drawing illustrations manually, article writing, article translation, translation editing, and final proofing. SM: project design, project implementation, digitizing Illustrations, article writing, article translation, and translation editing. AB: project design, project implementation, article writing. NN: project design, project implementation, translation editing. SF: project implementation. All authors contributed to manuscript revision, read, and approved the submitted version.

Funding

This study conducted as a self-funded project.

Acknowledgments

This manuscript was based on three approved dissertations at Islamic Azad University, Babol Branch, with registration numbers 15629206292865313981241 73 (method development) (48), 15629206292865313991623029 42 (postoperative pain) (49), and 15629206292865313981650 22 (postoperative serum-CRP) (50), authored by SM, AB, and SF, respectively. We are grateful for Iraj Nowrouzian's help and insightful suggestions. Mr. Mousavi-Kiasary S.H. is thanked for supplying the resources for these dissertations. The authors would like to thank Farshad Rajabi and Mohammadreza Abdullahzadeh-Delavari, who assisted us in the early planning stage prior to the start of the study. Particular appreciation is extended to the Adib Veterinary Surgical Center (AVSC) for providing equipment and facilities.

Conflict of interest

The correspondence supplied the idea of instrument shank-assisted OHE. This technique has been registered with the Patent Office-Real Estate Registration Organization of Iran under application number 140050140003000955, date of registration: 2021-04-25, patent number: 107195, date of patent: 2022-06-12, YEKTA identifier: 140150340003001229, verification code: 216204. Thereby, by releasing this article, the authors consider just the rights to intellectual property to be theirs.

The authors declare that the research was conducted in the absence of any commercial or financial relationships that could be construed as a potential conflict of interest.

Tabla de contenido:

Publisher's note

All claims expressed in this article are solely those of the authors and do not necessarily represent those of their affiliated organizations, or those of the publisher, the editors and the reviewers. Any product that may be evaluated in this article, or claim that may be made by its manufacturer, is not guaranteed or endorsed by the publisher.

Supplementary material

The Supplementary material for this article can be found online at: https://www.frontiersin.org/articles/10.3389/fvets.2023.1210089/full#supplementary-material

References

1. MacPhail, C, and Fossum, TW. Surgery of the reproductive and genital systems In: TW Fossum, editor. Small animal surgery. Philadelphia, Pennsylvania, USA: Elsevier Health Sciences (2018). 720–87.
2. Berzon, J. Complications of elective ovariohysterectomies in the dog and cat at a teaching institution: clinical review of 853 cases. Vet Surg. (1979) 8:89–91. doi: 10.1111/j.1532-950X.1979.tb00615.x
3. Pearson, H. The complications of ovariohysterectomy in the bitch. J Small Anim Pract. (1973) 14:257–66. doi: 10.1111/j.1748-5827.1973.tb06457.x
4. Freeman, LJ, Rahmani, EY, Sherman, S, Chiorean, MV, Selzer, DJ, Constable, PD, et al. Oophorectomy by natural orifice transluminal endoscopic surgery: feasibility study in dogs. Gastrointest Endosc. (2009) 69:1321–32. doi: 10.1016/j.gie.2008.10.028
5. Höglund, O, Olsson, K, Hagman, R, Öhlund, M, Olsson, U, and Lagerstedt, A-S. Comparison of Haemodynamic changes during two surgical methods for neutering female dogs. Res Vet Sci. (2011) 91:159–63. doi: 10.1016/j.rvsc.2010.08.013
6. Hansen, BD. Assessment of pain in dogs: veterinary clinical studies. ILAR J. (2003) 44:197–205. doi: 10.1093/ilar.44.3.197
7. Burrow, R, Batchelor, D, and Cripps, P. Complications observed during and after ovariohysterectomy of 142 bitches at a veterinary teaching hospital. Vet Rec. (2005) 157:829–33. doi: 10.1136/vr.157.26.829
8. Freeman, LJ, Rahmani, EY, Al-Haddad, M, Sherman, S, Chiorean, MV, Selzer, DJ, et al. Comparison of pain and postoperative stress in dogs undergoing natural orifice transluminal endoscopic surgery, laparoscopic, and open oophorectomy. Gastrointest Endosc. (2010) 72:373–80. doi: 10.1016/j.gie.2010.01.066
9. Fransson, BA, Lagerstedt, AS, Bergstrom, A, Hagman, R, Park, JS, Chew, BP, et al. C-reactive protein, tumor necrosis factor A, and Interleukin-6 in dogs with Pyometra and sirs. J Vet Emerg Crit Care. (2007) 17:373–81. doi: 10.1111/j.1476-4431.2006.00203.x
10. Bowlt, K, Murray, J, Herbert, G, Delisser, P, Ford-Fennah, V, Murrell, J, et al. Evaluation of the expectations, learning and competencies of surgical skills by undergraduate veterinary students performing canine ovariohysterectomies. J Small Anim Pract. (2011) 52:587–94. doi: 10.1111/j.1748-5827.2011.01120.x
11. Shivley, JM, Richardson, JM, Woodruff, KA, Brookshire, WC, Meyer, RE, and Smith, DR. Sharp transection of the suspensory ligament as an alternative to digital strumming during canine ovariohysterectomy. Vet Surg. (2019) 48:216–21. doi: 10.1111/vsu.13121
12. Devitt, CM, Cox, RE, and Hailey, JJ. Duration, complications, stress, and pain of open ovariohysterectomy versus a simple method of laparoscopic-assisted ovariohysterectomy in dogs. J Am Vet Med Assoc. (2005) 227:921–7. doi: 10.2460/javma.2005.227.921
13. Michelsen, J, Heller, J, Wills, F, and Noble, G. Effect of surgeon experience on postoperative plasma cortisol and C-reactive protein concentrations after ovariohysterectomy in the dog: a randomised trial. Aust Vet J. (2012) 90:474a–4478a. doi: 10.1111/j.1751-0813.2012.01013.x
14. Tsai, TY, Chang, SK, Chou, PY, and Yeh, LS. Comparison of postoperative effects between lidocaine infusion, meloxicam, and their combination in dogs undergoing ovariohysterectomy. Vet Anaesth Analg. (2013) 40:615–22. doi: 10.1111/vaa.12064

Tabla de contenido:

15. Campagnol, D, Teixeira-Neto, FJ, Monteiro, ER, Restitutti, F, and Minto, BW. Effect of intraperitoneal or incisional bupivacaine on pain and the analgesic requirement after ovariohysterectomy in dogs. Vet Anaesth Analg. (2012) 39:426–30. doi: 10.1111/j.1467-2995.2012.00728.x
16. Merskey, H, and Watson, G. The lateralisation of pain. Pain. (1979) 7:271–80. doi: 10.1016/0304-3959(79)90084-8
17. Morton, DB, and Griffiths, P. Guidelines on the recognition of pain, distress and discomfort in experimental animals and an hypothesis for assessment. Vet Rec. (1985) 116:431–6. doi: 10.1136/vr.116.16.431
18. Robertson, S, Taylor, P, Lascelles, B, and Dixon, M. Changes in thermal threshold response in eight cats after Administration of Buprenorphine, Butorphanol and morphine. Vet Rec. (2003) 153:462–5. doi: 10.1136/vr.153.15.462
19. Desborough, JP. The stress response to trauma and surgery. Br J Anaesth. (2000) 85:109–17. doi: 10.1093/bja/85.1.109
20. Hernández-Avalos, I, Flores-Gasca, E, Mota-Rojas, D, Casas-Alvarado, A, Miranda-Cortés, AE, and Domínguez-Oliva, A. Neurobiology of anesthetic-surgical stress and induced behavioral changes in dogs and cats: a review. Vet World. (2021) 14:393–404. doi: 10.14202/vetworld.2021.393-404
21. Goldberg, ME, and Shaffran, N. Pain Management for Veterinary Technicians and Nurses. Philadelphia, Pennsylvania, USA: John Wiley & Sons (2014).
22. Grisneaux, E, Pibarot, P, Dupuis, J, and Blais, D. Comparison of Ketoprofen and Carprofen administered prior to orthopedic surgery for control of postoperative pain in dogs. American Veterinary Medical Association (1999).
23. Hoffman, BM, Coons, MJ, and Kuo, PC. Personality differences between surgery residents, nonsurgery residents, and medical students. Surgery. (2010) 148:187–93. doi: 10.1016/j.surg.2010.04.005
24. Pfandler, M, Stefan, P, Mehren, C, Lazarovici, M, and Weigl, M. Technical and nontechnical skills in surgery: a simulated operating room environment study. Spine. (2019) 44:E1396–400. doi: 10.1097/brs.0000000000003154
25. Sadideen, H, Alvand, A, Saadeddin, M, and Kneebone, R. Surgical experts: born or made? Int J Surg. (2013) 11:773–8. doi: 10.1016/j.ijsu.2013.07.001
26. Hatala, R, Cook, DA, Brydges, R, and Hawkins, R. Constructing a validity argument for the objective structured assessment of technical skills (Osats): a systematic review of validity evidence. Adv Health Sci Educ Theory Pract. (2015) 20:1149–75. doi: 10.1007/s10459-015-9593-1
27. Niitsu, H, Hirabayashi, N, Yoshimitsu, M, Mimura, T, Taomoto, J, Sugiyama, Y, et al. Using the objective structured assessment of technical skills (Osats) global rating scale to evaluate the skills of surgical trainees in the operating room. Surg Today. (2013) 43:271–5. doi: 10.1007/s00595-012-0313-7
28. Brun, MV, Silva, MA, Mariano, MB, Motta, AC, Colomé, LM, Feranti, JP, et al. Ovariohysterectomy in a dog by a hybrid notes technique. Can Vet J. (2011) 52:637–40.
29. PubMed Abstract | 29. Pukacz, M, Kienzle, B, and Braun, J. Simple, minimally invasive technique for ovariohysterectomy in the dog. Vet Rec. (2009) 165:688–90. doi: 10.1136/vr.165.23.688
30. Mich, PM, Hellyer, PW, Kogan, L, and Schoenfeld-Tacher, R. Effects of a pilot training program on veterinary Students' pain knowledge, attitude, and assessment skills. J Vet Med Educ. (2010) 37:358–68. doi: 10.3138/jvme.37.4.358
31. Capner, A, Lascelles, B, and Waterman-Pearson, A. Current British veterinary attitudes to perioperative analgesia for dogs. Vet Rec. (1999) 145:95–9. doi: 10.1136/vr.145.4.95
32. Hernandez-Avalos, I, Mota-Rojas, D, Mora-Medina, P, Martínez-Burnes, J, Casas Alvarado, A, Verduzco-Mendoza, A, et al. Review of different methods used for clinical recognition and assessment of pain in dogs and cats. Int J Vet Sci Med. (2019) 7:43–54. doi: 10.1080/23144599.2019.1680044
33. Moldal, ER, Kjelgaard-Hansen, MJ, Peeters, ME, Nødtvedt, A, and Kirpensteijn, J. C-reactive protein, glucose and Iron concentrations are significantly altered in dogs undergoing open ovariohysterectomy or ovariectomy. Acta Vet Scand. (2018) 60:32. doi: 10.1186/s13028-018-0384-6
34. Donati, A, Ruzzi, M, Adrario, E, Pelaia, P, Coluzzi, F, Gabbanelli, V, et al. A new and feasible model for predicting operative risk. Br J Anaesth. (2004) 93:393–9. doi: 10.1093/bja/aeh210
35. Höglund, OV, Hagman, R, and Stridsberg, M. Chromogranin a and cortisol at intraoperative repeated noxious stimuli: surgical stress in a dog model. SAGE Open Med. (2015) 3:2050312115576432. doi: 10.1177/2050312115576432

Tabla de contenido:

36. Prete, A, Yan, Q, Al-Tarrah, K, Akturk, HK, Prokop, LJ, Alahdab, F, et al. The cortisol stress response induced by surgery: a systematic review and Meta-analysis. Clin Endocrinol. (2018) 89:554–67. doi: 10.1111/cen.13820
37. Cusack, B, and Buggy, DJ. Anaesthesia, analgesia, and the surgical stress response. BJA Educ. (2020) 20:321–8. doi: 10.1016/j.bjae.2020.04.006
38. Anand, K. The stress response to surgical trauma: from physiological basis to therapeutic implications. Prog Food Nutr Sci. (1986) 10:67–132.
39. PubMed Abstract | 39. Burton, D, Nicholson, G, and Hall, G. Endocrine and metabolic response to surgery. Cont Educ Anaesth Crit Care Pain. (2004) 4:144–7. doi: 10.1093/bjaceaccp/mkh040
40. Radunovic, M, Radunovic, M, Radunovic, M, Lazovic, R, Panic, N, and Bulajiic, M. Biohumoral and endocrine parameters in assessment of surgical trauma in open and laparoscopic cholecystectomy. Vojnosanit Pregl. (2013) 70:555–60. doi: 10.2298/vsp1306555r
41. James, K. Interactions between cytokines and A2-macroglobulin. Immunol Today. (1990) 11:163–6. doi: 10.1016/0167-5699(90)90067-J
42. Christensen, MB, Eriksen, T, and Kjelgaard-Hansen, M. C-reactive protein: quantitative marker of surgical trauma and post-surgical complications in dogs: a systematic review. Acta Vet Scand. (2015) 57:71. doi: 10.1186/s13028-015-0164-5
43. Wirtz, DC, Heller, KD, Miltner, O, Zilkens, KW, and Wolff, JM. Interleukin-6: a potential inflammatory marker after total joint replacement. Int Orthop. (2000) 24:194–6. doi: 10.1007/s002640000136
44. Reid, J, Scott, M, and Nolan, A. Pain assessment in companion animals: an update. In Pract. (2017) 39:446–51. doi: 10.1136/inp.j4513
45. Reid, J, Nolan, A, Hughes, J, Lascelles, D, Pawson, P, and Scott, E. Development of the short-form Glasgow composite measure pain scale (CMPS-SF) and derivation of an analgesic intervention score. J Appl Anim Welf Sci. (2007) 16:97–104. doi: 10.1017/S096272860003178X
46. Stahl, WM. Acute phase protein response to tissue injury. Crit Care Med. (1987) 15:545–50. doi: 10.1097/00003246-198706000-00001
47. Bradbury, G, and Morton, K. Using Behavioural science to improve pain management. In Pract. (2017) 39:339–41. doi: 10.1136/inp.j3251
48. Mousavi-Kiasary, SMS. Shank-assisted ovariohysterectomy in deep-chested mixed breed dogs [original research]. Babol: Babol Branch, Islamic Azad University (2020).
49. Behzadi, A. Qualitative evaluation of postoperative pain in shank-assisted ovariohysterectomized dogs compared to the conventional method [original research]. Babol: Babol Branch, Islamic Azad University (2021).
50. Mahmoodi-Ferdowsi, S. Evaluation of serum CRP changes in shank-assisted ovariohysterectomy dogs compared to the conventional method [original research]. Babol: Babol Branch, Islamic Azad University (2020).
51. Tomlinson, T. How to be fair, and power research? Select patients by flipping a coin. Am J Bioeth. (2020) 20:29–31. doi: 10.1080/15265161.2020.1795534
52. Schulz, KF, and Grimes, DA. Generation of allocation sequences in randomised trials: chance, not choice. Lancet. (2002) 359:515–9. doi: 10.1016/S0140-6736(02)07683-3
53. Brewin, CR, and Bradley, C. Patient preferences and randomised clinical trials. BMJ. (1989) 299:313–5. doi: 10.1136/bmj.299.6694.313
54. AHo, D. ASA physical status classification system. American Society of Anesthesiologists. (2018).
55. Höglund, OV, Hagman, R, Olsson, K, Olsson, U, and Lagerstedt, A-S. Intraoperative changes in blood pressure, heart rate, plasma vasopressin, and urinary noradrenalin during elective ovariohysterectomy in dogs: repeatability at removal of the 1st and 2nd ovary. Vet Surg. (2014) 43:852–9. doi: 10.1111/j.1532-950X.2014.12264.x
56. Höglund, OV, Lövebrant, J, Olsson, U, and Höglund, K. Blood pressure and heart rate during ovariohysterectomy in Pyometra and control dogs: a preliminary investigation. Acta Vet Scand. (2016) 58:80. doi: 10.1186/s13028-016-0263-y
57. Harris, KP, Adams, VJ, Fordyce, P, and Ladlow, J. Comparison of surgical duration of canine Ovariectomy and ovariohysterectomy in a veterinary teaching hospital. J Small Anim Pract. (2013) 54:579–83. doi: 10.1111/jsap.12147
58. Peeters, ME, and Kirpensteijn, J. Comparison of surgical variables and short-term postoperative complications in healthy dogs undergoing ovariohysterectomy or ovariectomy. J Am Vet Med Assoc. (2011) 238:189–94. doi: 10.2460/javma.238.2.189

Tabla de contenido:

59. Mathews, K, Kronen, PW, Lascelles, D, Nolan, A, Robertson, S, Steagall, PV, et al. Guidelines for recognition, assessment and treatment of pain: WSAVA global pain council members and co-authors of this document. J Small Anim Pract. (2014) 55:E10–68. doi: 10.1111/jsap.12200

60. Holton, L, Pawson, P, Nolan, A, Reid, J, and Scott, E. Development of a behaviour-based scale to measure acute pain in dogs. Vet Rec. (2001) 148:525–31. doi: 10.1136/vr.148.17.525

61. Firth, AM, and Haldane, SL. Development of a scale to evaluate postoperative pain in dogs. J Am Vet Med Assoc. (1999) 214:651–9.

PubMed Abstract | 62. Holton, L, Scott, E, Nolan, A, Reid, J, and Welsh, E. Relationship between physiological factors and clinical pain in dogs scored using a numerical rating scale. J Small Anim Pract. (1998) 39:469–74. doi: 10.1111/j.1748-5827.1998.tb03681.x

63. Allegranzi, B, Zayed, B, Bischoff, P, Kubilay, NZ, de Jonge, S, de Vries, F, et al. New who recommendations on intraoperative and postoperative measures for surgical site infection prevention: an evidence-based global perspective. Lancet Infect Dis. (2016) 16:e288–303. doi: 10.1016/S1473-3099(16)30402-9

64. Schober, P, Boer, C, and Schwarte, LA. Correlation coefficients: appropriate use and interpretation. Anesth Analg. (2018) 126:1763–8. doi: 10.1213/ANE.0000000000002864

65. Van Goethem, BS-OA, and Kirpensteijn, J. Making a rational choice between ovariectomy and ovariohysterectomy in the dog: a discussion of the benefits of either technique. Vet Surg. (2006) 35:136–43. doi: 10.1111/j.1532-950X.2006.00124.x

66. Hill, LN, and Smeak, DD. Suspensory ligament rupture technique during ovariohysterectomy in small animals. Compendium. (2010) 32:E1–7.

67. Anton, NE, Athanasiadis, DI, Karipidis, T, Keen, AY, Karim, A, Cha, J, et al. Surgeon stress negatively affects their non-technical skills in the operating room. Am J Surg. (2021) 222:1154–7. doi: 10.1016/j.amjsurg.2021.01.035

68. Rodriguez, FR, Kirby, BM, and Ryan, J. Evaluation of factors associated with retained surgical sponges in veterinary patients: a survey of veterinary practitioners. J Small Anim Pract. (2018) 59:570–7. doi: 10.1111/jsap.12873

69. Braungart, MM, Braungart, RG, and Gramet, P. Applying learning theories to healthcare practice. Jones and Bartlett Learning (2003).

70. Freeman, LJ, Ferguson, N, Fellenstein, C, Johnson, R, and Constable, PD. Evaluation of learning curves for ovariohysterectomy of dogs and cats and castration of dogs. J Am Vet Med Assoc. (2017) 251:322–32. doi: 10.2460/javma.251.3.322

71. Shaver, SL, Larrosa, M, and Hofmeister, EH. Factors affecting the duration of anesthesia and surgery of canine and feline Gonadectomies performed by veterinary students in a year-long preclinical surgery laboratory. Vet Surg. (2019) 48:352–9. doi: 10.1111/vsu.13163

72. Stulberg, JJ, Huang, R, Kreutzer, L, Ban, K, Champagne, BJ, Steele, SR, et al. Association between surgeon technical skills and patient outcomes. JAMA Surg. (2020) 155:960–8. doi: 10.1001/jamasurg.2020.3007

73. Ericsson, KA. Deliberate practice and the acquisition and maintenance of expert performance in medicine and related domains. Acad Med. (2004) 79:S70–81. doi: 10.1097/00001888-200410001-00022

74. Giannoudis, PV, Dinopoulos, H, Chalidis, B, and Hall, GM. Surgical stress response. Injury. (2006) 37:S3–9. doi: 10.1016/S0020-1383(07)70005-0

75. Engelmann, C, Schneider, M, Kirschbaum, C, Grote, G, Dingemann, J, Schoof, S, et al. Effects of intraoperative breaks on mental and somatic operator fatigue: a randomized clinical trial. Surg Endosc. (2011) 25:1245–50. doi: 10.1007/s00464-010-1350-1

76. Slack, P, Coulson, C, Ma, X, Webster, K, and Proops, D. The effect of operating time on Surgeons' muscular fatigue. Ann R Coll Surg Engl. (2008) 90:651–7. doi: 10.1308/003588408X321710

77. Haga, Y, Ikei, S, and Ogawa, M. Estimation of physiologic ability and surgical stress (E-pass) as a new prediction scoring system for postoperative morbidity and mortality following elective gastrointestinal surgery. Surg Today. (1999) 29:219–25. doi: 10.1007/BF02483010

78. Gillespie, BM, Chaboyer, W, and Fairweather, N. Factors that influence the expected length of operation: results of a prospective study. BMJ Qual Saf. (2012) 21:3–12. doi: 10.1136/bmjqs-2011-000169

79. Tallant, A, Ambros, B, Freire, C, and Sakals, S. Comparison of intraoperative and postoperative pain during canine ovariohysterectomy and ovariectomy. Can Vet J. (2016) 57:741–6.

Tabla de contenido:

PubMed Abstract | 80. Reid, J, Scott, M, Nolan, A, and Wiseman-Orr, L. Pain assessment in animals. In Pract. (2013) 35:51–6. doi: 10.1136/inp.f631

81. Hansen, BD, Hardie, EM, and Carroll, GS. Physiological measurements after ovariohysterectomy in dogs: what's normal? Appl Anim Behav Sci. (1997) 51:101–9. doi: 10.1016/S0168-1591(96)01079-9

82. Guillot, M, Rialland, P, Nadeau, MÈ, Del Castillo, J, Gauvin, D, and Troncy, E. Pain induced by a minor medical procedure (bone marrow aspiration) in dogs: comparison of pain scales in a pilot study. J Vet Intern Med. (2011) 25:1050–6. doi: 10.1111/j.1939-1676.2011.00786.x

83. Fajt, VR, Wagner, SA, and Norby, B. Analgesic drug administration and attitudes about analgesia in cattle among bovine practitioners in the United States. J Am Vet Med Assoc. (2011) 238:755–67. doi: 10.2460/javma.238.6.755

84. Gerbershagen, HJ, Aduckathil, S, van Wijck, AJM, Peelen, LM, Kalkman, CJ, and Meissner, W. Pain intensity on the first day after surgery: a prospective cohort study comparing 179 surgical procedures. Anesthesiology. (2013) 118:934–44. doi: 10.1097/ALN.0b013e31828866b3

85. Crompton, S. Reviewing pain assessment and scoring models in cats and dogs–part one. Vet Times. (2014) 14:15–8.

86. Horta, RS, Figueiredo, MS, Lavalle, GE, Costa, MP, Cunha, RMC, and Araújo, RB. Surgical stress and postoperative complications related to regional and radical mastectomy in dogs. Acta Vet Scand. (2015) 57:34. doi: 10.1186/s13028-015-0121-3

87. Cohen, FL. Postsurgical pain relief: Patients' status and Nurses' medication choices. Pain. (1980) 9:265–74. doi: 10.1016/0304-3959(80)90013-5

88. Peters, CL, Shirley, B, and Erickson, J. The effect of a new multimodal perioperative anesthetic regimen on postoperative pain, side effects, rehabilitation, and length of hospital stay after Total joint arthroplasty. J Arthroplast. (2006) 21:132–8. doi: 10.1016/j.arth.2006.04.017

89. Kehlet, H, and Dahl, JB. The value of "multimodal" or "balanced analgesia" in postoperative pain treatment. Anesth Analg. (1993) 77:1048–56. doi: 10.1213/00000539-199311000-00030

90. Filos, KS, and Lehmann, KA. Current concepts and practice in postoperative pain management: need for a change? Eur Surg Res. (1999) 31:97–107. doi: 10.1159/000008627

91. Ong, CK-S, Lirk, P, Seymour, RA, and Jenkins, BJ. The efficacy of preemptive analgesia for acute postoperative pain management: a meta-analysis. Anesth Analg. (2005) 100:757–73. doi: 10.1213/01.Ane.0000144428.98767.0e

92. Garimella, V, and Cellini, C. Postoperative pain control. Clin Colon Rectal Surg. (2013) 26:191–6. doi: 10.1055/s-0033-1351138

93. Lovich-Sapola, J, Smith, CE, and Brandt, CP. Postoperative pain control. Surg Clin. (2015) 95:301–18. doi: 10.1016/j.suc.2014.10.002

94. Dumville, JC, Gray, TA, Walter, CJ, Sharp, CA, Page, T, Macefield, R, et al. Dressings for the prevention of surgical site infection. Cochrane Database Syst Rev. (2016) 12:CD003091. doi: 10.1002/14651858.CD003091.pub4

95. Welsh, EM, Nolan, AM, and Reid, J. Beneficial effects of administering Carprofen before surgery in dogs. Vet Rec. (1997) 141:251–3. doi: 10.1136/vr.141.10.251

96. Lascelles, BD, Cripps, PJ, Jones, A, and Waterman-Pearson, AE. Efficacy and kinetics of Carprofen, administered preoperatively or postoperatively, for the prevention of pain in dogs undergoing ovariohysterectomy. Vet Surg. (1998) 27:568–82. doi: 10.1111/j.1532-950x.1998.tb00533.x

97. Riviere, JE, and Papich, MG. Veterinary pharmacology and therapeutics. Philadelphia, Pennsylvania, USA: John Wiley & Sons (2018).

98. Cagnardi, P, Zonca, A, Gallo, M, Villa, R, Carli, S, Beccaglia, M, et al. Pharmacokinetics and perioperative efficacy of intravenous ketorolac in dogs. J Vet Pharmacol Ther. (2013) 36:603–8. doi: 10.1111/jvp.12044

99. Papich, M. Papich mg Papich handbook of veterinary drugs. Philadelphia, Pennsylvania, USA: WB Saunders (2021).

100. Moaddel, R, Sanghvi, M, Ramamoorthy, A, Jozwiak, K, Singh, N, Green, C, et al. Subchronic administration of (R, S)-ketamine induces ketamine ring hydroxylation in Wistar rats. J Pharm Biomed Anal. (2016) 127:3–8. doi: 10.1016/j.jpba.2016.03.030

101. Hommeril, J-L, Bernard, J-M, Gouin, F, and Pinaud, M. Ketoprofen for pain after hip and knee arthroplasty. Br J Anaesth. (1994) 72:383–7. doi: 10.1093/bja/72.4.383

102. Mathews, KA, Pettifer, G, Foster, R, and McDonell, W. Safety and efficacy of preoperative Administration of Meloxicam, compared with that of Ketoprofen and Butorphanol in dogs undergoing abdominal surgery. Am J Vet Res. (2001) 62:882–8. doi: 10.2460/ajvr.2001.62.882

103. Slingsby, LS, and Waterman-Pearson, A. Postoperative analgesia in the cat after ovariohysterectomy by use of Carprofen, Ketoprofen, meloxicam or Tolfenamic acid. J Small Anim Pract. (2000) 41:447–50. doi: 10.1111/j.1748-5827.2000.tb03139.x

104. Rugytė, D, and Gudaitytė, J. Intravenous paracetamol in adjunct to intravenous Ketoprofen for postoperative pain in children undergoing general surgery: a double-blinded randomized study. Medicina. (2019) 55:86. doi: 10.3390/medicina55040086

105. Mathews, KA, Paley, DM, Foster, RA, Valliant, AE, and Young, SS. A comparison of ketorolac with Flunixin, Butorphanol, and Oxymorphone in controlling postoperative pain in dogs. Can Vet J. (1996) 37:557.

106. Hanson, PD, and Maddison, JE. Nonsteroidal anti-inflammatory drugs and Chondroprotective agents. Small Anim Clin Pharmacol. (2008) 5:287. doi: 10.1016/B978-070202858-8.50015-4

107. Mansour, C, Merlin, T, Bonnet-Garin, J-M, Chaaya, R, Mocci, R, Ruiz, CC, et al. Evaluation of the parasympathetic tone activity (PTA) index to assess the analgesia/nociception balance in anaesthetised dogs. Res Vet Sci. (2017) 115:271–7. doi: 10.1016/j.rvsc.2017.05.009

108. Hernández-Avalos, I, Valverde, A, Ibancovichi-Camarillo, JA, Sánchez-Aparicio, P, Recillas-Morales, S, Rodríguez-Velázquez, D, et al. Clinical use of the parasympathetic tone activity index as a measurement of postoperative analgaesia in dogs undergoing ovariohysterectomy. J Vet Res. (2021) 65:117–23. doi: 10.2478/jvetres-2021-0004

109. Casas-Alvarado, A, Mota-Rojas, D, Hernández-Ávalos, I, Mora-Medina, P, Olmos-Hernández, A, Verduzco-Mendoza, A, et al. Advances in infrared thermography: surgical aspects, vascular changes, and pain monitoring in veterinary medicine. J Therm Biol. (2020) 92:102664. doi: 10.1016/j.jtherbio.2020.102664

110. Küls, N, Blissitt, KJ, Shaw, DJ, Schöffmann, G, and Clutton, RE. Thermography as an early predictive measurement for evaluating epidural and femoral–sciatic block success in dogs. Vet Anaesth Analg. (2017) 44:1198–207. doi: 10.1016/j.vaa.2016.11.009

111. Boev, AN, Fountas, KN, Karampelas, I, Boev, C, Machinis, TG, Feltes, C, et al. Quantitative Pupillometry: normative data in healthy pediatric volunteers. J Neurosurg Pediatr. (2005) 103:496–500. doi: 10.3171/ped.2005.103.6.0496

112. Olson, DM, Stutzman, S, Saju, C, Wilson, M, Zhao, W, and Aiyagari, V. Interrater reliability of pupillary assessments. Neurocrit Care. (2016) 24:251–7. doi: 10.1007/s12028-015-0182-1

113. Kim, J, Heo, J, Ji, D, and Kim, MS. Quantitative assessment of pupillary light reflex in normal and anesthetized dogs: a preliminary study. J Vet Med Sci. (2015) 77:475–8. doi: 10.1292/jvms.14-0387

114. Dąbrowski, R, Wawron, W, and Kostro, K. Changes in CRP, SAA and haptoglobin produced in response to ovariohysterectomy in healthy bitches and those with Pyometra. Theriogenology. (2007) 67:321–7. doi: 10.1016/j.theriogenology.2006.07.019

115. Conner, J, Eckersall, P, Ferguson, J, and Douglas, T. Acute phase response in the dog following surgical trauma. Res Vet Sci. (1988) 45:107–10. doi: 10.1016/S0034-5288(18)30902-0

116. Kang, B-U, Lee, S-H, Ahn, Y, Choi, W-C, and Choi, Y-G. Surgical site infection in spinal surgery: detection and management based on serial C-reactive protein measurements. J Neurosurg Spine. (2010) 13:158–64. doi: 10.3171/2010.3.SPINE09403

117. Kjelgaard-Hansen, M, Strom, H, Mikkelsen, LF, Eriksen, T, Jensen, AL, and Luntang-Jensen, M. Canine serum C-reactive protein as a quantitative marker of the inflammatory stimulus of aseptic elective soft tissue surgery. Vet Clin Pathol. (2013) 42:342–5. doi: 10.1111/vcp.12063

118. Malin, K, and Witkowska-Piłaszewicz, O. C-reactive protein as a diagnostic marker in dogs: a review. Animals. (2022) 12:2888. doi: 10.3390/ani12202888

119. Pepys, MB, and Hirschfield, GM. C-reactive protein: a critical update. J Clin Invest. (2003) 111:1805–12. doi: 10.1172/JCI200318921

120. Neumaier, M, Metak, G, and Scherer, MA. C-reactive protein as a parameter of surgical trauma: CRP response after different types of surgery in 349 hip fractures. Acta Orthop. (2006) 77:788–90. doi: 10.1080/17453670610013006

Tabla de contenido:

121. Tylicka, M, Matuszczak, E, Karpińska, M, Hermanowicz, A, Dębek, W, and Ostrowska, H. Proteasome and C-reactive protein inflammatory response in children undergoing shorter and longer lasting laparoscopic cholecystectomy. Scand J Clin Lab Invest. (2017) 77:610–6. doi: 10.1080/00365513.2017.1385839

Citation: Ziaei Darounkolaei N, Mousavi Kiasary SMS, Behzadi A, Nabavi Mosavi N and Ferdowsi SM (2023) Instrument shank-assisted ovariohysterectomy: a randomized clinical trial of surgical and pain alleviation efficiency of a single-person modified technique. Front. Vet. Sci. 10:1210089. doi: 10.3389/fvets.2023.1210089

Received: 21 April 2023; Accepted: 03 October 2023; Published: 17 October 2023.

Edited by: Lynette Arnason Hart, University of California, Davis, United States

Reviewed by: Ismael Hernández Avalos, National Autonomous University of Mexico, Mexico Antonio González Cantalapiedra, University of Santiago de Compostela, Spain

*Correspondence: Navid Ziaei Darounkolaei, ziaei@baboliau.ac.ir

This article is part of the Research Topic

Effective Options Regarding Spay or Neuter of Dogs

https://axoncomunicacion.net/ovariohisterectomia-asistida-por-vastago-instrumental/

Tabla de contenido:

"Hemos desarrollado nuevas dietas de nuestra gama Gastrointestinal para el manejo nutricional de problemas digestivos, que incluyen prebióticos y fórmulas altamente digestibles"

María Ángeles Toscano

Corporate Affairs Director Royal Canin

¿Qué supone para Royal Canin estar presente en la WSAVA?

La presencia de Royal Canin en este 48º Congreso pone de manifiesto, un año más, el continuo compromiso que mantenemos con los profesionales de la salud de los animales de compañía, con los que compartimos el objetivo común de contribuir a la salud y el bienestar de cada gato y cada perro.

Nos consta que hubo una zona de formación habilitada por Royal Canin con ponentes de reconocido prestigio, ¿podría decirnos cuáles fueron los temas tratados y la repercusión que tuvieron los mismos?

El espacio de Royal Canin en WSAVA 2023 contó con más de 600 visitantes, que pudieron disfrutar de distintas ponencias impartidas por profesionales como la **Dra. Jane Ladlow**, especialista en medicina veterinaria de la Universidad de Cambridge, que expuso las herramientas necesarias para evaluar el síndrome obstructivo braquiocefálico de las vías respiratorias en perros, o la **Dra. Madalfa Pires Gonçalves**, veterinaria y especialista en prevención y tratamiento del sobrepeso y la obesidad de nuestras mascotas, que compartió los pasos a seguir para la intervención precoz en cachorros y gatitos. Mafalda abordó además los diversos problemas di-

ROYAL CANIN®
INCREÍBLE EN CADA DETALLE

gestivos que se pueden dar durante el crecimiento y las pautas a seguir para la recuperación de perros y gatos con estos problemas.

Además, junto al especialista **Thierry Correia**, compartimos el compromiso de Royal Canin con el planeta y cómo nuestra contribución a la salud de perros y gatos va directamente ligada con un modelo de negocio responsable y sostenible, que abarca desde el desarrollo de nuestros alimentos hasta su distribución. En este sentido, nuestros esfuerzos se centran en ofrecer una nutrición basada en ciencia diseñada para cubrir las necesidades reales de gatos y perros, pero siempre de forma responsable con el planeta y con las personas.

¿Qué novedades presentó la compañía en la WSAVA de Lisboa?

Tuvimos la oportunidad de presentar las últimas novedades de nuestra gama Gastrointestinal para el manejo nutricional de trastornos gastrointestinales en gatos y perros. Las nuevas fórmulas de la gama Gastrointestinal, Royal Canin® Fibre Response húmedo, Royal Canin® Low Fat Small Dogs y Royal Canin® High Fibre húmedo, con nuevos formatos, han sido desarrolladas gracias a los últimos avances científicos y son un ejemplo más del compromiso con la innovación continua.

¿Cuál es el elemento diferencial de las dietas gastrointestinales de Royal Canin? ¿Qué formatos tienen?

La gama Gastrointestinal ofrece una amplia variedad de dietas para dar una respuesta nutricional a las necesidades de cada animal ante los diversos problemas digestivos. Incluye fórmulas altamente digestibles y con prebióticos para favorecer una digestión saludable, con más o menos grasa o con distinto aporte de fibra según los requerimientos en cada enfermedad. También hay que destacar que están disponibles en presentaciones seca, húmeda y también líquida para administración por sonda, para poder adaptarnos mejor a cada necesidad.

¿Cuáles son los trastornos digestivos que requieren una dieta específica?

Cuando se trata de trastornos gastrointestinales es difícil generalizar, pero sí que podemos decir que el estreñimiento en gatos, la diarrea que responde a la fibra en perros o problemas digestivos que requieren un aporte bajo de grasa precisan una formulación específica. Además, en este último caso, podemos adaptar esa dieta digestiva y con bajo aporte de grasas a las particularidades de los perros pequeños y ofrecer una respuesta a medida.

¿Qué importancia tienen los prebióticos en la dieta?

Los prebióticos integrados en las fórmulas ayudan a mantener un microbioma saludable. En toda la gama se incluyen prebióticos como beneficio común y, por supuesto, hay prebióticos integrados en los tres nuevos lanzamientos. Además, estas dietas presentan una elevada digestibilidad gracias a su formulación, la selección de materias primas y los procesos de elaboración, para favorecer una digestión saludable.

Uno de los principales compromisos de Royal Canin con el planeta es su filosofía basada en los nutrientes. ¿Podrías arrojar más luz en este sentido?

Una parte importante del compromiso que en Royal Canin mantenemos con la sostenibilidad es la integración de ésta de forma transversal en nuestro modelo de negocio. En cuanto a nuestra filosofía basada en nutrientes, en Royal Canin trabajamos para optimizar nuestras fórmulas y buscamos fuentes de nutrientes lo más sostenibles posibles sin comprometer la calidad y el rendimiento de los alimentos. Por eso cuantificamos la huella de carbono del 100% de nuestras materias primas y optamos, por ejemplo, por el uso de subproductos de alta calidad. Los subproductos son ingredientes que no se destinan al consumo humano, tendiendo a desperdiciarse (corazón, hígado, cerebro), y que son una fuente rica en nutrientes de alta calidad.

ROYAL CANIN®
INCREÍBLE EN CADA DETALLE

(R) evolution
PEQUEÑOS ANIMALES

ROYAL CANIN®

INCREÍBLE EN CADA DETALLE

POR TU EXPERIENCIA,
SABES QUE TODO LO QUE COME CUENTA

El contenido de fibra del alimento puede tener impacto en la motilidad intestinal.

ROYAL CANIN® HIGH FIBRE húmedo es una dieta rica en fibra para ayudar a regular el tránsito intestinal. Es altamente digestible, contiene prebióticos para favorecer una digestión saludable y cubre las necesidades energéticas de mantenimiento, a pesar de tener un elevado contenido en fibra.

Para obtener más información, contacta con tu representante de Royal Canin o visita:
www.royalcanin.com/es

Nuevo

LA CIENCIA AL SERVICIO DE LA SALUD DIGESTIVA

Manejo nutricional de la cardiomiopatía hipertrófica felina

Nuevos estudios apoyan un nuevo enfoque nutricional para la cardiomiopatía hipertrófica felina, cuyos resultados muestran una reducción significativa del grosor tanto del tabique interventricular como de la pared ventricular

Los veterinarios generalistas deben estar alerta y detectar signos de CMH en sus pacientes felinos

Javier Manzanares

Especialista en Comunicación Científica
Royal Canin Iberia

La cardiomiopatía hipertrófica (CMH) se define como la **hipertrofia del ventrículo izquierdo no dilatado** en ausencia de condiciones anormales de carga, resultando en una reducción del volumen de la cámara cardíaca y disfunción diastólica. Es la forma de enfermedad cardíaca más común en los gatos y se puede presentar en todas las razas, aunque en algunas existe una predisposición genética, como en el Maine Coon, Persa, Ragdoll, British Shorthair, Sphynx o Chartreux. Como factores de riesgo: gatos machos (3x vs hembras), gatos de mayor tamaño y gatos con índices de condición corporal por encima de la ideal.

Aunque se desconoce la prevalencia exacta de la enfermedad, algunos estudios recientes muestran que alcanza al 15% de la población felina y aumenta con la edad, hasta casi el 30% a partir de los nueve años.

Respecto al tratamiento de la CMH felina, hay un consenso limitado sobre el tratamiento de la CMH en gatos sobre todo en las fases subclínicas. Todo ello ha llevado a buscar respuestas realizando nuevos estudios y desarrollando un nuevo enfoque nutricional para la CMH felina.

Hipótesis de fisiopatología

La fisiopatología de la CMH sigue siendo en parte desconocida, aunque investigaciones existentes sugerían que los gatos con CMH tenían niveles más altos de la proteína factor de crecimiento similar a la insulina 1 (IGF-1) y de marcadores inflamatorios, sobre todo amiloide sérico A o SAA. A partir de esta información, se planteó la hipótesis de que la fisiopatología de la CMH es un círculo vicioso, de forma que el engrosamiento de la pared cardiaca provoca inflamación y esta, a su vez, causa más hipertrofia. Además, la insulina y el IGF-1 se combinan para promover la síntesis de proteínas en el cardiomiocito, lo que también contribuye a empeorar la hipertrofia.

A partir de estos conocimientos se realizó un estudio inicial sobre el papel de la insulina, el IGF-1 y la inflamación en los gatos con CMH. Se incluyeron 51 gatos con CMH confirmada y se evaluaron distintos valores: se observó que el NT-ProBNP, marcador del aumento del estrés cardíaco, la C-TnI (Troponina-I cardíaca), marcador de la muerte celular cardíaca, el SAA y los niveles de insulina estaban significativamente elevados en los gatos afectados en comparación con el rango de referencia. Estos niveles elevados de insulina por un lado, y los niveles aumentados de SAA por otro, reforzaban la hipótesis sobre la fisiopatología sugerida.

Nuevo enfoque nutricional

Basándose en el estudio inicial y en la investigación disponible, se propuso un nuevo alimento dietético que incluía los nutrientes hipotéticamente claves. Esta dieta se caracterizaba por estar enriquecida en EPA/DHA, con el fin de interrumpir el círculo de hipertrofia e inflamación, además de incluir un nivel reducido de carbohidratos destinado a limitar la producción de insulina en el páncreas, la combinación de esta con el IGF-1 y, por tanto, la síntesis de proteínas en el cardiomiocito. Ambas modificaciones dietéticas estaban dirigidas a reducir la hipertrofia cardiaca.

Esta dieta teórica se probó en un ensayo clínico para ver si podía alterar la progresión de la CMH que incluyó gatos asintomáticos con CMH en estadio 1B según la clasificación del Consejo Internacional de Salud Cardiaca de Pequeños Animales (ISACHC). En el estudio se permitieron medicamentos, incluidos atenolol, enalapril y clopidogrel, siempre que hubieran sido administrados durante más de ocho semanas. Se aceptaban todas las razas y se dio preferencia a los gatos de interior, ya que sería más probable que se alimentaran exclusivamente de la dieta de estudio. En relación a las exclusiones, no se in-

(R) evolution

PEQUEÑOS ANIMALES

ROYAL CANIN®
INCREÍBLE EN CADA DETALLE

cluyeron en el estudio gatos con enfermedades concurrentes, siendo la diabetes la exclusión más notable.

En cuanto al diseño del estudio, fue un estudio prospectivo, aleatorio, doble ciego y multicéntrico, que incluyó 44 gatos, asignados aleatoriamente a un grupo de control de 21 gatos y un grupo de prueba de 23 gatos. Recibieron una dieta de control o a una dieta de prueba durante 12 meses. A los 6 y 12 meses se realizaron las mismas evaluaciones.

El contenido proteico de la dieta de prueba era significativamente mayor que el de la dieta de control, al igual que los niveles de EPA/DHA. Asimismo, era significativamente más baja en contenido de almidón, con lo que se pretendía reducir los picos de insulina, limitando teóricamente la insulina disponible para unirse a la IGF-1. También era ligeramente restringida en sodio.

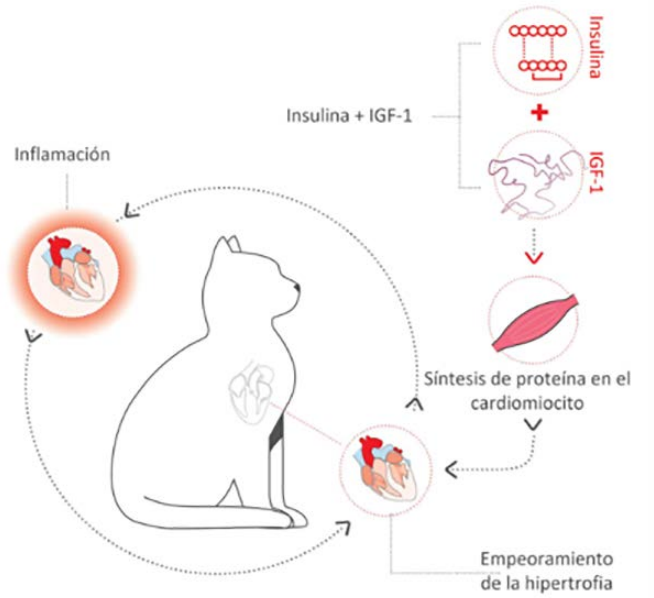

Figura 1. *Hipótesis de la fisiopatología de la CMH felina*

Los resultados mostraron una disminución significativa del grosor de la pared ventricular en diástole en el grupo que consumió la dieta de prueba que no se observó en los gatos de control. A los 12 meses el grosor de la pared estaba por debajo del umbral de 6mm (corte CMH).

Además, se produjo una reducción significativa de la Troponina-I cardíaca y de IGF-1 en el grupo de prueba (a los 6 y 12 meses respectivamente).

Conclusiones

Estos resultados apoyan el potencial de la adaptación de la dieta alta en proteína, baja en almidón y enriquecida en EPA/DHA, además del control de los niveles de sodio, en gatos con CMH.

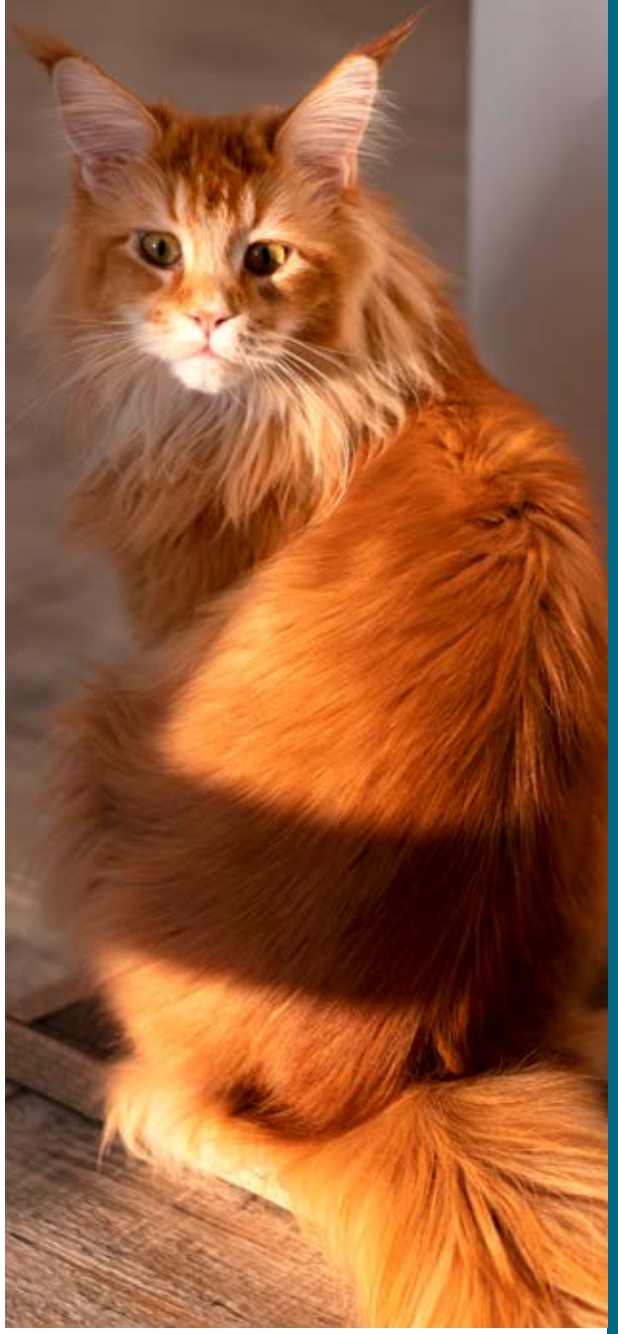

(R) evolution
PEQUEÑOS ANIMALES

ROYAL CANIN®
INCREÍBLE EN CADA DETALLE

Bibliografía

- Payne JR, Brodbelt DC, Luis Fuentes V. Cardiomyopathy prevalence in 780 apparently healthy cats in rehoming centres (the CatScan study). J Vet Cardiol. 2015 Dec;17 Suppl 1:S244-57.
- Freeman LM, Rush JE, Stern JA, Huggins GS, Maron MS. Feline Hypertrophic Cardiomyopathy: A Spontaneous Large Animal Model of Human HCM. Cardiol Res. 2017 Aug;8(4):139-142. doi: 10.14740/cr578w. Epub 2017 Aug 23. PMID: 28868097; PMCID: PMC5574284.
- Fazio S, Palmieri EA, Biondi B, Cittadini A, Saccà L. The role of the GH-IGF-I axis in the regulation of myocardial growth: from experimental models to human evidence. Eur J Endocrinol. 2000 Mar;142(3):211-6.
- Freeman LM. Beneficial effects of omega-3 fatty acids in cardiovascular disease. J Small Anim Pract. 2010 Sep;51(9):462-70.
- Freeman LM, Rush JE, Meurs KM, Bulmer BJ, Cunningham SM. Body size and metabolic differences in Maine Coon cats with and without hypertrophic cardiomyopathy. J Feline Med Surg. 2013 Feb;15(2):74-80
- Meurs KM, Fox PR, Miller MW, Kapadia S, Mann DL. Plasma concentrations of tumor necrosis factor-alpha in cats with congestive heart failure. Am J Vet Res. 2002 May;63(5):640-2.
- Payne JR, Borgeat K, Connolly DJ, Boswood A, Dennis S, Wagner T, Menaut P, Maerz I, Evans D, Simons VE, Brodbelt DC, Luis Fuentes V. Prognostic indicators in cats with hypertrophic cardiomyopathy. J Vet Intern Med. 2013 Nov-Dec;27(6):1427-36.
- Sharma N, Okere IC, Duda MK, Chess DJ, O'Shea KM, Stanley WC. Potential impact of carbohydrate and fat intake on pathological left ventricular hypertrophy. Cardiovasc Res. 2007 Jan 15;73(2):257-68.
- Wrigley BJ, Lip GY, Shantsila E. The role of monocytes and inflammation in the pathophysiology of heart failure. Eur J Heart Fail. 2011 Nov;13(11):1161-71.
- Hoek, Ingrid & Hodgkiss-Geere, Hannah & Bode, Elizabeth & Hamilton-Elliott, Julie & Mõtsküla, Paul & Palermo, Valentina & Martinez Pereira, Yolanda & Culshaw, Geoff & Ivanova, Anna & Dukes-McEwan, Joanna. (2020). Associations among echocardiography, cardiac biomarkers, insulin metabolism, morphology, and inflammation in cats with asymptomatic hypertrophic cardiomyopathy. Journal of Veterinary Internal Medicine. 34.
- Van Hoek I, Hodgkiss-Geere H, Bode EF, et al. Association of diet with left ventricular wall thickness, troponin I and IGF-1 in cats with subclinical hypertrophic cardiomyopathy. J. Vet. Intern. Med. 2020;34(6):2197-2210.

(R) evolution

PEQUEÑOS ANIMALES

ROYAL CANIN®
INCREÍBLE EN CADA DETALLE

Comparative analysis of the aberrant immunophenotype and clinical characteristics in dogs with lymphoma: a study of 27 cases

Análisis comparativo del inmunofenotipo en perros con linfoma

Keywords: *lymphoma, immunophenotyping, flow cytometry, aberrancies, dog*

Palabras clave: linfoma, inmunofenotipado, citometría de flujo, aberrancias, perro

https://www.frontiersin.org/articles/10.3389/fvets.2023.1254458/full

Hyeona Bae[1†], Sang-Ki Kim[2†], DoHyeon Yu[1*†]

1. College of Veterinary Medicine, Gyeongsang National University, Jinju, Republic of Korea
2. College of Industrial Science, Kongju National University, Yesan, Republic of Korea

Tabla de contenido:

Introducción: *Los fenotipos de linfoma aberrante se encuentran con frecuencia en perros, pero las implicaciones clínicas son escasas. Métodos: Se analizaron veintisiete perros con linfoma aberrante diagnosticado mediante citometría de flujo entre 2017 y 2023. Los síndromes paraneoplásicos mayores, los factores pronósticos y las características clínicas del linfoma se compararon con sus inmunofenotipos.*

Resultados: *Veintisiete perros tenían inmunofenotipos aberrantes, siendo MHCII- (48%) y CD3+/CD21+ (44%) las aberrancias más comúnmente identificadas. En el linfoma de células B, las aberraciones más frecuentes fueron MHC II- (53%), CD3+/CD21+ (41%), CD34+ (24%) y CD79a- (24%).*

ntroduction: Aberrant lymphoma phenotypes are frequently found in dogs, but the clinical implications are sparse.

Methods: Twenty-seven dogs with aberrant lymphoma diagnosed using flow cytometry between 2017 and 2023 were analyzed. Major paraneoplastic syndromes, prognostic factors, and clinical features of lymphoma were compared to their immunophenotypes.

Results: Twenty-seven dogs had aberrant immunophenotypes, with MHCII- (48%) and CD3+/CD21+ (44%) being the most commonly identified aberrancies. In B-cell lymphoma, the most frequent aberrancies were MHC II- (53%), CD3+/CD21+ (41%), CD34+ (24%), and CD79a- (24%). Meanwhile, in T-cell lymphoma, CD3+/CD21+ (63%), CD4-/CD8-(50%), CD5- (50%), and CD45- (50%) were the most common. The platelet–neutrophil ratio was significantly higher in the CD3+/CD21+ group than in the other groups, where either one or both markers were not expressed (55.23 ± 39.64; 18.72 ± 14.95, respectively; $p = 0.001$). Serum albumin concentration was significantly lower in the MHCII-group (2.59 g/dL, 95% CI 2.31–2.87) than in the MHCII+ group (3.06 g/dL, 95% CI 2.88–3.23; $p = 0.009$). CD34 expression showed significant correlations with cranial mediastinal mass, WHO clinical substage, and fever ($p = 0.028$, $p = 0.041$, and $p = 0.047$, respectively). MHCII expression was correlated with adverse reactions to chemotherapy, cranial mediastinal masses, and fever ($p = 0.009$, $p = 0.023$, and $p < 0.001$, respectively). No statistically significant differences in the survival period were observed for any of the phenotypic aberrancies.

Conclusion: Aberrant lymphomas are common in dogs. Some clinical prognostic factors that significantly correlate with aberrant immunophenotypes have been identified and can be applied clinically.

1. Introduction

When compared to experimental animals, naturally occurring diseases in dogs could reflect human diseases such as cancer. Studying these similarities can provide valuable insights into disease mechanisms, treatments, and potential therapeutic targets for dogs as well as humans.

Immunophenotyping plays a crucial role in the accurate diagnosis and classification of canine lymphoma, similar to human lymphoma. Despite of limited availability of commercially specific dog antibodies, a significant prognostic factor based on the immunophenotyping in canine lymphoma has been established (1–3). The immunophenotypes of lymphoma in dogs is catego-

rized according to the origin of B-and T-cells, with representative markers of CD21/CD79a and CD3/CD4/CD8 commonly used in dogs. Furthermore, various phenotypes have been identified in detail, such as CD45 in all leukocytes, CD34 in precursor hematopoietic cells, and major histocompatibility complex class II (MHCII) in antigen-presenting cells. Among these, aberrant phenotypes characterized by either increased or decreased expression of specific antigens are well established in both human and veterinary medicine (4–7). Several studies are being conducted to explore the possibility of utilizing immunophenotypes, including various aberrancies, for clinical purposes and prognosis prediction in humans (8–13).

Clinical prognostic factors such as World Health Organization (WHO) substage, mediastinal lymphadenopathy (14), and paraneoplastic syndrome (PNS) (15) have been studied in canine lymphoma, but the clinical implications of aberrant phenotypes have yet to be studied in dogs.

Thus, the aims of this study were [1] the identification of aberrant phenotypes in dogs with various types of lymphoma and [2] the investigation of associated types with the severity of clinical signs, PNS, and prognosis of the aberrant phenotypes.

2. Materials and methods

A retrospective in vitro analysis of the clinicopathological parameters and immunophenotypes of dogs with lymphoma was conducted using lymph node aspirates and peripheral whole blood samples collected at the time of diagnosis. This study was approved by the Institutional Animal Care and Committee (IACUC) GNU-230425-D0087.

Among the dogs diagnosed with lymphoma that visited Gyeongsang National University Veterinary Teaching Hospital between 2017 and 2023, 35 dogs that were immunophenotyped by flow cytometry were included in this study. The inclusion criteria were as follows: [1] dogs diagnosed with lymphoma through the following diagnostic procedures: cytology, histopathology, immunophenotyping, and clonality test (through fine needle aspiration (FNA) or a biopsy sample of enlarged lymph nodes or target lesions); [2] dogs without underlying diseases other than lymphoma that may affect hematological changes; and [3] dogs with naïve lymphoma who had not received chemotherapy prior to admission or dogs with relapsed lymphoma six months after the last chemotherapy. Both nodal and extranodal forms were included, and all dogs were staged according to the WHO staging system (16). Cytologic grading was evaluated according to the updated Kiel classification (17, 18). Histopathology and polymerase chain reaction for antigen receptor rearrangement were requested from an external laboratory (IDEXX, Westbrook, ME, United States), while cytology and immunophenotyping using flow cytometry.

The classification criteria for each lymphocyte lineage in immunophenotyping were as follows: [1] B-cell lymphoma, if the tumor cells were CD21+ (>70% of the major cells) and the T-cell marker was negative; [2] T-cell lymphoma, if the tumor cells were CD3+ (>70% of the major cells) and the B-cell marker was negative; and [3] non-B and non-T lymphomas, if the tumor cells were negative for both B-cell and T-cell markers.

Phenotypic aberrancies were defined as follows: [1] reduced or absent expression of pan-leukocyte or lymphocyte markers (CD45 and MHCII), [2] simultaneous expression of lymphocyte markers of different lineages (CD3 and CD21) or different stages of differentiation (markers of mature stage and CD34), [3] in T-cell, CD4 and CD8 markers were expressed simultaneously, or neither was expressed, [4] in B-cell, loss of CD79a, which is expressed in all maturation stages of B-cells (7, 19, 20).

At the time of diagnosis, the presence of PNS was assessed in all dogs to determine the clinical course and prognosis. The correlation between WHO substage

'b' (clinically ill), anemia, hypercalcemia, thrombocytopenia, and immunophenotype was analyzed. Survival time was defined as the period from the date of diagnosis at our hospital to the day of death due to lymphoma. Dogs that died from causes unrelated to the tumor or whose follow-up was discontinued were considered 'censored'. Treatment response was evaluated in dogs that had received chemotherapy or equivalent medication and was divided into complete remission (CR), partial remission (PR), progressive disease (PD), and stable disease (SD) according to previous literature (21).

Upon admission, laboratory examinations were performed to assess the overall clinical condition of the dogs and to detect any underlying diseases, including PNS. A complete blood count (Procyte Dx hematology analyzer, IDEXX, Westbrook, ME, United States) and blood film analysis, including platelet-to-lymphocyte ratio (PLR), platelet-to-neutrophil ratio (PNR), lymphocyte-to-monocyte ratio (LMR), and neutrophil-to-lymphocyte ratio (NLR) were performed. Acid–base balance and electrolyte concentrations (Nova pHOX analyzer, Nova Biochemical, Waltham, MA, United States), serum biochemical analysis (Catalyst Dx® Chemistry Analyzer, IDEXX, Westbrook, ME, United States), coagulation tests (Coag Dx™ analyzer with citrate PT and citrate aPTT cartridges, IDEXX), and complete urinalysis (VetLab UA Analyzer, IDEXX) were also performed. The fibrinogen levels were evaluated using the Millar's method (22).

FNA aspirates were collected from the prescapular or inguinal lymph nodes of dogs with generalized lymphadenopathy, and peripheral blood was collected to evaluate WHO staging. For cases of extranodal lymphoma, FNA aspirates were collected from regional lymph nodes suspected of involvement near the target lesions (stomach, intestinal segments, liver, spleen, and cutaneous lesions) and pleural or abdominal free fluids were also collected. All aspirates were suspended in 0.3–0.5 mL of 5% dextrose saline, and peripheral blood was collected in ethylene-diamine-tetraacetic acid tubes. All samples were analyzed within 24 h of collection by the same operator, and those with ambiguous diagnoses, low cellularity, or low viability were excluded.

The antibodies used in this study were based on previous studies (23). Multi-color flow cytometric analysis was conducted to evaluate the contemporary expression of different antigens within the same cellular population. The sample preparation and analysis method was similar to previous studies (6), with the exception that CD14-negative cells were sorted (CD14 is expressed on monocytes and macrophages), and only lymphocytes were selected using the difference in granularity and lymphocyte-specific markers. The major cells were first identified through cytology, and flow cytometric analysis was primarily performed on lymphocytes, which constituted the largest population (>60%). Lymphocytes exhibiting a tumorigenic phenotype, even at a small percentage, were also analyzed. The samples were acquired using the MACSQuant Analyzer 10 (Miltenyi Biotech, Bergisch Gladbach, Germany) and analyzed using FlowJo software version 10.8.0 (Ashland, OR, United States).

All statistical analyses (Student's t-test, Mann–Whitney U test, Fisher's exact test, and Kaplan–Meier curve) were performed using SPSS Statistics version 27.0, for Windows (SPSS Inc., Chicago, IL, United States). Clinical data on admission, including signalment, temperature, body weight, presence of abnormalities in hematological parameters, and clinical substages, were evaluated for their impact on survival time using Kaplan–Meier estimators and log-rank tests. For Fisher's exact test, clinical, clinicopathological, and immunophenotypic data were dichotomized and evaluated. The p values were two-sided and were considered significant at $p < 0.05$.

Tabla de contenido:

3. Results

3.1. Study population and prevalence of immunophenotypic aberrancies

The characteristics of the dogs included in this study are summarized in Supplementary Table S1. Among the dogs initially recruited for the study, 27 were included, all of whom showed immunophenotypic aberrancies with immunophenotyping by flow cytometry at the time of diagnosis. The mean (± standard deviation) age of 27 dogs was 9 ± 3.5 years (range, 3–15 years). The breeds included Maltese (n = 7), Mixed (n = 5), Shih-Tzu (n = 4), Golden Retriever (n = 3), Miniature Poodle (n = 2), Yorkshire Terrier (n = 1), Dogo Canario (n = 1), Dachshund (n = 1), Chihuahua (n = 1), Cocker Spaniel (n = 1), and Shiba (n = 1). The multicentric lymphoma was the most common (n = 24), followed by as an extranodal lymphoma, the alimentary (n = 1), tongue (n = 1), and liver (n = 1) forms were identified. When classified by WHO clinical stage, one was WHO stage I, two were stage III, 13 were stage IV, and 11 were stage V. Of the 27 dogs, 11 were WHO substage 'a' (asymptomatic) and 16 were substage 'b' (clinically ill).

A total of 21 dogs received chemotherapy after being diagnosed with lymphoma. Among these, 14 dogs underwent the L-CHOP protocol, three dogs were administered chlorambucil, and protocols CHOP, COP, and doxorubicin alone were applied to one dog each. Two of the dogs that received the L-CHOP protocol, died of tumor progression and were lost to follow-up immediately after chemotherapy in the first week (L-asparaginase and vincristine). One dog that was treated with chlorambucil showed a poor response and was treated with a combination of prednisolone, imatinib, and cyclophosphamide. Upon evaluation of the response after chemotherapy, five dogs with CR, six dogs with PR, four dogs with SD, and 8 with PD were identified.

On cytological examination, 12 dogs had large cells, 7 dogs had intermediate cells, and five dogs had small cells. In three dogs, intermediate and large cells were identified as heterogeneous. Among the 22 dogs that could be analyzed by the updated Kiel classification, five dogs (23%) were found to have low-grade lymphoma and 17 dogs (77%) were found to have high-grade lymphoma (Supplementary Tables S2, S3). In the low-grade lymphoma group, there were three clear cells, one prolymphocytic-like cell, and one centrocytic-like cell type. In the high-grade lymphoma group, there were seven centroblastic polymorphic (predominantly large cells), three Burkitt-type, three plasmacytoids, two pleomorphic, one centroblastic polymorphic (predominantly small cells) cell, and one anaplastic lymphoma. Of the eight dogs that could be diagnosed through histopathological and immunohistochemical methods, diffuse large B-cell lymphoma (DLBCL) was identified in five, TZL in two, and diffuse small B-cell lymphoma in one.

A total of 27 dogs were identified as having an aberrant immunophenotype (Table 1). Among the total aberrancies, MHCII- (13/27, 48%) and CD3+/CD21+ (12/27, 44%) were the most frequently identified, whereas 19% of these dogs (5/27) did not express CD3 or CD21. All 22 dogs that could be analyzed by the updated Kiel classification showed immunophenotypic aberrancies. Among the dogs that showed aberrancy, five were found have low-grade lymphoma, and 17 were found to have high-grade lymphoma, with the high-grade lymphoma group showing more immunophenotypic aberrancies. CD3+/CD21+ (4/5, 80%) and MHCII- (7/17, 41%) were the most frequently identified in low-and high-grade lymphomas, respectively. The most represented aberrancies in B-cell lymphoma were MHCII- (9/17, 53%), CD3+/CD21+ (7/17, 41%), CD34+ (4/17, 24%), CD79a- (4/17, 24%), while CD3+/CD21+ (5/8, 63%), CD4-/CD8- (4/8, 50%), CD45- (4/8, 50%), CD5- (4/8, 50%) were expressed in T-cell lymphoma. In the two cases showing the

non-B/non-T phenotype, CD3-/CD21-, CD4-/CD8-, expression of CD5, and MHCII-were confirmed at a rate of 50%. In both cases, the canine natural killer cell (NK cell) marker, NKp46, was highly expressed, suggesting NK cell-derived lymphoma.

3.2. Correlation with aberrant immunophenotype and clinicopathologic, paraneoplastic syndrome measurements

As a result of analyzing the clinical measurement in the CD3+/CD21+ group, which was identified as most frequent among the aberrant phenotypes, the PNR was significantly higher in the group identified as CD3+/CD21+ than in the other groups (either one or both were not expressed) (55.23 ± 38.52; 18.13 ± 17.12, respectively; p = 0.003), CD45-group than in CD45+ group (90.01 ± 43.30; 26.85 ± 22.66, respectively; p = 0.007). NLR was significantly lower in the CD45-group (7.45 ± 10.58; 0.47 ± 0.22; p = 0.041). The ionized calcium concentration was also significantly higher in the group identified as CD3+/CD21+ than in the other groups (1.32 mmol/L, 95% CI 1.29–1.35; 1.24 mmol/L, 95% CI 1.19–1.29, respectively; p = 0.01). Serum albumin concentration was significantly lower in the group of MHCII- (2.59 g/dL, 95% CI 2.31–2.87) than in the group of MHCII+ (3.10 g/dL, 95% CI 2.94–3.26; p = 0.005) (**Figure 1**).

When analyzing the association between phenotypic aberrancies and clinical measurements, the expression of

Aberrancy	Percentage (aberrant/tested) (%)			
	Total (*n* = 27/35)	B-cell (*n* = 17/23)	T-cell (*n* = 8/10)	Non-B & non-T-cell (*n* = 2/2)
CD3+/CD21+	12/27 (44%)	7/17 (41%)	5/8 (63%)	0/2
CD3-/CD21-	2/27 (7%)	1/17 (6%)	0/8	1/2 (50%)
CD4+/CD8+	1/27 (4%)	0/17	1/8 (13%)	0/2
CD4-/CD8-	5/27 (19%)	–	4/8 (50%)	1/2 (50%)
CD5+	–	0/17	–	1/2 (50%)
CD5-	–	–	4/8 (50%)	1/2 (50%)
CD79a-	-	4/17 (24%)	–	0/2
CD45-	4/27 (15%)	0/17	4/8 (50%)	0/2
CD34+	5/27 (19%)	4/17 (24%)	1/8 (13%)	0/2
MHCII-	13/27 (48%)	9/17 (53%)	3/8 (38%)	1/2 (50%)

MHCII, major histocompatibility complex class II.

Table 1. *Aberrant phenotype epidemiology.*

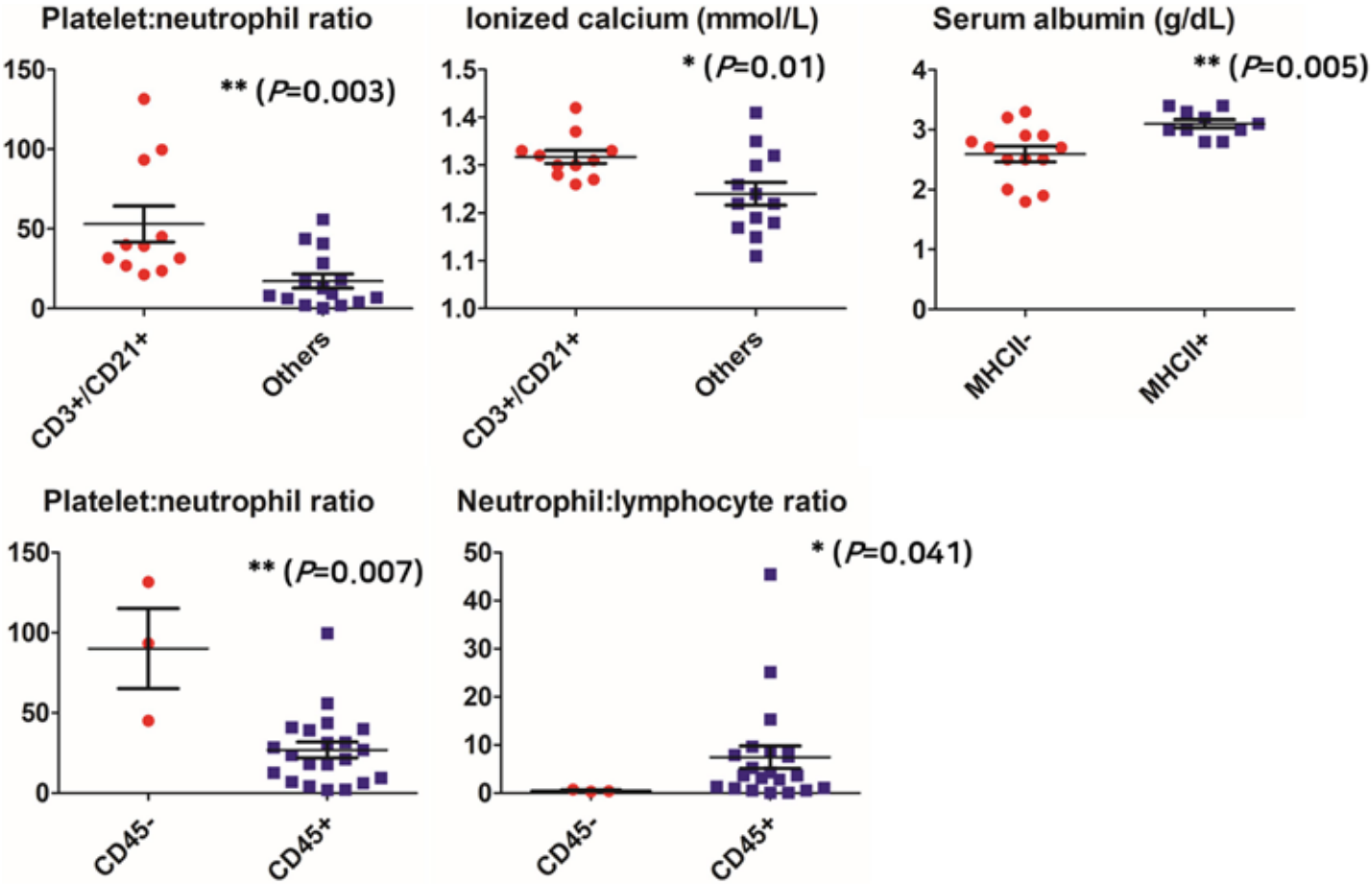

Figure 1. *Comparison of clinicopathological parameters according to aberrant phenotypes. *p < 0.05, **p < 0.01, ***p < 0.001.*

CD34 showed significant correlations with cranial mediastinal lymphadenopathy, WHO clinical substage, and fever (p = 0.017, p = 0.037, and p = 0.033, respectively). Cranial mediastinal lymphadenopathy was present in four out of the five dogs (80%) that expressed CD34, whereas only three of the 18 dogs (16.7%) that did not express CD34 had cranial mediastinal lymphadenopathy. Five (41.7%) of 12 dogs with substage "b" expressed CD34, whereas none of the 11 dogs with substage "a" expressed CD34; four out of five dogs (80%) with CD34+ had fever, whereas only four of 18 dogs (22.2%) with CD34- had fever. The odds of cranial mediastinal lymphadenopathy were 20 times higher in CD34+ than those in CD34- dogs. CD34+ dogs were 2.6 times more likely to be evaluated as WHO clinical substage "b" than CD34- dogs, and their odds of having fever were 14 times higher.

A significant correlation was observed between the presence of MHCII expression and fever (p < 0.001), and the presence of chemotherapy adverse reactions (p = 0.022). Fever was pres-

ent in seven of 10 MHCII+ dogs (70%), whereas none showed fever in the 13 MHCII-group. Chemotherapy adverse effects were present in seven of nine MHCII+ dogs (77.8%), whereas only two of 11 dogs with MHCII-showed chemotherapy adverse reactions. The odds of adverse reactions to chemotherapy were 16 times higher in the MHCII+ group than in the MHCII-group, and the odds of expressing MHCII were 5.3 times greater when fever was present than when fever was absent (**Table 2**).

3.3. Survival analysis

The overall median survival time was 365 days (range 1–1,138 days). Ten dogs died due to lymphoma, while two dogs died due to other reasons unrelated to the tumor. Twelve dogs survived the entire study duration, and follow-up was discontinued for three dogs.

No statistically significant differences in the survival period were observed for any of the phenotypic aberrancies. The survival time was significantly shorter in the substage "b" group (p = 0.006) and in the group with anemia and monocytosis among those with PNS (p = 0.028 and p = 0.024, respectively) (Supplementary Table S4).

	Frequency (%)		Total
Cranial mediastinal lymphadenopathy	CD34+	CD34-	
Yes	4 (57.1%)	3 (42.9%)	7
No	1 (6.3%)	15 (93.8%)	16
Fisher's exact test (*P*) [95% CI]	0.017 [1.613–247.981]		
WHO clinical substage	CD34+	CD34-	
a	0 (0%)	11 (100%)	11
b	5 (41.7%)	7 (58.3%)	12
Fisher's exact test (*P*) [95% CI]	0.037 [1.441–4.589]		
Fever	CD34+	CD34-	
Yes	4 (50%)	4 (50%)	8
No	1 (6.7%)	14 (93.3%)	15
Fisher's exact test (*P*) [95% CI]	0.033 [1.200–163.367]		
Chemotherapy adverse reactions	MHCII+	MHCII-	
Yes	7 (77.8%)	2 (22.2%)	9
No	2 (22.2%)	9 (81.8%)	11
Fisher's exact test (*P*) [95% CI]	0.022 [1.754–141.404]		
Fever	MHCII+	MHCII-	
Yes	7 (100%)	0 (0%)	7
No	3 (18.8%)	13 (81.3%)	16
Fisher's exact test (*P*) [95% CI]	<0.001 [1.923–14.790]		

Table 2. *Association analysis between prognostic factors of lymphoma and aberrant immunophenotypes using Fisher's exact test.*

4. Discussion

Companion animals serve as excellent models for human diseases, particularly spontaneously occurring cancers, which reflect similar pathobiologies and comorbidities. Dogs and humans share common cytogenetic and clinical features, pathology, tumor biology, tumor behavior, and genetic aberrations in the case of lymphoma (24, 25). In this study, flow cytometry was used to analyze immunophenotypes, an important prognostic factor in dogs diagnosed with lymphoma, and aberrancies were identified in 77% of the dogs (27/35 dogs). Dogs with high-grade lymphoma classified by the updated Kiel classification showed much more immunophenotypic aberrancies than ones with low-grade lymphoma. Furthermore, correlations between clinical, hematological, and serological findings were identified in dogs with aberrant phenotypes. As hypothesized, aberrancies associated with prognostic markers of lymphoma and PNS were identified, but no significant difference in survival time was observed according to the aberrant phenotype.

Previous studies have reported a slight difference in the incidence of aberrant phenotypes depending on the definition used. Specifically, Celant et al. found that 12% (310/2,612) of dogs had specific antigen aberrancies (20), while Wilkerson et al. reported an incidence of 22% (5). The incidence of loss of MHCII expression or low expression, which was the most frequently identified aberrancy in our study, has been reported to be approximately 14–72% in previous studies (2, 11). Additionally, the co-expression of CD3 and CD21 has been reported to range from as low as 0.7% (20), to as high as 31–50% (5, 19), while one study reported no cases of CD3/CD21 co-expression (26).

The MHCII proteins are specifically expressed on professional antigen-presenting cells such as B lymphocytes, monocytes, and dendritic cells (27). The MHCII gene expression signature suggests that antigen presentation to the immune system plays a significant role in therapeutic responses (27). The reduced MHCII expression may hinder sufficient tumor immunosurveillance, which could have contributed to the unfavorable outcome (27). In this study, the loss of MHCII expression was identified in the seven dogs with high-grade morphotypes (7/17, 41%). Although this study did not find a significant difference in survival time depending on MHCII expression, several previous human and dog studies have stablished its potential use as a prognostic factor.

CD3 is a complex molecule associated with the T-cell receptor and is expressed during maturation in early thymocytes (5). It is a representative marker expressed in T-cell lymphocytes and is present in all stages of T-cells from early precursor T-cells to mature T-cells that enter the circulation and lymph nodes. On the other hand, CD21 is a marker of mature B-cells, and when immature B-cells naïve to antigen exposure are released from the bone marrow, CD21 antigen is expressed on the surface (28).

In this study, the most frequently identified aberrancies in all lineages were double positive for CD3 and CD21. The co-expression of different lineage markers is a characteristic feature of tumors that cannot be identified in reactive lymph nodes (19). Four of the five dogs with low-grade lymphoma showed CD3+/CD21+, and three of them showed clear cell types and were diagnosed with TZL in histopathology. Eight dogs co-expressed CD21 among T cells, of which four dogs were presumed to have TZL and one dog had clinically aggressive multicentric T-cell lymphoma (no biopsy available). These were expected results since TZL is low grade indolent lymphoma and expresses CD21, as previously reported (29). However, in the case of the other dog, it was not clinically indolent. Six out of seventeen dogs with high-grade lymphoma showed CD3+/CD21+ expression, which is assumed to be aberrant expression.

CD21-positivity has already been described in canine T-cell neoplasms in the past (5, 19). Since it is a tumor cell, it is possible that the phenotype of the antigen expressed during the maturation stage of lymphocytes is altered. It is also possible that these two types of tumors occurred concurrently. One dog with CD3-expressing B-cell lymphoma was histopathologically diagnosed with DLBCL. However, in the clonality test, both T and B cells were confirmed to be clonal, suggesting that both tumor lineages occurred concurrently.

The loss of CD45, CD5, and CD4/CD8 double negativity was the second most common abnormality in T cells. CD45 is a transmembrane protein tyrosine phosphatase that serves as a common leukocyte marker due to its expression in all leukocytes irrespective of lineage (30). CD45 loss has also been regarded as a tumor hallmark in previous studies (19, 31). Among the histologic subtypes of lymphoma, CD45 is a characteristic finding of TZL, and as mentioned above, is clinically indolent. In our study, two dogs with CD45-were histopathologically diagnosed with TZL. One of the two dogs without histopathology had a tongue mass as the primary complaint and exhibited an immunophenotype of CD3+/CD4-/CD8+/CD21+/CD45-in the regional lymph nodes. Although the phenotype of the tongue mass was not analyzed, cytology confirmed that the main population was small lymphocytes (data not shown). The possibility of TZL originating from the tongue is also high in this dog, considering a previous case of TZL in the tongue (32). However, in another study, 5.3% of T-cell not otherwise specified dogs were identified as CD45- (20). Although this study did not find any aggressive lymphoma with CD45-, it is expected that the frequency of this aberrant type will increase as the population size increases.

T lymphocytes differentiate from double-negative (CD4-/CD8-) thymocytes to double-positive (CD4+/CD8+) cells before leaving the thymus and evolving into CD4+ and CD8+ cells (7). Since CD4 and CD8 are not expressed in mature T-cells, which are marked by CD3+, the phenotype observed in this study was considered aberrant. The CD4-/CD8-phenotype has been in various anatomical forms of T-cell lymphoma. For example, the phenotype of neoplastic lymphocytes in cutaneous epitheliotropic lymphoma was CD4-/CD8+ or CD4-/CD8- (33), and CD4-/CD8+ or CD4-/CD8-patterns were also identified in hepatosplenic and hepatocytotropic lymphoma (34). Regarding the survival period, a recent study found that dogs with a CD4-/CD8-/MHCII+ phenotype had a relatively long progression-free interval (2), while another study reported a more aggressive progression (35). Among lymphoma in dogs, lymphoblastic lymphoma, which has the most aggressive progression, has been shown to express CD4-/CD8-or CD4+/CD8+ (36). In this study, there was no significant difference in survival time, and no significant association with prognostic factors was confirmed. The four dogs with the CD4/CD8 double-negative phenotype did not show any common anatomical tumor regions.

In B-cells, MHCII-was identified in approximately 53% of cases, followed by CD3+/CD21+ in 41%, CD34+ in 24%, and CD79-in 24%. As previously mentioned, low MHCII expression is well known as one of the most reliable indicators of poor outcomes in human B-cell lymphoma (27, 37). Studies in dogs with B-cell lymphoma have also demonstrated an association between low MHCII expression and high mortality and relapse rates (11). There is evidence to suggest that MHCII expression is correlated with more robust immunosurveillance in B-cell lymphomas, as well as longer survival in T-cell lymphomas (12). However, in studies investigating MHCII expression in T-cell lymphoma, it remains unclear whether it can be used as a prognostic factor, as dogs with strong MHCII expression have been shown to have shorter survival times (2). Additionally, no difference in survival time was found depending on MHCII expression in a cohort of DLBCLs in a later study (38). Nevertheless, in this study,

Tabla de contenido:

there was a strong correlation between MHCII expression and clinical signs and PNS caused by lymphoma, such as fever and cranial mediastinal lymphadenopathy, which suggests that MHCII expression may impact the severity or prognosis of the disease.

CD34 is a well-known hematopoietic precursor cell marker that has been clinically used to distinguish between acute lymphoblastic leukemia, chronic lymphocytic leukemia, and the leukemic stage (Stage V) of lymphoma (28). Although aberrant expression of CD34 has been observed in lymphoma without bone marrow involvement, its biological significance remains unclear (5, 6, 39). In case of precursor lymphoma, antigens expressed in lymphocytes at a relatively early stage of differentiation, including CD34, may also be identified. In this study, 19% (5/27) of dogs showed CD34 expression, and all showed high-grade morphotypes in the updated Kiel classification. Four of them were positive for CD21, a mature B-cell marker, suggesting aberrant expression in mature B-cell lymphoma. Among the T cells, one dog was identified as CD34+ and CD4-/CD8-, suggesting the possibility of precursor lymphoma. In previous studies, the expression rate of CD34 was 10–29%. When CD34 is co-expressed with CD21, a mature B-cell marker, as in this study, it is considered an aberrant phenotype (5, 11). Unfortunately, due to the lack of histopathology and a bone marrow analysis, the WHO classification and bone marrow infiltration was unknown. However, in the case of CD34+ B-cell lymphoma, considering various clinical and immunophenotypic characteristics, and tumor course, the possibility of acute leukemia or precursor lymphoma was estimated to be low. The response to chemotherapy of dogs with CD34+ B-cell lymphoma was poor, as it recurred during the induction (L-CHOP) protocol. Despite conducting a rescue protocol, the disease was considered progressive with a survival time of 99 days.

Next, the relationship between the phenotypic aberrations and clinical measurements was analyzed. The clinical significance of blood cell ratios as a biomarker has already been accepted for several diseases in humans, and investigations are being conducted on tumors of various origins in dogs. Inflammation plays a fundamental role in lymphomagenesis and tumor progression, and vice versa, and can lead to changes in peripheral blood leukocyte composition (neutrophil, monocyte, and lymphocyte, especially), depending on the severity and extent of inflammation (40, 41). PNR was confirmed as an independent prognostic factor in dogs diagnosed with DLBCL, with a cutoff value of 0.032; a higher value increases the risk of tumor progression before 180 days (42). Platelet–neutrophil interactions in malignant conditions are directly related to PNR, especially in humans and dogs with lymphomas presenting malignant hypercoagulability as a frequent PNS (42–45). In our study, PNR was significantly higher in the CD3+/CD21+ and CD45-group than in the group without this phenotype. Although there was no statistically significant difference in survival time among the PNR, CD45, and CD3+/CD21+ phenotypes, dogs with a low PNR generally tended to be 'clinically ill' upon admission. However, this was not related to tumor progression, and the relationship with phenotypic aberrancies could not be confirmed. Additionally, NLR was higher in the CD45+ group than in the CD45 + group. In human non-Hodgkin's lymphoma, an NLR of 3.5 or higher was identified as a negative prognostic factor (46, 47). In this study, two out of four dogs with CD45-were diagnosed with TZL, and both had lymphocytosis at diagnosis, with neutrophils within the reference range. The difference in NLR is speculated to be largely due to the influence of lymphocytosis. However, the low NLR compared to lymphomas showing aggressive clinical features (e.g., DLBCL, peripheral T-cell lymphoma not otherwise specified) is probably due to the mild degree of tumor-induced inflammatory response (neutrophil change) and host immunity change

Tabla de contenido:

(lymphocyte change) compared to aggressive lymphoma. This is presumed to be in line with the clinically indolent type and clinical signs similar to those of aggressive lymphomas, such as generalized lymphadenopathy and lymphocytosis, but different progression is thought to be related to changes in the blood cell ratio. The TZL population was too small to detect differences between TZL and other lymphomas or between TZL and healthy dogs.

Compared to the serum chemistry data, the concentration of ionized calcium was significantly higher in the CD3+/CD21+ group. However, their clinical relevance remains unknown. Among the dogs studied, two had hypercalcemia, which was evaluated as PNS due to parathyroid hormone related hormone, while one was found to have hypocalcemia. Several significant results were found in the Fisher's exact test, most of which were related to PNS. Neoplastic fever is thought to be due to the innate immune response to a tumor antigen or the development of necrotic cells within the tumor, and is particularly common in hematopoietic cancers such as lymphoma (14). In this study, a significant difference in the presence or absence of fever was identified according to MHCII expression ($p < 0.001$). This is thought to be related to the function of MHCII and the mechanism of its upregulation in dogs with tumors. Cytokines such as TNF-α, IFN-γ, and IL-1 upregulate MHCII expression (48), and these cytokines also activate the arachidonic acid cascade to produce prostaglandin E2, which acts on the thermoregulatory center of the hypothalamus to regulate the development of fever (49). Although the direct causal relationship between MHCII expression and fever is unknown, further research is needed to determine the clinical relevance of MHCII as a negative prognostic factor and fever as a PNS. There was a correlation between MHCII expression and adverse reactions to chemotherapy as well. When MHCII was expressed, the risk of chemotherapy adverse reactions was higher than when it was not expressed. Most adverse reactions were myelosuppression, mainly neutropenia. Grade III or IV chemotherapy-induced neutropenia is known as a favorable prognostic factor of lymphoma in dogs (50, 51). Likewise, although the direct relationship between MHCII expression and chemotherapy adverse reactions could not be identified, it is presumed that there is an unknown mechanism between them.

In the case of CD34+ lymphoma, it can be presumed to be a precursor-derived or remaining aberrancy in the differentiation stage of tumor cells or leukemic involvement in high-grade lymphoma (52). WHO clinical substage "b" refers to a state with clinical signs such as lethargy, inappetence, weight loss, polyuria/polydipsia, or fever due to lymphoma, and it is a negative prognostic factor for lymphoma (1, 53). In this study, all 11 dogs in WHO substage "a" did not express CD34, while five out of 12 dogs (41.7%) in substage "b" expressed CD34. One of the five dogs expressing CD34 was of T-cell origin, and the other was of B-cell origin. There was no statistically significant difference in survival time, likely due to the small sample size, but four of the CD34+ dogs showed rapid tumor progression after or during the induction protocol (L-CHOP). Chemotherapy response in all four dogs was assessed as PD, and euthanasia was performed, or the dogs died due to tumor progression. When the correlation with cranial mediastinal masses, another negative prognostic factor, was analyzed, CD34 was expressed in four out of seven dogs (57.1%) with masses and only one (6.3%) out of 16 dogs without masses. Again, a causal relationship between these factors could not be confirmed, but it is presumed that there is a possible clinical association between CD34 expression, response to chemotherapy, and the progression-free interval.

When the Kaplan–Meier curve was used to analyze survival time based on the aberrant phenotype, no statistically significant difference in median survival time was observed for any phenotype.

Previous studies have shown that the prognosis of T cells is poorer than that of B cells, but this study did not identify any differences in survival time according to immunophenotype. Although the dogs with high-grade lymphoma in the updated Kiel classification showed more immunopheonotypic aberrancies, it was not confirmed if it is related to the prognosis. There are prior studies that show that the prognosis is related to specific morphotypes with the updated Kiel classification (54). However, this study did not confirm the association with detailed morphotypes, immunophenotypic aberrations, and prognosis due to the small population. The survival period was significantly shorter in the PNS group, particularly in dogs with anemia and monocytosis. These results align with previously known negative prognostic factors for lymphoma. The small sample size and cases where tumor progression was not confirmed due to loss during follow-up may have contributed to these findings.

This study had some limitations associated with its retrospective nature. First, due to the small number of individuals, there were limitations in analyzing various aspects of phenotypic aberrations, which are known to have a particularly low frequency. In this study, two out of 19 dogs were identified as having non-B, non-T cell origin, and both were confirmed to be positive for the NK cell marker NKp46. Therefore, NK cell lymphoma could be diagnosed. However, it was difficult to compare the clinical characteristics because there were only two dogs. Second, there are still a few antibodies produced that target dogs for flow cytometry, and the majority of those used in this study are antibodies that cross-react with human, rat, or mouse cells. In this case, a false expression could be observed because of the risk of nonspecific binding. However, in this study, this was unlikely because the background cells, including neutrophils, monocytes, and reactive lymphocytes, did not show nonspecific binding to each antibody. Additionally, there are few antibodies available to further subdivide the phenotypes within the same lineage. By identifying phenotypic changes according to lymphocyte maturation stage and comparing them with clinical measurements, subtypes that are not yet widely known in veterinary medicine, such as precursor lymphoma, can be identified. Third, the WHO classification based on histopathology and bone marrow analysis remains a key tool for the diagnosis and classification of lymphoma and distinguishing it from bone marrow-originated diseases such as leukemia. In particular, a bone marrow analysis is necessary to determine whether the CD34 expression identified in this study is an aberrant immunophenotype, precursor lymphoma, or acute lymphoblastic leukemia, and peripheral blood tests are insufficient. Although it is not possible to evaluate the treatment response or prognosis using these methods alone, a clear evaluation is important as histological classification and grading is a strong prognostic factor. In clinical practice, surgical resection is not often attempted as diagnosis can typically be achieved to some extent with less invasive cytology and immunophenotyping. Future studies in populations with secured pathology results may enable accurate analysis between prognostic factors and clinical measurements. Such studies are expected to help our understanding of various subtypes of lymphoma in dogs by analyzing how the functions that are changed by aberrant antigen expression are clinically expressed at the gene expression level.

Data availability statement

The original contributions presented in the study are included in the article/Supplementary material, further inquiries can be directed to the corresponding author.

Ethics statement

The animal studies were approved by Gyengsang National University, IACUC no. GNU-230425-D0087. The studies

were conducted in accordance with the local legislation and institutional requirements. Written informed consent was obtained from the owners for the participation of their animals in this study.

Author contributions

HB: Conceptualization, Resources, Software, Writing – review & editing, Data curation, Formal analysis, Investigation, Methodology, Visualization, Writing – original draft. S-KK: Data curation, Formal analysis, Resources, Writing – review & editing, Funding acquisition, Validation. DY: Funding acquisition, Resources, Validation, Writing – review & editing, Conceptualization, Project administration, Software, Supervision.

Funding

The author(s) declare financial support was received for the research, authorship, and/or publication of this article. This research was supported by Korea Institute of Planning and Evaluation for Technology in Food, Agriculture and Forestry (IPET) through Companion Animal Life Cycle Industry Technology Development Program, funded by Ministry of Agriculture, Food and Rural Affairs (MAFRA) (322092-04-1-HD030).

Conflict of interest

The authors declare that the research was conducted in the absence of any commercial or financial relationships that could be construed as a potential conflict of interest.

Publisher's note

All claims expressed in this article are solely those of the authors and do not necessarily represent those of their affiliated organizations, or those of the publisher, the editors and the reviewers. Any product that may be evaluated in this article, or claim that may be made by its manufacturer, is not guaranteed or endorsed by the publisher.

Supplementary material

The Supplementary material for this article can be found online at: https://www.frontiersin.org/articles/10.3389/fvets.2023.1254458/full#supplementary-material

References

1. Teske, E, van Heerde, P, Rutteman, GR, Kurzman, ID, Moore, PF, and MacEwen, EG. Prognostic factors for treatment of malignant lymphoma in dogs. J Am Vet Med Assoc. (1994) 205:1722–8.
2. Deravi, N, Berke, O, Woods, JP, and Bienzle, D. Specific immunotypes of canine T cell lymphoma are associated with different outcomes. Vet Immunol Immunopathol. (2017) 191:5–13. doi: 10.1016/j.vetimm.2017.07.008
3. Ruslander, DA, Gebhard, DH, Tompkins, MB, Grindem, CB, and Page, RL. Immunophenotypic characterization of canine lymphoproliferative disorders. In Vivo. (1997) 11:169–72.
4. Schmidt, CJ, Domenico, L, Ward, P, Barcos, MP, and Stewart, CC. Aberrant antigen expression detected by multiparameter three color flow cytometry in intermediate and high grade B-cell lymphomas. Leuk Lymphoma. (1999) 34:539–44. doi: 10.3109/10428199909058481
5. Wilkerson, MJ, Dolce, K, Koopman, T, Shuman, W, Chun, R, Garrett, L, et al. Lineage differentiation of canine lymphoma/leukemias and aberrant expression of CD molecules. Vet Immunol Immunopathol. (2005) 106:179–96. doi: 10.1016/j.vetimm.2005.02.020
6. Gelain, ME, Mazzilli, M, Riondato, F, Marconato, L, and Comazzi, S. Aberrant phenotypes and quantitative antigen expression in different subtypes of canine lymphoma by flow cytometry. Vet Immunol Immunopathol. (2008) 121:179–88. doi: 10.1016/j.vetimm.2007.09.018

7. Comazzi, S, and Gelain, ME. Use of flow cytometric immunophenotyping to refine the cytological diagnosis of canine lymphoma. Vet J. (2011) 188:149–55. doi: 10.1016/j.tvjl.2010.03.011
8. Sehn, LH. Optimal use of prognostic factors in non-Hodgkin lymphoma. Hematology Am Soc Hematol Educ Program. (2006) 2006:295–302. doi: 10.1182/asheducation-2006.1.295
9. Berglund, M, Thunberg, U, Amini, RM, Book, M, Roos, G, Erlanson, M, et al. Evaluation of immunophenotype in diffuse large B-cell lymphoma and its impact on prognosis. Mod Pathol. (2005) 18:1113–20. doi: 10.1038/modpathol.3800396
10. Rahemtullah, A, Longtine, JA, Harris, NL, Dorn, M, Zembowicz, A, Quintanilla-Fend, L, et al. CD20+ T-cell lymphoma: clinicopathologic analysis of 9 cases and a review of the literature. Am J Surg Pathol. (2008) 32:1593–607. doi: 10.1097/PAS.0b013e31817d7452
11. Rao, S, Lana, S, Eickhoff, J, Marcus, E, Avery, PR, Morley, PS, et al. Class II major histocompatibility complex expression and cell size independently predict survival in canine B-cell lymphoma. J Vet Intern Med. (2011) 25:1097–105. doi: 10.1111/j.1939-1676.2011.0767.x
12. Avery, PR, Burton, J, Bromberek, JL, Seelig, DM, Elmslie, R, Correa, S, et al. Flow cytometric characterization and clinical outcome of CD4+ T-cell lymphoma in dogs: 67 cases. J Vet Intern Med. (2014) 28:538–46. doi: 10.1111/jvim.12304
13. Williams, MJ, Avery, AC, Lana, SE, Hillers, KR, Bachand, AM, and Avery, PR. Canine lymphoproliferative disease characterized by lymphocytosis: immunophenotypic markers of prognosis. J Vet Intern Med. (2008) 22:596–601. doi: 10.1111/j.1939-1676.2008.0041.x
14. Vail, DM, Thamm, DH, and Liptak, JM. Withrow and MacEwen's small animal clinical Oncology-E-Book, 6th ed. Edinburgh, UK: Elsevier Health Sciences (2019).
15. Huang, W-H, Lee, J-J, Liao, AT, and Wang, S-L. Paraneoplastic syndrome as a prognostic factor in dogs with multicentric lymphoma. Intern J Appl Res Vet Med. (2020):18.
16. Valli, VE, San Myint, M, Barthel, A, Bienzle, D, Caswell, J, Colbatzky, F, et al. Classification of canine malignant lymphomas according to the World Health Organization criteria. Vet Pathol. (2011) 48:198–211. doi: 10.1177/0300985810379428
17. Ponce, F, Marchal, T, Magnol, JP, Turinelli, V, Ledieu, D, Bonnefont, C, et al. A morphological study of 608 cases of canine malignant lymphoma in France with a focus on comparative similarities between canine and human lymphoma morphology. Vet Pathol. (2010) 47:414–33. doi: 10.1177/0300985810363902
18. Fournel-Fleury, C, Magnol, JP, Bricaire, P, Marchal, T, Chabanne, L, Delverdier, A, et al. Cytohistological and immunological classification of canine malignant lymphomas: comparison with human non-Hodgkin's lymphomas. J Comp Pathol. (1997) 117:35–59. doi: 10.1016/S0021-9975(97)80065-5
19. Martini, V, Poggi, A, Riondato, F, Gelain, ME, Aresu, L, and Comazzi, S. Flow-cytometric detection of phenotypic aberrancies in canine small clear cell lymphoma. Vet Comp Oncol. (2015) 13:281–7. doi: 10.1111/vco.12043
20. Celant, E, Marconato, L, Stefanello, D, Moretti, P, Aresu, L, Comazzi, S, et al. Clinical and clinical pathological presentation of 310 dogs affected by lymphoma with aberrant antigen expression identified via flow cytometry. Vet Sci. (2022) 9:9. doi: 10.3390/vetsci9040184
21. Vail, DM, Michels, GM, Khanna, C, Selting, KA, London, CA, and Veterinary Cooperative Oncology, G. Response evaluation criteria for peripheral nodal lymphoma in dogs (v1.0)--a Veterinary Cooperative Oncology group (VCOG) consensus document. Vet Comp Oncol. (2010) 8:28–37. doi: 10.1111/j.1476-5829.2009.00200.x
22. Millar, HR, Simpson, JG, and Stalker, AL. An evaluation of the heat precipitation method for plasma fibrinogen estimation. J Clin Pathol. (1971) 24:827–30. doi: 10.1136/jcp.24.9.827
23. Shin, SW, Jin Lim, Y, Bae, H, Kim, J, Cho, A, Park, J, et al. CD3+/CD4+/CD5+/CD8+/CD21+/CD34-/CD45-/CD79a-/TCRαβ+/TCRγδ-/MHCII+ T-zone lymphoma in a dog with generalized lymphadenopathy: a case report. Korean Journal of Veterinary Research. (2021) 61:e21. doi: 10.14405/kjvr.2021.61.e21
24. Seelig, DM, Avery, AC, Ehrhart, EJ, and Linden, MA. The comparative diagnostic features of canine and human lymphoma. Vet Sci. (2016) 3:3. doi: 10.3390/vetsci3020011

Tabla de contenido:

25. Ito, D, Frantz, AM, and Modiano, JF. Canine lymphoma as a comparative model for human non-Hodgkin lymphoma: recent progress and applications. Vet Immunol Immunopathol. (2014) 159:192–201. doi: 10.1016/j.vetimm.2014.02.016
26. Pawlak, A, Rapak, A, Drynda, A, Poradowski, D, Zbyryt, I, Dzimira, S, et al. Immunophenotypic characterization of canine malignant lymphoma: a retrospective study of cases diagnosed in Poland lower Silesia, over the period 2011-2013. Vet Comp Oncol. (2016) 14:52–60. doi: 10.1111/vco.12112
27. Rimsza, LM, Roberts, RA, Miller, TP, Unger, JM, LeBlanc, M, Braziel, RM, et al. Loss of MHC class II gene and protein expression in diffuse large B-cell lymphoma is related to decreased tumor immunosurveillance and poor patient survival regardless of other prognostic factors: a follow-up study from the leukemia and lymphoma molecular profiling project. Blood. (2004) 103:4251–8. doi: 10.1182/blood-2003-07-2365
28. Moore, P, and Vernau, W. Lymphocytes: differentiation molecules in diagnosis and prognosis. Schalm's veterinary hematology, 5th ed. (2000):247–55.
29. Seelig, DM, Avery, P, Webb, T, Yoshimoto, J, Bromberek, J, Ehrhart, EJ, et al. Canine T-zone lymphoma: unique immunophenotypic features, outcome, and population characteristics. J Vet Intern Med. (2014) 28:878–86. doi: 10.1111/jvim.12343
30. Dahlke, MH, Larsen, SR, Rasko, JE, and Schlitt, HJ. The biology of CD45 and its use as a therapeutic target. Leuk Lymphoma. (2004) 45:229–36. doi: 10.1080/1042819031000151932
31. Martini, V, Cozzi, M, Arico, A, Dalla Rovere, G, Poggi, A, Albonico, F, et al. Loss of CD45 cell surface expression in canine T-zone lymphoma results from reduced gene expression. Vet Immunol Immunopathol. (2017) 187:14–9. doi: 10.1016/j.vetimm.2017.03.006
32. Borin-Crivellenti, S, De Nardi, AB, Varallo, GR, Tinucci-Costa, M, Raposo-Ferreira, TMM, Laufer-Amorim, R, et al. T-cell lymphoma in the tongue of a dog with cutaneous and striated forelimb muscle involvement. Acta Sci Vet. (2014) 42:1–6.
33. Moore, PF, Affolter, VK, Graham, PS, and Hirt, B. Canine epitheliotropic cutaneous T-cell lymphoma: an investigation of T-cell receptor immunophenotype, lesion topography and molecular clonality. Vet Dermatol. (2009) 20:569–76. doi: 10.1111/j.1365-3164.2009.00814.x
34. Keller, SM, Vernau, W, Hodges, J, Kass, PH, Vilches-Moure, JG, McElliot, V, et al. Hepatosplenic and hepatocytotropic T-cell lymphoma: two distinct types of T-cell lymphoma in dogs. Vet Pathol. (2013) 50:281–90. doi: 10.1177/0300985812451625
35. Lurie, DM, Milner, RJ, Suter, SE, and Vernau, W. Immunophenotypic and cytomorphologic subclassification of T-cell lymphoma in the boxer breed. Vet Immunol Immunopathol. (2008) 125:102–10. doi: 10.1016/j.vetimm.2008.05.009
36. Ponce, F, Magnol, J, Blavier, A, Bonnefont, C, Ghernati, I, Felman, P, et al. Clinical, morphological and immunological study of 13 cases of canine lymphoblastic lymphoma: comparison with the human entity. Comp Clin Pathol. (2003) 12:75–83. doi: 10.1007/s00580-003-0480-4
37. Veelken, H, Dannheim, SV, Moenting, JS, Martens, U, Finke, J, and Schmitt-Graeff, A. Immunophenotype as prognostic factor for diffuse large B-cell lymphoma in patients undergoing clinical risk-adapted therapy. Ann Oncol. (2007) 18:931–9. doi: 10.1093/annonc/mdm012
38. Wolf-Ringwall, A, Lopez, L, Elmslie, R, Fowler, B, Lori, J, Sfiligoi, G, et al. Prospective evaluation of flow cytometric characteristics, histopathologic diagnosis and clinical outcome in dogs with naive B-cell lymphoma treated with a 19-week CHOP protocol. Vet Comp Oncol. (2020) 18:342–52. doi: 10.1111/vco.12553
39. Marconato, L, Gelain, ME, and Comazzi, S. The dog as a possible animal model for human non-Hodgkin lymphoma: a review. Hematol Oncol. (2013) 31:1–9. doi: 10.1002/hon.2017
40. Hjelmström, P. Lymphoid neogenesis: de novo formation of lymphoid tissue in chronic inflammation through expression of homing chemokines. J Leukoc Biol. (2001) 69:331–9. doi: 10.1189/jlb.69.3.331
41. Carbone, A, Tripodo, C, Carlo-Stella, C, Santoro, A, and Gloghini, A. The role of inflammation in lymphoma. Adv Exp Med Biol. (2014) 816:315–33. doi: 10.1007/978-3-0348-0837-8_12
42. Henriques, J, Felisberto, R, Constantino-Casas, F, Cabeçadas, J, and Dobson, J. Peripheral blood cell ratios as prognostic factors in canine diffuse large B-cell lymphoma treated with CHOP protocol. Vet Comp Oncol. (2021) 19:242–52. doi: 10.1111/vco.12668
43. Kol, A, Marks, SL, Skorupski, KA, Kass, PH, Guerrero, T, Gosselin, RC, et al. Serial haemostatic monitoring of dogs with multicentric lymphoma. Vet Comp Oncol. (2015) 13:255–66. doi: 10.1111/vco.12041

Tabla de contenido:

44. Caruso, V, Di Castelnuovo, A, Meschengieser, S, Lazzari, MA, De Gaetano, G, Storti, S, et al. Thrombotic complications in adult patients with lymphoma: a meta-analysis of 29 independent cohorts including 18 018 patients and 1149 events Blood. J Am Soc Hematol. (2010) 115:5322–8. doi: 10.1182/blood-2010-01-258624

45. Caine, GJ, Stonelake, PS, Lip, GY, and Kehoe, ST. The hypercoagulable state of malignancy: pathogenesis and current debate. Neoplasia. (2002) 4:465–73. doi: 10.1038/sj.neo.7900263

46. Mutz, M, Boudreaux, B, Kearney, M, Stroda, K, Gaunt, S, and Shiomitsu, K. Prognostic value of baseline absolute lymphocyte concentration and neutrophil/lymphocyte ratio in dogs with newly diagnosed multicentric lymphoma. Vet Comp Oncol. (2015) 13:337–47. doi: 10.1111/vco.12045

47. Porrata, LF, Ristow, K, Habermann, T, Inwards, DJ, Micallef, IN, and Markovic, SN. Predicting survival for diffuse large B-cell lymphoma patients using baseline neutrophil/lymphocyte ratio. Am J Hematol. (2010) 85:896–9. doi: 10.1002/ajh.21849

48. Guardiola, J, and Maffei, A. Control of MHC class II gene expression in autoimmune, infectious, and neoplastic diseases. Crit Rev Immunol. (1993) 13:247–68.

49. Ettinger, SJ, Feldman, EC, and Cote, E. Texbook of Veterinary internal medicine, 8th ed. Missouri, USA: Elsevier health sciences (2016).

50. Wang, SL, Lee, JJ, and Liao, AT. Chemotherapy-induced neutropenia is associated with prolonged remission duration and survival time in canine lymphoma. Vet J. (2015) 205:69–73. doi: 10.1016/j.tvjl.2015.04.032

51. Vaughan, A, Johnson, JL, and Williams, LE. Impact of chemotherapeutic dose intensity and hematologic toxicity on first remission duration in dogs with lymphoma treated with a Chemoradiotherapy protocol. J Vet Intern Med. (2007) 21:1332–9. doi: 10.1111/j.1939-1676.2007.tb01956.x

52. Tasca, S, Carli, E, Caldin, M, Menegazzo, L, Furlanello, T, and Gallego, LS. Hematologic abnormalities and flow cytometric immunophenotyping results in dogs with hematopoietic neoplasia: 210 cases (2002-2006). Vet Clin Pathol. (2009) 38:2–12. doi: 10.1111/j.1939-165X.2008.00099.x

53. Jagielski, D, Lechowski, R, Hoffmann-Jagielska, M, and Winiarczyk, S. A retrospective study of the incidence and prognostic factors of multicentric lymphoma in dogs (1998-2000). J Vet Med A Physiol Pathol Clin Med. (2002) 49:419–24. doi: 10.1046/j.1439-0442.2002.00458.x

54. Sayag, D, Fournel-Fleury, C, and Ponce, F. Prognostic significance of morphotypes in canine lymphomas: a systematic review of literature. Vet Comp Oncol. (2018) 16:12–9. doi: 10.1111/vco.12320

Citation: Bae H, Kim S-K and Yu D (2023) Comparative analysis of the aberrant immunophenotype and clinical characteristics in dogs with lymphoma: a study of 27 cases. Front. Vet. Sci. 10:1254458. doi: 10.3389/fvets.2023.1254458

Received: 07 July 2023; Accepted: 03 October 2023; Published: 16 October 2023.

Edited by: Carlos Eduardo Fonseca-Alves, Paulista University, Brazil

Reviewed by: Joy Archer, University of Cambridge, United Kingdom Maria Elena Gelain, University of Padua, Italy

*Correspondence: DoHyeon Yu, yudh@gnu.ac.kr

†ORCID: Hyeona Bae orcid.org/0000-0002-2888-5782Sang-Ki Kim orcid.org/0000-0003-0292-8200DoHyeon Yu orcid.org/0000-0001-7645-6926

Tabla de contenido:

https://axoncomunicacion.net/analisis-comparativo-del-inmunofenotipo-en-perros-con-linfoma/

(R) evolution

PEQUEÑOS ANIMALES

Tabla de contenido:

Inhibidores de la enzima de conversión de angiotensia, aún seguimos ahí

Susana Garcia Pérez de Ayala, DVM

GPCert cardio, GPCert FeLP, Acred. AVEPA Med. Felina

VetPartners ES

Introducción

Los inhibidores de la enzima de conversión de angiotensina (IECAs) son profármacos que inhiben la síntesis a nivel renal de angiotensina II que es un potente vasoconstrictor.

Actúan, por tanto, como vasodilatadores y se recomiendan en el tratamiento de la enfermedad renal crónica (ERC), hipertensión arterial, proteinuria y del fallo cardiaco congestivo (FCC).

El benazepril, enalapril, imidapril y ramipril están aprobados para el tratamiento de perros con FCC y su eficacia está demostrada ya que mejoran la función hemodinámica y los signos clínicos, aumentando la supervivencia. Son prodrogas que se administran por vía oral y se activan dentro del organismo.

Al inhibir el paso de angiotensina I a angiotensina II presentan un efecto hipotensivo leve a moderado.

Existe también evidencia de que los IECAs están recomendados en perros y gatos con ERC ya que reducen la presión capilar glomerular, tienen efectos antiproteinúricos, tienden a retrasar la progresión de la enfermedad y limitan la extensión de las lesiones renales.

Una de las mayores ventajas es su tolerabilidad.

En perros presentan eliminación renal (45%) y hepática (55%) y en gatos se excretan principalmente por el hígado (casi 85%).

Sistema renina-angiotensina-aldosterona (RASS)

Sistema de emergencia que conecta el corazón con el riñón para regular la presión arterial.

Está siempre preparado, el hígado libera continuamente angiotensinógeno.

Cuando hay un problema cardiaco, el corazón no bombea la sangre con eficiencia y el resultado es la reducción del volumen sanguíneo circulante. Lo detecta el riñón y provoca en el aparato yuxtaglomerular la liberación de renina, que desencadena la activación del eje. El angiotensinógeno se transforma en angiotensina I, casi sin actividad, que en los capilares pulmonares se encuentra a la ECA y se transforma en angiotensina II.

La angiotensina II es un potente vasoconstrictor que actúa a nivel de la corteza adrenal para liberar aldosterona. La angiotensiona II provoca vasoconstricción y la aldosterona reabsorción de sodio y agua aumentando la volemia. Ambos provocan el aumento de la presión arterial.

La aldosterona se une a los receptores mineralocorticoides del corazón provocando alteraciones ventriculares, arritmias, fibrosis cardiovascular y edema pulmonar. Por tanto, la activación del RAAS puede provocar la sobrecarga del corazón.

La acción completa sobre el eje requiere el control sobre la angiotensina II y la aldosterona. Los IECAs controlan la transformación de angiotensina I a II, pero no el escape de la aldosterona.

El escape de la aldosterona (EA) es una condición en la cual la IECA y/o el receptor bloqueador de angiotensina fallan en suprimir la actividad del sistema angiotensina-aldosterona. El bloqueo incompleto del SRAA es común en perros con EVM que están recibiendo un IECA. Mientras que el mecanismo del EA es probablemente multifactorial y aún no se conoce bien, la existencia demostrada de EA en perros ofrece la posibilidad de mejorar el pronóstico de la EVM con la adición de un bloqueante del receptor mineralocorticoide a las terapias actuales. En un estudio se comprobó que, aproximadamente, el 30% de los perros en tratamiento por cardiopatía y FCC presentaban EA. La identificación de subpoblaciones de pacientes que experimentan EA puede ayudar a guiar el diseño de futuros estudios y la toma de decisiones clínicas.

La deshidratación, hipotensión, FCC grave, la administración de dosis elevadas de diuréticos o una alteración renal previa, son algunas de las situaciones que incrementan el riesgo de complicación renal durante la terapia con IECAs.

La funcionalidad renal debe evaluarse antes de iniciar una terapia y los valores de urea y creatinina deberán ser controlados periódicamente durante el tratamiento

Fallo cardiaco congestivo

Una de las principales causas de morbilidad y mortalidad en perros. Al igual que en humanos, la activación del SRAA juega un papel central en la patofisiología del FCC, su activación crónica contribuye a la progresión de la enfermedad. Uno de los principales tratamientos es el uso de IECAs que mitigan el SRAA.

Los IECAs en perros disminuyen la presión arterial sistémica (PA), la fracción de regurgitación mitral y la presión de la aurícula izquierda.

Dosis más altas de 0,5 mg/kg/12h bajan los niveles de AngII y aumentan los niveles de Ang 1-7 comparando con niveles más bajos, lo que es más favorable ya que se mantiene la ruta de protección con efecto antifibrótico, antihipertrófico, vasodilatador y antioxidante pero en un estudio no se vieron diferencias relevantes entre los grupos de dosis más bajas y más altas en

cuanto a la presión arterial o las variables ecocardiográficas. El conocimiento de las alteraciones dependientes de la dosis en los biomarcadores de las vías clásicas y alternativas del SRAA podría ayudar a optimizar el tratamiento.

La edad, aumento progresivo de tamaño cardiaco (A y VI), incremento de la velocidad de flujo transmitral (E), aumento del NT-proBNP y el aumento en reposo de la frecuencia cardiaca son, al menos, moderadamente predictivos de la progresión de la EVM y pueden ayudar a identificar perros con riesgo de FCC.

Las repeticiones en la aparición del edema pulmonar indica un mal ajuste de la medicación y deben revisarse la terapia diurética y neurohormonal (IECAs).

El objetivo fundamental del tratamiento de la insuficiencia cardiaca consiste en reducir la severidad de los signos clínicos, mejorar la calidad de vida, prolongar la vida y reducir el riesgo de muerte súbita.

- Reducir edema y derrame
  - Diuréticos: furosemida, espironolactona, hidroclorotiazida.
  - Vasodilatadores venosos: IECAs, pimobendan
- Mejorar el gasto cardiaco:
  - Inotropos positivos: pimobendan
  - Vasodilatadores arteriales: IECAs, amlodipino, pimobendan
- Manejo de las arritmias:
  - Diltiazem, digoxina, sotalol, amiodarona, β-bloqueantes
- Reducir ejercicio físico
- Control nutricional
- Terapia múltiple recomendada por el ACVIM:
- IECA: evitar el paso de angiotensina I a angiotensina II
- Espironolactona: evitar escape aldosterona
- Furosemida: evitar el edema pulmonar
- Pimobendan: Inodilatador

Lo racional para el uso de IECAs es que la supresión del SRAA tiene el potencial de conducir a una situación más favorable hemodinámicamente ya que producen vasodilatación, contrarrestan la retención de líquidos y la progresión de la remodelación auricular y ventricular que ocurre en respuesta a la regurgitación mitral.

Sin embargo, dos estudios, con perros asintomáticos, no mostraron diferencias en el retraso en el desarrollo de FCC entre perros que se les administró enalapril y otros con placebo. Lo que indica que pueden no ser eficaces en el tratamiento de perros asintomáticos.

Por tanto, se recomienda empezar tratamiento con IECAs en estadio C, episodio de FCC que no es refractario al tratamiento estándar. En fase C el tratamiento recomendado por el ACVIM:

- Diurético: furosemida o torasemida. Se recomienda uso de furosemida hasta que falle y entonces torasemida. No cortar el tratamiento si ya ha habido FCC.
  - Furosemida: 2-4 mg/kg/8-12 horas
  - Torasemida 0,2 mg/kg/8-12h
- Inodilatador:
  - Pimobendan: Estudio QUEST. 0,2-0,3 mg/kg/12h
- Espironolactona + IECAs: benazeprilo el más utilizado: Estudio BESST. Mejora la esperanza y calidad de vida. Reduce el riesgo de edema pulmonar.
  - Espironolactona: 2 mg/kg/24h
  - IECAs: 0,25 mg/kg/12-24h

En cuanto a la nutrición se está estudiando el efecto de añadir ciertos nutrientes al tratamiento del FCC. Lo importante es que el animal coma adecuadamente y cubra sus necesidades calóricas y proteica (60 Kcal/kg/dia).

- Ácidos grasos omega 3: reducen las arritmias y tratamiento caquexia cardiaca
- Proteínas: no restringir proteínas, acelera la caquexia cardiaca
- Estudio de supervivencia reducida en perros que consumían dieta sin grano
- L-carnitina y taurina
- Modesta restricción sodio

También es importante la restricción del ejercicio físico dando solo paseos con correa.

Se deben medir la creatinina sérica y electrolitos 14 días después de empezar con el tratamiento. Posible desarrollo de ERA si las concentraciones de creatinina sérica aumentan en ≥30% de la concentración inicial.

Los IECAs son inhibidores enzimáticos competitivos. Se precisa inhibir >95% del ECA para inhibir significativamente la formación de Angiotensina II. Dosis altas demostraron mayores beneficios. A mayor grado de insuficiencia cardiaca, se deben administrar dosis mayores. No son útiles para reducir la presión en AI ya que se ha visto que la presión se reduce muy poco a pesar de la reducción de la postcarga.

La administración crónica de furosemida debe acompañarse de la administración de IECAs para contrarrestar la activación de mecanismos vasoconstrictores y desequilibrios electrolíticos que puedan surgir. Los IECAs y la reducción en la ingesta de sodio ayudan a reducir la dosis diaria de diuréticos.

La aldosterona provoca retención de sodio y líquidos, estimula la inflamación de arterias vasos, desajusta baroreceptores, puede provocar hipertensión y arritmias.

La secreción persistente de aldosterona, a pesar de la presunta reducción de la actividad plasmática de la ECA y de la producción de angiotensina II, se ha denominado "escape de aldosterona". Tanto los IECAs como los diuréticos del asa como el amlodipino, provocan escape de aldosterona. Hay diferentes rutas de producción de aldosterona y escapa a su ruta habitual, además, los IECAs bloquean el SRAA plasmático no el tisular. No se sabe con certeza por qué se produce este escape.

La espironolactona (2.0 mg/kg PO q12 - 24 h) se recomienda como terapia adyuvante para el tratamiento crónico en fase C. El beneficio se basa en ser antagonista de la aldosterona.

En el estudio DeLay se falló en demostrar que la administración combinada de espironolactona y benazepril retrasara la aparición de FCC en perros en fase preclínica. Sin embargo, el tratamiento proporciona efectos beneficiosos en la remodelación cardiaca y estos resultados sí pueden tener relevancia clínica. El bloqueo de los receptores de mineralocorticoides reduce la remodelación cardiaca y con el tratamiento se vio que mejoraron valores como el índice vertebral cardiaco o VHS (vertebral heart score), ratio aurícula izquierda/aorta, diámetro interno del ventrículo izquierdo en diástole normalizado (LVEDDn) y el flujo transmitral que son factores predictivos negativos. NT-proBNP tampoco aumento en el grupo tratado y si en el placebo.

La espironolactona bloquea receptores de aldosterona, es un diurético muy débil, previene la reabsorción distal de sodio y ahorra potasio, antagoniza efectos cardiotóxicos de la aldosterona, previene la fibrosis miocárdica y contrarresta el escape de la aldosterona a los IECAs. Las dosis sugeridas son de 0,5-2,0mg/kg VO una o dos veces al día.

Hay pocos estudios sobre el manejo terapéutico del FCC en gatos. Normalmente la terapia crónica consiste en:

- Furosemida PO 1-3 mg/kg q12 -24h o menor
- IECA PO, enalapril o benazepril 0.25 a 0.5 mg/kg q12-24h
- Diltiazem PO 1.5-2.5 mg/kg q8h (no en gatos con FCC)

A la mayoría de los gatos se les trata con IECAs y furosemida. Beta bloqueantes cuando no hay FCC o para tratar arritmias u obstrucción severa del tracto de salida del ventrículo izquierdo. El diltiazem es más eficaz, pero se usa menos por su administración más frecuente.

En un estudio con benazepril utilizado en gatos con CMH en fase subclínica se vió que se mejoraba la función diastólica y la hipertrofia ventricular aunque se consideró que los hallazgos podían ser inicidentales.

No se ha demostrado efecto sobre el tiempo de aparición de FCC, ni que se retrase el paso de estadio C a D, aunque se sigue usando por algunos cardiólogos.

Ne necesitan más estudios en pacientes felinos para evaluar su eficacia.

Enfermedad renal crónica

Enfermedad irreversible y progresiva que avanza a glomeruloesclerosis y fibrosis intersticial y, en ocasiones, a estadios finales de fallo renal.

Varios sistemas endocrinos y citoquinas están involucradas en el desarrollo de hipertensión renal y progresión de la enfermedad. La hiperactivación del SRAA juega un papel primordial.

La AngII contrae las arteriolas eferentes aumentando la presión capilar glomerular y la filtración. A su vez, contrae los vasos sanguíneos periféricos y, por tanto, eleva la presión arterial sistémica. Estimula la corteza adrenal para secretar aldosterona que reduce la pérdida de sodio y fluidos en túbulos distales, contribuyendo también al incremento de la presión arterial.

La hipótesis de la hiperfiltración nos dice que el aumento de la filtración glomerular provoca daños físicos en los glomérulos, lo que lleva a una lesión renal progresiva. El exceso de AngII desempeña su papel patógeno principal al aumentar la presión de perfusión glomerular provocando lesiones tubulointersticiales, daño en las nefronas remanentes y agravando el deterioro y la disfunción estructural renal.

La proteinuria es un fuerte factor de progresión y su reducción tiene efectos críticos.

Todos los perros con proteinuria renal o azotemia deben ser evaluados para detectar hipertensión. Los gatos mayores, en particular aquellos con enfermedad renal crónica (ERC), deben someterse a exámenes de presión arterial desde el inicio de la enfermedad y durante el curso de la misma ya que aproximadamente el 10 % tendrá hipertensión.

La indicación general es reducir la presión arterial <150 mm Hg

Se cree que el mecanismo de la hipertensión renal implica la retención de líquidos corporales asociada con la insuficiencia renal, el aumento del gasto cardíaco y la resistencia de los vasos periféricos, la activación del sistema renina-angiotensina-aldosterona (RAA) y la supresión del sistema calicreína-cinina-prostaglandina.

Las inhibir la ECA y por tanto la producción de AngII obtendremos un efecto renoprotector con reducción en la presión arterial sistémica, la presión capilar glomerular y el volumen de filtrado glomerular.

En los gatos, la pérdida de masa renal provoca la activación del SRAA y la hipertensión renal asociada que juegan un papel fundamental en la progresión de la insuficiencia renal.

La respuesta a los IECAs es menor que en perros, es posible que exista heterogeneidad en el grado de afectación del SRAA en gatos con enfermedad renal natural y, por tanto, en la respuesta a la inhibición de la ECA. Su administración en estos pacientes provoca una reducción moderada de la hipertensión sistémica. Aun así, pueden ser un tratamiento eficaz para frenar la tasa de progresión de la insuficiencia renal en gatos ya que disminuyen la hipertensión glomerular presumiblemente por su efecto en el SRAA intrarrenal.

En algunos gatos se pueden desarrollar disminuciones transitorias y reversibles de la TFG en respuesta a la vasodilatación arteriolar eferente durante el tratamiento con inhibidores de la ECA.

En un estudio con benazepril, corrigió la hipertensión sistémica y redujo significativamente la angiotensina II y la aldosterona. Se redujeron los valores de creatinina sérica y la proteinuria. Además, se excreta la mayoria en bilis (85%), de esta forma no se acumula en animales con disfunción renal lo que indica su potencial terapéutico seguro en ERC.

En perros, la ERC suele tener un origen glomerular y por eso presentan más proteinuria que los gatos. En IRIS I no suelen presentar signos clínicos a menos que esté muy baja la albúmina o en glomerulonefritis.

La hipertensión sistémica también es común en perros con ERC y puede conducir a una progresión más rápida de la insuficiencia renal. La activación del SRAA es una de las principales causas y el tratamiento con IECA se considera una de las estrategias terapéuticas más eficaces.

Los IECAs producen disminución en la hipertensión capilar glomerular y la gravedad de la proteinuria y un retraso en la progresión de las lesiones renales. Presentan un efecto positivo sobre la TFG y se reduce la liberación de matriz extracelular y colágeno de las células mesangiales y tubulares que disminuye la fibrosis glomerular e intersticial.

Estudios adicionales deberían investigar si los IECA pueden minimizar la hipercoagulabilidad renal.

La administración de benazepril en perros parece ser segura y bien tolerada, con efectos adversos mínimos.

Proteinuria

La hipertensión glomerular causa proteinuria debido al aumento de la tasa de filtración glomerular (TFG) de una sola nefrona que aumenta el radio de los poros dentro de la barrera de filtración y, por lo tanto, se produce la ultrafiltración de proteínas.

La pérdida renal de proteínas plasmáticas puede contribuir a la hipoalbuminemia, alteraciones en los factores de coagulación, disminución de la inmunidad y desarrollo de hiperlipidemia en algunos casos.

Se ha demostrado que la proteinuria crónica se asocia con fibrosis intersticial, así como con degeneración y atrofia tubular.

La proteinuria es un importante marcador para diagnóstico precoz y pronóstico. Está altamente relacionada con la reducción de la supervivencia en perros y gatos azotémicos y no azotémicos. En perros azotémicos, un ratio proteína/creatinina en orina (UPC por sus siglas en inglés) igual o mayor a 1 está asociado con un mayor riesgo de crisis urémica y muerte.

Las fuerzas hemodinámicas influyen en el movimiento transglomerular de

las proteínas, por lo que alterar la hemodinámica renal sería eficaz para reducir la proteinuria.

Se debe medir la proteinuria en varios controles y descartar la pre y la postrenal.

Los perros normales y la mayoría de los gatos normales deben tener una relación proteína: creatinina en la orina inferior a 0,4 e inferior a 0,2, respectivamente.

Los perros que tienen proteinuria renal y un UPC de 2,0 o mayor suelen tener enfermedad glomerular, mientras que los perros con un UPC inferior a 2,0 pueden tener enfermedad glomerular o enfermedad tubulointersticial. Las enfermedades glomerulares ocurren con mucha menos frecuencia en los gatos, pero deben sospecharse cuando el UPC es 2 o mayor. La hipoalbuminuria concurrente es evidencia adicional de que hay enfermedad glomerular

El sistema renina-angiotensina-aldosterona (SRAA) ha sido el principal sistema objetivo de este enfoque para reducir la proteinuria. La administración de IECAs y/o bloqueadores de los receptores de angiotensina (ARB) se consideran un tratamiento estándar en perros y gatos con proteinuria renal.

Los mecanismos propuestos para estos efectos incluyen la disminución de la resistencia arteriolar glomerular eferente que conduce a una disminución o normalización de la presión hidráulica transcapilar glomerular, reducción de la pérdida de sulfato de heparina glomerular, disminución del tamaño de los poros endoteliales de los capilares glomerulares, mejora del metabolismo de las lipoproteínas, crecimiento y proliferación mesangial glomerular más lentos. En perros y gatos, el objetivo terapéutico ideal es una reducción de la UPC, una reducción de la UPC del 50 % o más sin un empeoramiento inapropiado de la función renal.

La hiperpotasemia parece ser un efecto secundario común de la inhibición de SRAA en perros con enfermedad renal, pero probablemente sea poco común en gatos.

El tratamiento de la proteinuria en perros reduce la progresión de la ERC y, en un estudio, el grupo tratado con enalapril mostró una reducción significativa del UPC tras 30 días de tratamiento. Además, demostró minimizar los signos clínico de uremia y mantener una óptima condición corporal.

Hipertensión

La hipertensión no tratada pone en riesgo de daño a otros órganos diana (cerebro, corazón, ojo, riñón, grandes vasos), lo que aumenta la morbilidad y la mortalidad.

Se estima una incidencia en gatos del 19.5%.

La presión arterial sistólica (PAS) media debe ser de 120 mmHg (rango 110–132 mmHg) pero aumenta con la edad y en gatos con ERC.

Se distinguen varios tipos de hipertensión:

- Situacional
- Primaria o idiopática
- Secundaria

Si un gato presenta hipertensión sostenida >160 mmHg en las siguientes revisiones, debe tratarse.

Ideal obtener presiones desde los 3 años, cada 12 meses (ACVIM)

En el tratamiento es fundamental valorar cada caso individualmente, tratar la causa y que la reducción sea gradual.

En gatos hipertensos se recomienda una reducción de 20-30 mmHg y los tratamientos de elección son el amlodipino (antagonista canales del Ca) y el telmisartán (inhibidor de angiotensina II). Los IECAs se utilizan más en caso de proteinuria.

En perros, los IECAs constituyen el tratamiento de primera elección, seguidos del amlodipino, inhibidores de la angiotensina II y los beta-bloqueantes.

Objetivo de la terapia: disminuir al máximo el riesgo de daño en órganos diana (PAS < 150 mm Hg y PAD < 95 mm Hg). La terapia debe ajustarse si la PA es > 150/95 mm Hg o <120 mm Hg.

Los IECAs en hipertensión presentan una serie de ventajas e inconvenientes:

- Ventajas:
  - Dilatan las arteriolas eferentes
  - Bajan la presión intraglomerular
  - Frecuentemente bajan la magnitud de la proteinuria
  - Los efectos adversos cardiacos y renales de la angiotensina II y aldosterona pueden ser atenuados por esta clase de agentes.
- Inconvenientes:
  - Una consecuencia secundaria de la dilatación arteriolar eferente es una tendencia teórica a la disminución de la tasa de filtración glomerular (TFG)., poco importante en perros y gatos
  - Un modesto incremento en los valores de creatinina sérica
  - No deberían usarse en pacientes deshidratados en los cuales la TFG puede descender precipitadamente
  - En gatos, no se recomiendan como monoterapia ya que el descenso de la presión arterial es muy leve

Bibliografía

- Atkins C, Bonagura J, Ettinger S, Fox P, Gordon S, Häggström J, et al. Guidelines for the Diagnosis and Treatment of Canine Chronic Valvular Heart Disease. J Vet Intern Med 2009; 23:1142–1150
- Brown SA, Brown CA, Jacobs G, Stiles J, Hendi RS, Wilson S. Effects of the angiotensin converting enzyme inhibitor benazepril in cats with induced renal insufficiency. AJVR, Vol 62, No. 3, March 2001
- Brown S, Atkins C, Bagley R, Carr A, Cowgill L, Davidson M, et al. Guidelines for the Identification, Evaluation, and Management of Systemic Hypertension in Dogs and Cats. J Vet Intern Med 2007; 21:542–558
- Ishikawa T, Tanaka R, Suzuki S, Miyaishi Y, Akagi H, Lino Y. The Effect of Angiotensin-Converting Enzyme Inhibitors of Left Atrial Pressure in Dogs with Mitral Valve Regurgitation. J Vet Intern Med 2010; 24:342–347
- Keene BW, Atkins CE, Bonagura JD, Fox PR, Häggström J, Luis Fuentes V, Oyama MA, Rush JE, Stepien JE, Uechi M. Guidelines for the Diagnosis and Treatment of Canine Chronic Valvular Heart Disease. J Vet Intern Med. 2019; 33:1127–1140.
- Kvart C, Häggström J, Pedersen HD, Hansson K, Eriksson A, Järvinen AK, et al. Efficacy of Enalapril for Prevention of Congestive Heart Failure in Dogs with Myxomatous Valve Disease and Asymptomatic Mitral Regurgitation. J Vet Intern Med 2002; 16:80–88
- Lantis AC, Ames MK, Atkins CE, De Francesco TC, Keene BW, Werre SR. Aldosterone breakthrough with benazepril in furosemide-activated renin-angiotensin-aldosterone system in normal dogs. J. vet. Pharmacol. Therap. 38, 65--73.
- Luis Fuentes V, Abbott J, Chetboul V, Côté E, Fox PR, Häggström J, Kittelson MD, Schober K, Stern JA. ACVIM consensus statement guidelines for the classification, diagnosis, and management of cardiomyopathies in cats. *J Vet Intern Med.* 2020; 34:1062–1077.
- Mizutani H, Koyama H, Watanabe T, Kitagawa H, Nakato M, Kajiwara K, et al. Evaluation of the Clinical Efficacy of Benazepril in the Treatment of Chronic Renal Insufficiency in Cats. J Vet Intern Med 2006; 20:1074–1079
- Pouchelon JL, Chetboul V, Lugardon B, Rousselot JF, Corlouer JP, Bussadori C, et al. The BENCH (BENazepril in Canine Heart disease) Study Group. The effect of benazepril on survival times and clinical signs of dogs with congestive heart failure: Results of a multicenter, prospective, randomized, double-blinded, placebo-controlled, long-term clinical trial.. Journal of Veterinary Cardiology, Vol. 1, No. 1, May 1999
- Quimby JM. Update on Medical Management of Clinical Manifestations of Chronic Kidney Disease. Vet Clin Small Anim 46 (2016) 1163–1181
- Suzuki S, Fukushima R, Ishikawa T, Yamamoto Y, Hamabe L, et al. Comparative effects of amlodipine and benazepril on Left Atrial Pressure in Dogs with experimentally-induced Mitral Valve Regurgitation. BMC Veterinary Research 2012, 8:166
- Taillefer M, Fruscia RD. Benazepril and subclinical feline hypertrophic cardiomyopathy: a prospective, blinded, controlled study. *Can Vet J* 2006; 47:437–445
- Tenhündfeld J, Wefstaedt P, Nolte IJ. A randomized controlled clinical trial of the use of benazepril and heparin for the treatment of chronic kidney disease in dogs. JAVMA, Vol 234, No. 8, April 15, 2009
- Thompson J. Management of hypertension in a geriatric cat. Can Vet J 2004; 45:427–429
- Vaden SL, Elliott J. Management of Proteinuria in Dogs and Cats with Chronic Kidney Disease. Vet Clin Small Anim 46 (2016) 1115–1130
- Watanabe T, Mishina M. Effects of Benazepril Hydrochloride in Cats with Experimentally Induced or Spontaneously Occurring Chronic Renal Failure. *J. Vet. Med. Sci.* 69(10): 1015–1023, 2007

Doble protección para su corazón

CALIER

El nuevo complemento alimentario en formato gel para perros y gatos que da soporte a BANACEP®, nuestro fármaco indicado para el tratamiento de patologías cardíacas.

Compuesto por Benazepril

MOLÉCULA ÚNICA

UNA SOLA TOMA DIARIA

Compuesto por hidrolizado de levadura de cerveza, L-carnitina y Taurina

PALATABLE

FÁCIL ADMINISTRACIÓN

HIPOALERGÉNICO

Cardiocep Gel

BANACEP® Vet 5 mg

BANACEP® Vet 20 mg

Natural History of Histopathologic Changes in Cardiomyopathy of Golden Retriever Muscular Dystrophy

Cambios histopatológicos en la miocardiopatía de la distrofia muscular del Golden Retriever

Keywords: *cardiomyopathy, dystrophinopathy, golden retriever muscular dystrophy (GRMD), duchenne muscular dystrophy (DMD), natural history*

Palabras clave: miocardiopatía, distrofinopatía, distrofia muscular golden retriever (DMG), distrofia muscular de Duchenne (DMD), historia natural

https://www.frontiersin.org/articles/10.3389/fvets.2021.759585/full

Sarah M. Schneider[1*†], Garett T. Sansom[2], Lee-Jae Guo[3], Shinji Furuya[3†], Brad R. Weeks[1], Joe N. Kornegay[1,3]

1. Department of Veterinary Pathobiology, Texas A&M University, College Station, TX, United States
2. Department of Environmental and Occupational Health, Texas A&M University, College Station, TX, United States
3. Department of Veterinary Integrative Biosciences, Texas A&M University, College Station, TX, United States

Tabla de contenido:

La distrofia muscular de Duchenne (DMD, por sus siglas en inglés) es una miopatía hereditaria ligada al cromosoma X que causa enfermedad progresiva del músculo esquelético y cardíaco. Las lesiones cardíacas se describieron en los primeros informes de DMD, y la miocardiopatía es ahora la principal causa de muerte. Sin embargo, el diagnóstico y el tratamiento de la miocardiopatía se han quedado rezagados con respecto a los de la enfermedad del músculo esquelético apendicular y respiratorio. La mayoría de los estudios en modelos animales se han realizado en el ratón mdx, que tiene una forma relativamente leve de miocardiopatía. Los perros con la enfermedad genéticamente homóloga Golden Retriever distrofia muscular (DMR) desarrollan una miocardiopatía progresiva análoga a la observada en la DMD. Los estudios descriptivos previos de la miocardiopatía GRMD se han limitado principalmente a la toma selectiva de muestras de corazones de perros jóvenes.

Background: Duchenne muscular dystrophy (DMD) is an X-linked inherited myopathy that causes progressive skeletal and cardiac muscle disease. Heart lesions were described in the earliest DMD reports, and cardiomyopathy is now the leading cause of death. However, diagnostics and treatment for cardiomyopathy have lagged behind those for appendicular and respiratory skeletal muscle disease. Most animal model studies have been done in the mdx mouse, which has a relatively mild form of cardiomyopathy. Dogs with the genetically homologous condition, Golden Retriever muscular dystrophy (GRMD), develop progressive cardiomyopathy analogous to that seen in DMD. Previous descriptive studies of GRMD cardiomyopathy have mostly been limited to selective sampling of the hearts from young dogs.

Methods and Results: We systematically assessed cardiac lesions in 31 GRMD and carrier dogs aged 3 to 76 months and a separate cohort of 2–10-year-old normal hounds. Both semi-quantitative lesion scoring and quantitation of the cross-sectional area of fibrosis distinguished dogs with GRMD disease from normal dogs. The carriers generally had intermediate involvement but had even greater fibrosis than GRMD dogs. Fatty infiltration was the most prominent feature in some older GRMD dogs. Vascular hypertrophy was increased in GRMD dogs and correlated positively with lesion severity. Purkinje fiber vacuolation was also increased but did not correlate with lesion severity. Histopathologic changes correlated with late gadolinium enhancement on cardiac MRI.

Conclusion: These features are generally compatible with those of DMD and further validate GRMD as a useful model to study cardiomyopathy pathogenesis and treatment. Additionally, the nature of some degenerative lesions suggests that functional hypoxia or non-thrombotic ischemia may contribute to disease progression.

Introduction

Duchenne muscular dystrophy (DMD) and Golden Retriever muscular dystrophy (GRMD) are genetically homologous, phenotypically analogous degenerative muscle diseases caused by mutations in the DMD gene, which encodes the dystrophin protein (1, 2). Loss of dystrophin at the sarcolemma leads to membrane fragility and both skeletal (3) and cardiac muscle lesions (4, 5). Cardiac complications are the leading cause of death in young men with DMD (6).

Although the heart and skeletal muscle both lack dystrophin, differences in Ca2+ homeostasis (7–9), metabo-

(R) evolution

PEQUEÑOS ANIMALES

Tabla de contenido:

lism (10), and dystrophin–glycoprotein complex localization (11–13) contribute to variable pathologic changes in the two tissues. While some studies have shown that skeletal and cardiac muscle functional deficits track together, others have demonstrated variable progression (5, 6, 14–16). This potential for discordance has clinical significance. Features typical of cardiac disease may not be present in wheelchair-bound DMD boys (17, 18), precluding the assessment of treatment effects on the heart. More importantly, improvement in skeletal muscle function alone could increase strain on the heart and accelerate cardiac disease progression (6, 17–21).

The GRMD dog is an important large animal model of DMD (1, 2). Cardiac disease features in affected dogs that closely parallel those in boys include ECG abnormalities (22–24), initial lesion onset around adolescence (4, 5, 25), changes predominantly in the basolateral left ventricle (LV) (4, 5, 25, 26), and eventual progression to clinically evident dilated cardiomyopathy with reduced ejection fraction and heart failure (1, 2, 4, 5). Previous pathologic descriptive studies, including the first paper by Valentine et al. (25), established the basic features of GRMD cardiomyopathy (1, 25–29). However, these studies often focused on young dogs, and some assessed a limited number of cardiac anatomic sites. The Valentine study was comprehensive in that twenty four dogs were assessed, and 13 to 17 cardiac sections were sampled in each of them, but 19 of the 24 dogs were <12 weeks old and had no detectable abnormalities. Accordingly, the study focused on only five dogs ranging from 6.5 months (m) to 6 years (y). All five dogs had lesions, establishing 6.5 m as the age of onset for pathologic changes. Based on a study of eight crossbred beagles (CXMDJ) with the GRMD mutation, Yugeta et al. (26) suggested that the pathologic onset might be delayed until 12 months. Their pathologic assessment included only four dogs >12 m of age, with the oldest being 21 m. No histopathologic lesions were seen in dogs <12 m, and only 3 of the 4 older dogs had changes. While the most recent descriptive study out of Brazil (29) included 18 GRMD dogs and also made the most concerted effort to differentiate lesions among age groups, only single sites from the LV and right ventricle (RV) were examined for each dog. Since all the dogs in the Brazil study purportedly died of heart failure, the pathologic findings across all age groups might be more typical of end-stage disease vs. the full spectrum of lesion development.

Women carriers heterozygous for DMD gene mutations are also at an increased risk for clinical heart disease (30–33) due to mosaic cardiac dystrophin expression (30). Canine GRMD carriers have an analogous mosaic cardiac dystrophin expression pattern (34) and lesions similar to affected dogs, including variable degrees of myocardial fibrosis, necrosis, mineralization, and fatty infiltration concentrated in the LV free wall (35).

Given the similarities between the DMD and GRMD cardiomyopathies, preclinical studies in affected dogs should inform the management of DMD patients. Pathologic studies typically serve as the gold standard for establishing disease progression and aid in selecting appropriate diagnostic and prognostic markers. We report a semi-quantitative natural history of histopathologic cardiomyopathy changes in a large cohort of GRMD dogs across a wide age range.

Materials and Methods

Animals

Care of the dogs in this study was governed by principles outlined in the Guide for the Care and Use of Laboratory Animals of the National Research Council and the protocols approved by the institutional animal care and use committee at Texas A&M University. Typically, in our colony, the carrier females are bred with semen from affected males, producing 25% each of

normal males, carrier females, dystrophic hemizygous males, and dystrophic homozygous females.

Hearts were collected from thirty eight dogs, including 7 normal hounds (controls; 2–10 y; 5 female and 2 male), 5 GRMD carriers (3 m–4.5 y), and 26 GRMD-affected dogs [divided among four age groups: <6 m (five dogs), 6–12 m (seven dogs), 12–24 m (five dogs), and >24 m up to 76 m (nine dogs)]. The GRMD dogs were evenly split between hemizygous males and homozygous females.

Hearts

We collected hearts from GRMD-affected dogs that died or were euthanized due to declining quality of life (defined as an inability to maintain sternal recumbence or progression to end-stage heart failure) or at terminal end-points for studies unrelated to cardiomyopathy. Of the GRMD dogs, only one was euthanized due to reasons related to intractable heart failure; four died or were euthanized for other reasons. Hearts from carrier dogs were collected at terminal end-points for studies unrelated to cardiomyopathy and from one dog (3 m) that died under anesthesia with no previous clinical symptoms of heart disease. Unaffected hearts were collected from an unrelated colony of working hound dogs euthanized for non-cardiac events.

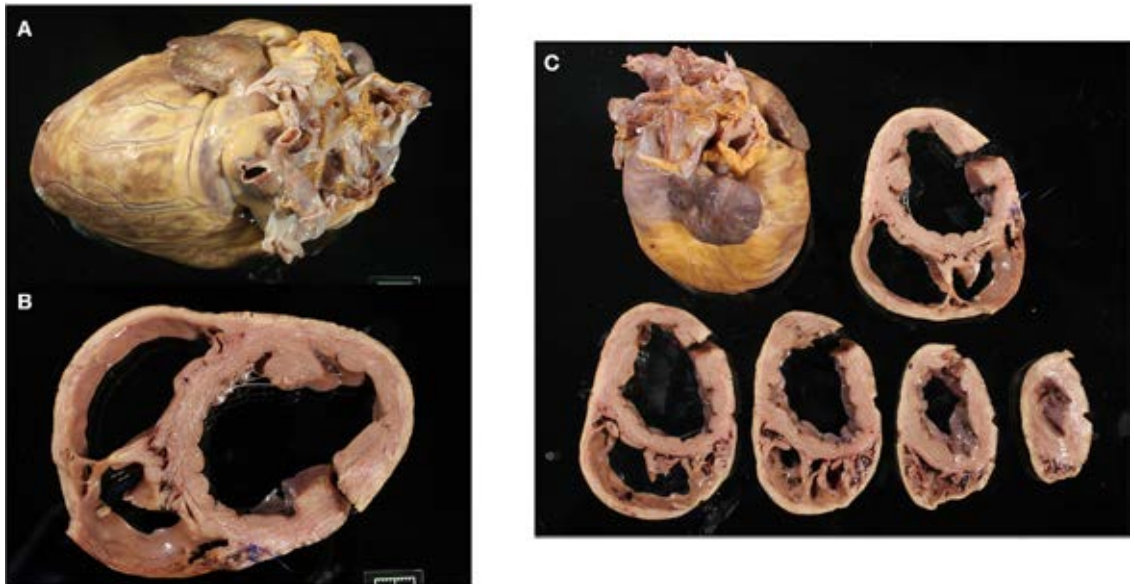

Figure 1. *Representative gross images of a Golden Retriever muscular dystrophy heart showing the whole heart (**A**), the basal cross-section with left ventricle and right ventricle dilation (**B**), and all ventricular cross-sections (**C**).*

In all hearts, samples from the LV and RV free walls were snap-frozen at necropsy and banked for potential gene expression and immunohistochemistry studies. The remaining whole heart was placed in formalin.

Gross Pathology and Sectioning

Fixed hearts were weighed and photographed in six views (cranial, caudal, lateral from left and right sides, base, and apex). Each heart was cross-sectioned through the ventricular short axis at 1-cm intervals to the level of the atrioventricular valves and photographed (**Figure 1**). The hearts were weighed, and the thicknesses of the fixed LV, RV, and interventricular septum were measured (**Table 1** and **Supplementary Table 1**). The hearts were evaluated grossly and in the images for subjective dilation, pallor, and mineralization.

Each heart was systematically sectioned for histology. Seventeen sections of the LV (including septum) were taken to correspond with standard segmentation for advanced imaging (36). Additionally, four sections of the RV (anterior and inferior as available at the basal and mid-level) and the left and right atria were collected. The atrioven-

tricular node was isolated by sectioning the septal junction of the right atrium below the foramen ovale and the non-coronary cusp of the aortic valve. The sinoatrial node was sectioned at the junction of the vena cava and the right atrium (37). Tissue cassettes containing the sections were photographed for reference, paraffin-embedded, and routinely processed. Slides were cut at 5-10 m thickness and stained with hematoxylin and eosin (H&E) and Masson's trichrome. All slides were digitally scanned at × 20 on a Hamamatsu NanoZoomer 2.0-HT whole-slide imager (Hamamatsu Corporation; Bridgewater, NJ, USA).

Microscopic Pathology

Digital slide images were evaluated by a single pathologist (SS) using two methods to assess disease severity. Each section was given a semi-quantitative grade for approximate percentage of the cross-sectional area affected by histopathologic lesions, generally following the system described by Kane et al. (35) (0 = none, 1 = 1–10%, 2 = 11–20%, 3 = 21–30%, and 4 >30%) (Supplementary **Figure 1**). These scores were averaged across sections and groups for statistical comparisons (Supplementary **Table 2**). In a second method, specific histopathologic changes were scored as absent/present, and notations were made for the nature of some

Group (*N*)	Averages (±SD) HW (g)	BW (kg)	LV (cm)	RV (cm)	Septum (cm)	HW/BW (g/kg)	RV/LV	LV/Sept	LV/HW (mm/g)
All GRMD (26)	118.04 (±50.9)	15.43 (±7.47)	1.09 (±0.27)	0.46 (±0.14)	0.98 (±0.25)	8.74 (±5.33)	0.43 (±0.11)	1.15 (±0.33)	0.11 (±0.04)
GRMD >6 months (21)	135.14 (±41.1)*	17.4 (±6.98)*	1.16 (±0.25)*‡	0.5 (±0.13)*†	1.03 (±0.24)*	9.27 (±5.8)	0.44 (±0.12)	1.18 (±0.34)‡	0.09 (±0.02)
Carrier (5)	175.6 (±68.1)	15.32 (±3.22)†	1.38 (±0.16)‡§	0.66 (±0.05)†‡	1.22 (±0.17)†	12.32 (±6.44)	0.48 (±0.06)	1.14 (±0.12)§	0.09 (±0.05)
Normal (7)	210.83 (±30)*	25.09 (±0.9)*†	1.86 (±0.05)*§	0.9 (±0.14)*‡	1.91 (±0.05)*†	8.48 (±0.10)	0.49 (±0.04)	0.99 (±0.09)‡§	0.09 (±0)
GRMD by age (*N*)									
<6 months (5)	46.2 (±3.87)	7.16 (±1)	0.8 (±0.14)	0.3 (±0)	0.78 (±0.17)	6.52 (±0.62)	0.39 (±0.07)	1.05 (±0.21)	0.11 (±0.04)
6–12 months (7)	109.86 (±17.14)	17.67 (±7.12)	1.19 (±0.2)	0.57 (±0.12)	1.17 (±0.22)	6.90 (±1.88)	0.48 (±0.07)	1.02 (±0.11)	0.1 (±0.01)
>12–24 months (4)	94.75 (±8.1)	16.78 (±6.1)	0.95 (±0.21)	0.39 (±0.05)	0.98 (±0.04)	6.36 (±1.96)	0.42 (±0.06)	0.97 (±0.19)	0.1 (±0.02)
6–24 months (11)	104.36 (±16.24)	17.35 (±6.78)	1.10 (±0.23)	0.50 (±0.13)	1.10 (±0.20)	6.70 (±1.93)	0.46 (±0.07)	1.00 (±0.15)	0.11 (±0.01)
>24 months (10)	169 (±32.57)	17.46 (±7.2)	1.23 (±0.25)	0.5 (0±.12)	0.95 (±0.25)	12.09 (±7.16)	0.43 (±0.15)	1.37 (±0.39)	0.09 (±0.02)

*/†, $p < 0.001$; ‡/§, $p < 0.05$.

Table 1. *Averages of gross heart measurements for Golden Retriever muscular dystrophy (GRMD), carrier, and normal dogs.*

Group (*N*)	Semi-quantitative average lesion score	Frequency for individual lesions: Fatty infiltration	Inflammation	Acute necrosis	Mineral	Vascular changes	Purkinje fiber vacuolation
GRMD age groups (*N*)							
<6 months (5)	0.33	-	-	-	-	-/+	+
6–12 months (7)	0.85	+	+++	+	+++	++	++
>12–24 months (4)	0.73	+	++	+	+	+	+++
>2 years (10)	1.63	++++	++	-/+	+++	++	++
Carrier (5)	0.55	++++	+	-/+	+	+	+
Normal (7)	0.30	+	+	-/+	-	+	+

The second column from the left depicts the semi-quantitative average score severity of all lesions taken together across left ventricle and right ventricle. The six columns to the right depict the percentage of all examined sections with the individual lesions listed: - = 0, -/+ <0.5, + = 0.5–20, ++ = 20–30, +++ = 30–40, ++++ >40.

Table 2. *Averages of histologic changes for groups.*

changes. The six assessed lesions included the following: fatty infiltration (absent/present), acute necrosis (absent/present), inflammatory infiltrates (none, primarily histiocytic, or primarily lymphoplasmacytic), mineralization (absent/present), Purkinje fiber vacuolation (positive if 50% or more of overall fiber cytoplasm was affected by vacuolation), and the nature of vascular changes (none, fibrosis, wall hypertrophy, and intimal hypertrophy).

The approximate percentage of examined sections from the whole heart with the six individual lesions mentioned above was semi-quantitatively scored using a modified "+" approach, whereby (–) = 0, (–/+) <0.5%, (+) = 0.5–20%, (++) = 20–30%, (+++) = 30–40%, and (++++) >40% (**Tables 2, 3**). Additionally, the primary lesion localization within each segment was classified as either subepicardial (outer 1/3), mid-myocardial (middle 1/3), subendocardial (inner 1/3), or panmyocardial (evenly distributed across the wall) (**Figure 2**).

Trichrome slides were quantitatively analyzed for percentage fibrosis. The NDPI files for each slide were exported as a JPEG at × 5 magnification using the NDPI to OME-TIFF Converter v1.5 (https://matthias-baldauf.at/software/ndpi-converter/). These JPEGs were cropped in Graphic Converter (http://www.graphic-converter.net/) to remove duplicate tissue sections and

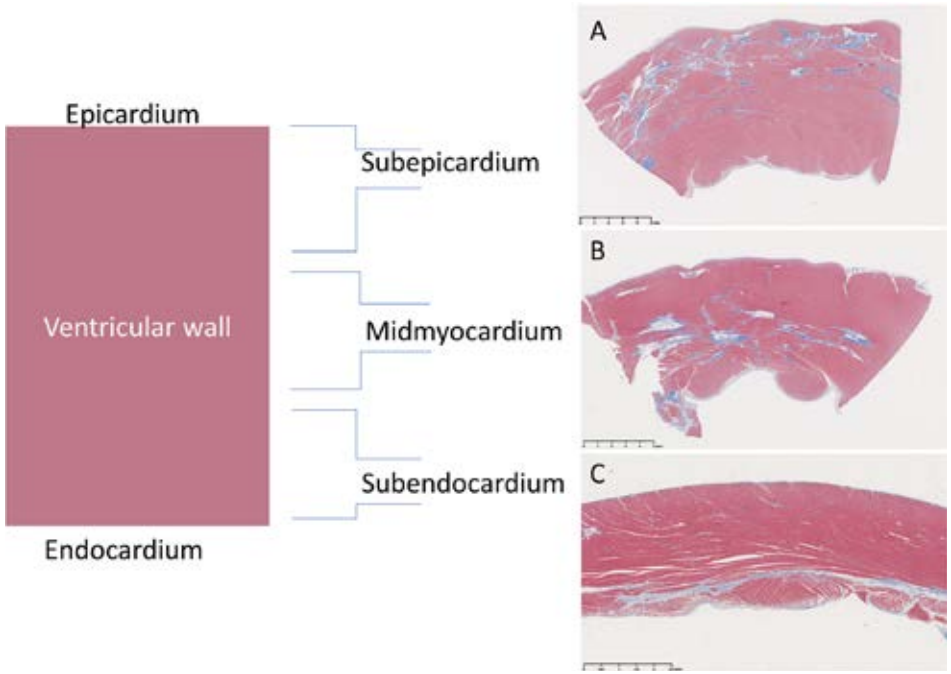

Figure 2. *Representation of distributions of fibrotic lesions within the ventricular wall of Golden Retriever muscular dystrophy (GRMD) dogs using a trichrome stain which stains collagen blue and muscle fibers red. (**A**) The sub-epicardial myocardium (male, 3-years-old) is reportedly preferentially affected in GRMD dogs (pictured) and Duchenne muscular dystrophy boys (not pictured). (**B**) However, the mid-myocardium (male, 4-years-old) may predominate. (**C**) Subendocardial changes were rare and only seen in the right ventricle (female, 1-year-old).*

large blood clots. The final JPEGS were analyzed in ImageJ using batch macros (Supplementary Data S1) to distinguish the percentage of blue staining from the total area with staining.

Cardiac Magnetic Resonance Imaging

Some affected GRMD dogs in this study were part of a separate natural history imaging study (38) and had their cardiac function assessed prior to pathological collection. The cardiac magnetic resonance (CMR) scans were performed as previously described (38), using a 3-T MRI machine (Siemens 3T Magnetom Verio, Siemens Medical Solutions) while the dogs were under general anesthesia. To identify the fibrotic lesions, late gadolinium enhancement (LGE) and a semi-quantitative scoring method (from 0 to 2; none to marked enhancement) was applied to indicate the

Age (months) and sex	Semi-quantitative lesion score	Frequency for individual lesions listed					
		Fatty infiltration	Inflammation	Acute necrosis	Mineral	Vascular changes	Purkinje fiber vacuolation
GRMD							
3 F	0.2	-	-	-	-	-	+
3 F	0.4	-	-	-	-	-	+++
3 F	0.58	-	-	-	-	-/+	-
3 M	0.16	-	-	-	-	-	-/+
3 M	0.22	-	-	-	-	-/+	+++
10 M	0.19	-/+	-/+	-	-	+	++++
11 F	1.05	++	++++	-/+	++++	+	-
11 M	0.3	-/+	+	-	-	+	++
12 F	1.47	++++	++++	-/+	++++	+++	+++
12 F	0.76	-	++++	++++	++++	++	-/+
12 F	1.39	-	++++	++	+++	+	+
12 M	0.81	-	++	+	+	++	++++
15 M	0.67	-	+	-	-/+	+	++
17 M	0	-	-	-	-	+	++++
21 F	1.29	++	++++	+	+	+	++
21 F	0.95	-/+	++	-/+	+	+	+++
28 F	1.93	+++	++	-/+	+++	+	-
36 M	0.95	++++	+++	-/+	++++	-/+	++++
38 M	1.19	++++	+	+	-	+++	++++
40 F	1.74	++++	+	+	++++	+	+
40 F	1.95	++++	-	-	+++	++++	-
40 M	1.86	++++	+	-	+	++	++
45 F	2.26	++++	+	-	++++	++++	+
51 M	2.38	++++	++++	-	+	+	++++
76 M	1.07	++++	++++	-	++++	+++*+	-
76 M	1	++++	+	-	+	+	++
Carrier							
3 F	0.13	-	-	-	-	-	-
12 F	0.05	+	-/+	-	++	+	+
46 F	1.4	++++	++++	+	+	++	-
56 F	0.37	++++	-	-	-	+	-
65 F	0.80	++++	+	-/+	-	++	+
Normal							
22 F	0.38	+	-	-/+	-	-	+
36 F	0	-	+	-	-	+	-/+
46 F	0.68	-/+	++++	-	-	-/+	-
61 M	0.14	-	-	-	-	+	+
75 F	0.35	+++	-/+	+	-	+	++
102 F	0.09	+	-	-	-	-/+	-
124 M	0.45	++	+	+	-	-	-

Table 3. *Lesion frequency across the heart for individual dogs.*

severity of fibrosis in each myocardial segment as previously described (38). The LV segmentation method in CMR was similar to the histologic segmentation, with both based on the same standard of 17 LV segments (36) and modified for canine heart. The LV lesion distribution was further compared between the CMR and pathologic assessments.

Statistics

Descriptive statistics were calculated for each variable, including sex and age. Gross measurements were averaged for groups, and means were compared with t-tests. Two-sample F-test for variance was done to compare variability in heart weight (HW)/body weight (BW) ratios between groups. Sections of the heart were categorized into 25 regions for comparisons (as described above, 17 LV segments, 4 RV segments, the left and right atria, and the atrioventricular and sinoatrial nodes). One-way analysis of variance (ANOVA) was conducted by comparing the mean and standard deviation of fibrosis percentage and semi-quantitative lesion scores across all regions of the heart and comparing fibrosis percentage among GRMD, carrier, and normal specimens. Ordinal logistic regression was used to determine

if the ordered independent variable, age, was associated with an increase in semi-quantitative cross-sectional lesion score. The average number of sections with each of the six individual lesions detailed above was calculated, and an ANOVA was used to compare the frequency of change among GRMD, carrier, and normal as well as between GRMD age groups for each feature. An independent-sample t-test comparing fibrosis percentage was calculated, stratified by the sex of the dog from which the specimen was obtained. An ordered logistic regression was run, comparing a rise in semi-quantitative lesion and vascular scores. Finally, Spearman's rank-order analysis was performed to evaluate the correlation between the LGE and pathological scores, and an ANOVA was performed to compare the mean value of fibrosis percentage and LGE scores within the LV sections across the hearts of seven dogs. Statistics were calculated using STATA 15 (College Station, TX, USA) and Microsoft Excel (Redmond, WA, USA).

Results

Gross Findings

No gross lesions were noted in any of the five affected dogs under 6 m of age. Older dogs had multiple lesions that varied in severity and distribution. Of the 10–12-m-old dogs, 5/7 had gross changes, including LV (3/7) or RV (1/7) pallor and streaking, and 3/7 had fibrotic or mineralized foci in the papillary muscle. Only 1/7 had clear concomitant LV and RV dilation on gross exam. In the four dogs 12–24 m old, one each had RV (1/4) or LV (1/4) dilation. All ten dogs >24 m had gross changes, including LV dilation (7/10); RV dilation (4/10); atrial dilation (2/10); thin ventricular walls (2/10); and pallor and streaking in the LV (6/10), RV (3/10), and septum (3/10) or pallor with mineralization in the papillary muscle (3/10). In carrier dogs, 4/5 (all >12 m) had gross changes, including thickening of the LV and septum (3/5), right auricle enlargement (1/5), and LV and septal pallor and streaking (1/5).

Furthermore, t-tests were used to compare mean gross measurements among groups (**Table 1**). For BW, HW, and ventricular wall measurement comparisons, the immature (<6 m) dogs were excluded, unless otherwise noted, since HW/BW and ventricular ratios differ even between normal immature and adult dogs (39). Based on BW, normal hounds were significantly heavier (25.09 ± 0.09 kg) than either the carrier (15.32 ± 3.22 kg) or adult GRMD dogs (17.4 ± 6.98 kg; $p < 0.001$ for both); the BW of carrier and adult GRMD dogs was not significantly different. Similarly, average HW differed among groups, with adult GRMD (135.14 ± 41.05 g) < carrier (175.6 ± 68.9 g) < normal (210.83 ± 0.05g) (**Table 1**), but the HW disparity was only significant ($p < 0.001$) between normal and GRMD. To better account for the effect of body size on heart weight, HW/BW ratios were calculated. The HW/BW ratio did not differ among GRMD (8.74 ± 5.33), carrier (12.32 ± 6.44), and normal dogs (8.48 ± 0.10) when comparing all ages or when comparing only dogs >6 m (9.27 ± 5.80) (**Table 1**), suggesting that the lower HW in GRMD dogs was due to their smaller stature. The results for individual dogs are included in (Supplementary **Table 1**).

A two-sample F-test for variance was done to compare the variability in HW/BW ratios in the dogs. Interestingly, GRMD dogs >24 m and carriers >12 m had a significantly greater variance in the HW/BW ratios than either normal dogs or GRMD dogs <24 m, reflecting the wide phenotypic variation and disease progression in older dogs. In the GRMD dogs >24 m, the HW/BW ratio ranged from 5.85 to 31.4 g/kg (Supplementary **Table 1**), with four dogs falling well-above the previously reported range of 4.53 to 10.04 g/kg in large adult dogs (39, 40). Similarly, the 3 carrier dogs >24 m (28–76 m) had higher HW/BW ratios of 13.5 to 23.1 g/kg. The BW did not differ between GRMD dogs >24 m vs. those <24 m of age, but the HW was significantly higher in the older

group (169 ± 32.6 vs. 104.4 ± 16.2 g; p < 0.001). This suggests that increased the HW/BW ratio is driven by a relative increase in HW in the older dogs.

Comparing the measurements among groups, the average LV thickness varied significantly: GRMD (1.09 ± 0.27 cm) < carrier (1.38 ± 0.16 cm) < normal (1.86 ± 0.05 cm) (p < 0.05) (**Table 1**), but the ratio of RV to LV thickness did not differ. Of the five carriers, four had subjective wall and papillary muscle thickening relative to the heart size on gross exam. However, when correcting the LV thickness for overall HW, the groups were not significantly different (**Table 1**), which suggests that hearts with thicker walls were proportionally heavier.

Semi-quantitative Lesion Scoring in GRMD Dogs

Using both H&E- and trichrome-stained images, the sections were scored semi-quantitatively based on the total cross-sectional area percentage, as generally described by Kane et al. (35) (0 = none, 1 = 1–10%, 2 = 11–20%, 3 = 21–30%, and 4 >30%). The heart sections were categorized into 25 regions for comparisons, as described above. Among GRMD dogs, the scores for individual sections varied from 0.7 (several sites) to 1.4 (basal anterolateral). The scores for carriers were lower, varying from 0.3 to 1.2, and the sites with greater/lesser involvement did not correspond to the GRMD group. Normal dogs had lower scores, ranging from 0.1 to 0.7. The overall average cross-sectional lesion area was higher in the GRMD vs. normal dogs (1.02 vs. 0.3; p < 0.001). While the average score for carriers (0.6) was intermediate, it was not significantly different from either GRMD or normal dogs. On evaluation of one-way ANOVA comparing the average cross-sectional area score among sections, no section had a significantly higher or lower cross-sectional area score. The values for individual dogs and section averages are shown in (Supplementary **Table 2**).

Ordinal logistic regression was used to determine if the ordered independent variable, age, was associated with an increase in semi-quantitative lesion score. The scores for each section showed a highly statistically significant (p < 0.001) correlation with age, consistent with disease progression over time.

Fatty Infiltration

Fatty infiltration (**Figures 3A,B**) was frequently seen in the hearts from older GRMD and carrier dogs (**Table 2**). While the percentage of affected sections in each normal heart ranged from 0 to 30%, GRMD and carrier dogs >24 m all had >50% of sections showing fatty infiltration and degeneration. In GRMD dogs >24 m, 195/232 (84%) of the examined sections had fatty change. A similar percentage of sections (56/76, 74%) in carriers also showed fatty degeneration, while only 18/149 (12%) of normal sections had this lesion. However, only the differences between GRMD and normal dogs were significant (p < 0.01), probably due to the relatively low number of carriers.

Fatty infiltration and degeneration increased with age. None was seen in any dog <6 m. The GRMD dogs >24 m had a significantly higher proportion of sections with fatty infiltration (84.05%) than any of the younger GRMD groups (0%, 6 m; 14.75%, 6–12 m; 16.95%, >12–24 m; p < 0.001) (**Table 2**). The same was likely true for carriers, in which only two sections in one dog <12 m had fatty infiltration, although the numbers were too small to determine significance. No normal dog was <22 m; the oldest three dogs had the highest number of affected sections in this group (**Table 3**).

Fatty replacement of the mid-myocardium was a prominent feature in the RV of some GRMD dogs (**Figure 3C**), with only small bands of muscle remaining on either side of a central band of adipose tissue. This pattern was not observed in the left ventricle, where patchy areas of fat tended to surround vessels and be mixed with fibrosis (**Figure 3A**).

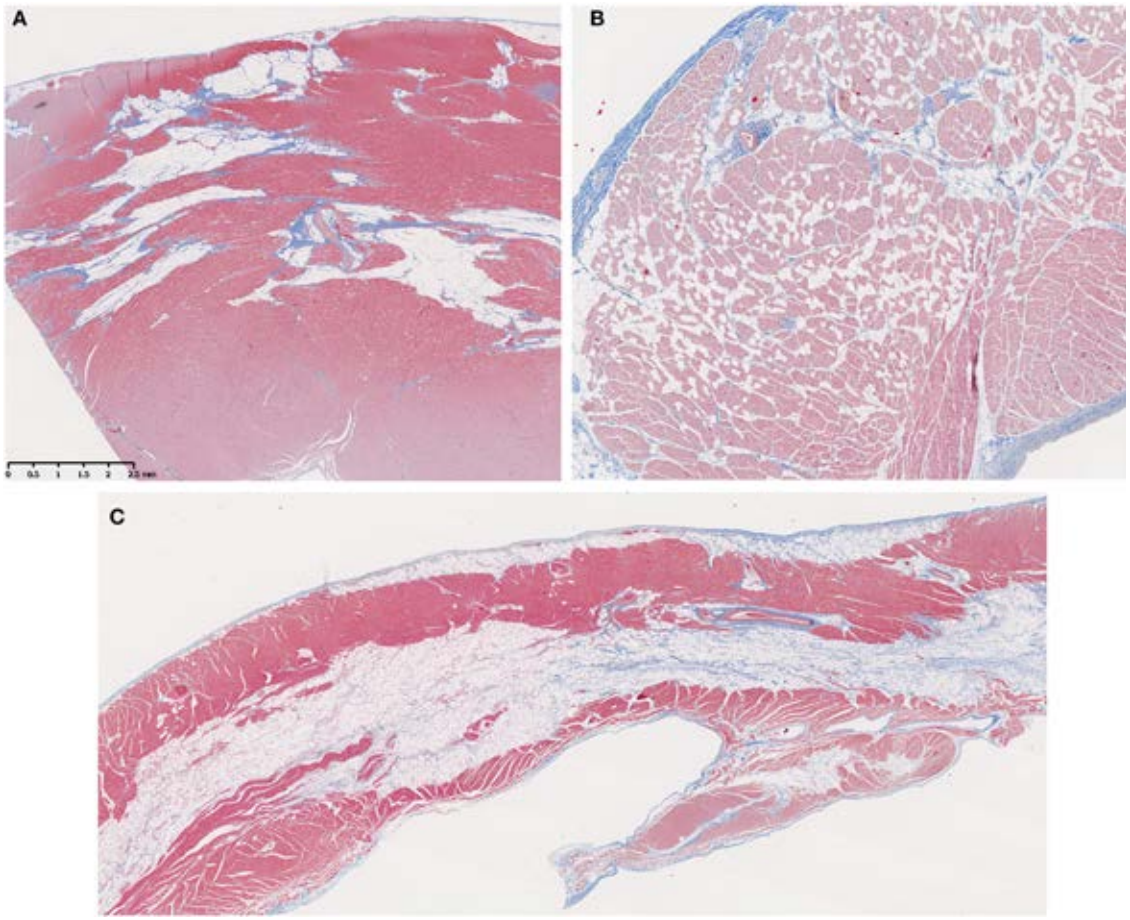

Figure 3. *Fatty infiltration was a prominent feature in older Golden Retriever muscular dystrophy (GRMD) dogs. (**A**) A section of left ventricle free wall from a 3-years-old female GRMD dog shows large bands of fat (non-staining vacuolated tissue) replacing normal myocardial muscle (red) and predominating over fibrosis (blue). (**B**) In some cases, fatty infiltration was more diffuse with individual or small clusters of fat cells scattered throughout the myocardium (male, 1-year-old). (**C**) In several dogs, the RV showed striking mid-myocardial replacement by bands of fat with minimal fibrotic tissue (male, 3.5-years-old). In these trichrome-stained sections, muscle fibers = red, collagen = blue, and fat cells = non-staining vacuolated tissue; × 10 original magnification.*

Acute Necrosis

Of the 26 GRMD dogs, 0/5 <6 m (0%), 5/7 6–12 m (71%), 2/4 12–24 m (50%), and 4/10 >24 m (40%) had at least one section with acute coagulative necrosis (**Figure 4**). Nearly half the number of GRMD dogs with this change (5/11) had three or more sections with acute necrosis. Over half the number of dogs with acute necrosis (7/11) were 6–24 m, pointing to the relatively early onset of this lesion. Acute necrosis was found at least once in the 17 LV and 4 RV sections that were examined in each dog, with no one heart section having a higher likelihood of lesions. Acute necrosis was not found in the atria. Incidentally, 3/7 normal dogs and 2/5 carrier dogs, each >24 m, also had at least one, but no more than three, sections with acute myocardial necrosis (**Table 3**).

One 12-m-old female GRMD dog had markedly more affected sections (14/27 heart segments) with acute myocardial necrosis. This dog had an incident of marked abdominal breathing and dark urine of undetermined cause following anesthesia for wound treatment at ~6 m of age. No hyperthermia was documented, and blood oxygenation was maintained in the normal range. As part of a non-cardiac study, she was euthanized while under anesthesia at 12 m of age.

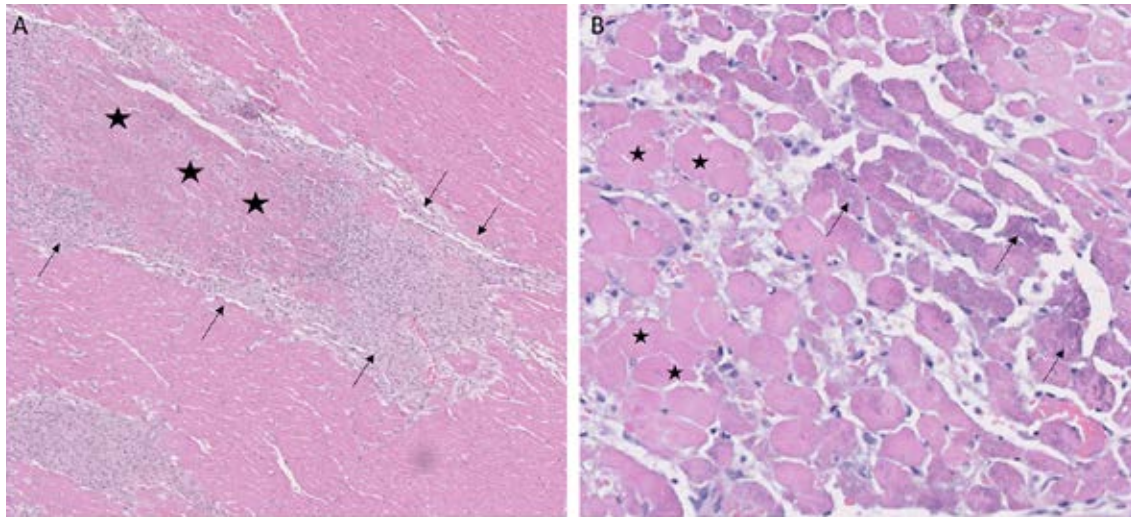

Figure 4. *Coagulative myocardial necrosis was a feature in some Golden Retriever muscular dystrophy hearts. (**A**) Areas of infarct-like coagulative necrosis characterized by loss of cytoplasmic detail and maintenance of tissue architecture (stars) are surrounded by proliferating macrophages and pericytes (arrows); H&E, × 5 magnification. (**B**) Acute coagulative necrosis with loss of nuclei and hypereosinophilic cytoplasm (representative cells with stars); cells on the margins of lesions have granular basophilic mineralization (arrows). 1-year-old female, H&E, × 20 magnification.*

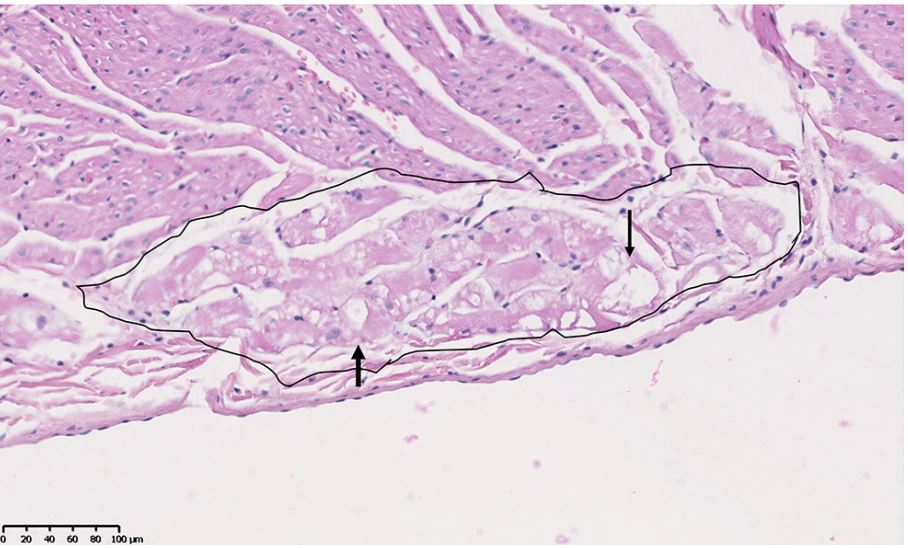

Figure 5. *Purkinje fiber (circled area) vacuolation (clear spaces indicated by arrowheads) in the heart of an 18-month-old male Golden Retriever muscular dystrophy dog. H&E, × 20 magnification.*

Inflammation

Inflammatory cells were seen in all disease groups and did not differ among ages, even if the youngest dogs were excluded (**Table 2**). While the overall scores for inflammation among normal, GRMD, and carrier dogs did not differ, there were differences in the cell types. Normal dogs had lymphoplasmacytic infiltrates, with one 46-m-old dog having infiltrates in almost every examined section. Although normal dogs were euthanized for non-cardiac lesions, two dogs initially examined for the study were excluded due to chronic Chagas disease (Trypanosoma cruzi) detected histologically and by PCR. T. cruzi was not detected in the remaining dogs, but exposure with associated lesions may explain the unexpected inflammation in some dogs from this group. Conversely, carriers and GRMD dogs had few sections with lymphoplasmacytic infiltration (four in all the examined dogs), with predominantly histiocytic inflammation. Histiocytic inflammation is typical secondary to degeneration and acute necrosis, initially occurring within 48 h and peaking at around 6 to 10 days, with slow resolution as the tissue remodels (41, 42).

Interestingly, when comparing the age groups, dogs <6 m had significantly fewer sections with inflammation (no inflammation) than 10–12- and

>24-m-old dogs ($p < 0.05$ and $p < 0.01$) but were not significantly different from the small group of 12–24-m-old dogs. Dogs of 10–12 m trended toward more inflamed sections than 12–24-m-old dogs ($p = 0.054$), while dogs >24 m had significantly more affected sections than 12–24-m-old dogs ($p < 0.05$). However, the 10–12-m- and >24-m-old dogs did not differ.

Mineralization

No mineral was noted in the hearts from normal dogs. All GRMD dogs >10 m had mineral in at least 1 section, with the exception of a 17-m-old male that had few lesions of any type (**Table 3**). The average number of sections containing mineral differed significantly ($p < 0.05$) among the GRMD age groups (<6 m: 0 sections, no detectable mineral; 6–12 m: 8.4 sections; 12–24 m: 2 sections; >24 m: 8.8 sections). The low numbers in the 12–24-m group likely reflect the relatively mild lesions in this age group in our study, as the degree of mineralization has previously been shown to decline with age (25). Two of five carriers also had mineral in at least one section.

Purkinje Fibers

Previous studies described but did not score Purkinje fiber vacuolation starting at under 6 m in the GRMD (CXMDJ) heart (27). Degenerative changes have also been described in Purkinje fibers of DMD boys (43). We scored Purkinje fiber vacuolation as present if vacuoles affected 50% or more of overall fiber cytoplasm (**Figure 5**). Of the 26 GRMD dogs, 4/5 (80%) <6 m, 6/7 (86%) 6–12 m, 4/4 (100%) 12–24 m, and 7/10 (70%) >24 m had at least one segment with vacuolation. The GRMD dogs had significantly increased fiber vacuolation (average, 6.9 affected sections; range, 0–19) compared to both carriers (1.4 sections; $p < 0.01$) and normal dogs (1.6 sections; $p < 0.01$) (**Tables 2, 3**). Purkinje fiber vacuolation did not differ between carrier and normal dogs nor among age groups in the GRMD cohort. Unlike the previous CXMDJ study, some GRMD dogs had no Purkinje fiber vacuolation detected. Moreover, vacuolation was not correlated with age nor with either semi-quantitative or quantitative lesion scores. Indeed, vacuolation was marked in some of the youngest dogs that otherwise had no lesions. The examination of H&E slides did not show an appreciable visual difference in the vacuoles among groups. The sinoatrial and atrioventricular nodes did not have observable abnormalities with H&E or trichrome staining.

Vascular Changes

Vascular changes of fibrosis and medial hypertrophy (**Figure 6**) were evaluated. Hearts from GRMD dogs <6 m had only rare changes. Those from adult (>6 m) GRMD dogs had a significantly greater frequency of vascular wall hypertrophy than normal dogs (5.2 vs. 1.7 sections; $p < 0.01$). Although low numbers prevented the detection of a difference between normal and carrier dogs, two of the carriers had hypertrophy in twice as many sections as the highest normal dogs.

Ordered logistic regression comparing a rise in the semi-quantitative cross-sectional score (which did not include vascular changes) and vascular scores in GRMD dogs showed a highly significant association between arteriolar hypertrophy and a rise in semi-quantitative severity score. For every 1-point increase in the vascular score, there was a 0.32 rise in the semi-quantitative severity score (z-score = 3.91, $p < 0.001$). Although correlated, it is not clear if there is a causative association or if both represent a cumulative increase in degenerative changes with age.

Additionally, aortic mineralization was a prominent feature in GRMD dogs, with 11/26 having prominent mineralization in the aorta: 0/5 <6 m, 4/7 6–12 m, 1/4 12–24 m, and 6/10 >24 m of age. Aortic mineralization was not noted in the carriers, while 2/7 of the oldest normal hounds had much smaller mineral deposits in the aortic wall.

Although endothelial hypertrophy was described by Valentine et al. in one dog, it was not detected in this study.

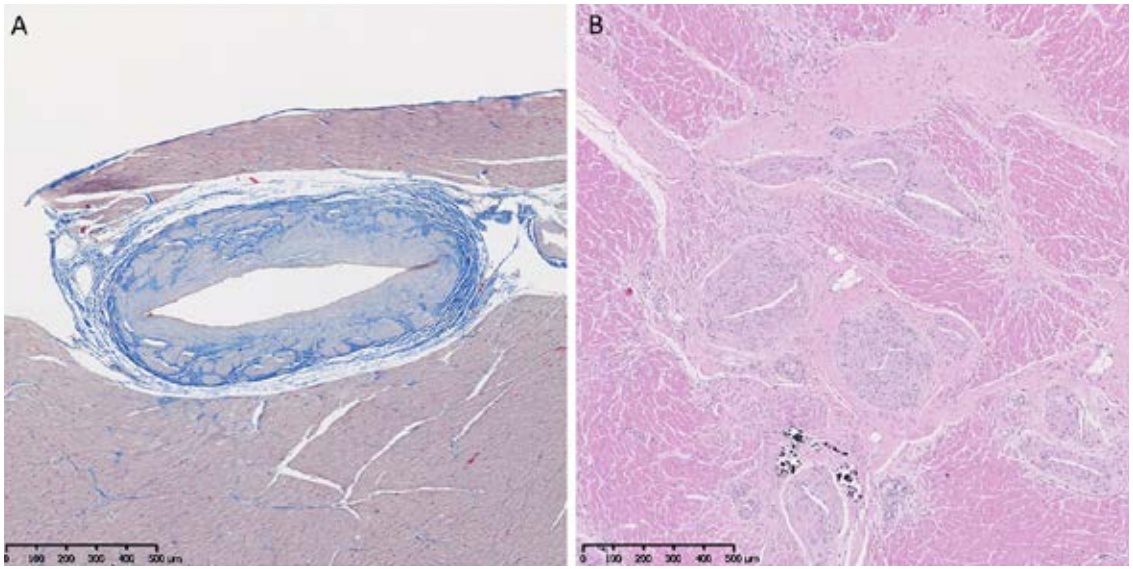

Figure 6. *(**A**) Increased fibrous tissue (blue) in an arteriole of a normal 3-year-old female. Trichrome, × 5 magnification. (**B**) Marked medial and intimal hypertrophy and vascular proliferation in arterioles in the heart of a 6-year-old male Golden Retriever muscular dystrophy dog. H&E, × 5 magnification.*

Quantitative Fibrosis

An analysis of variance was performed to assess the relationship between disease status and the percentage of cross-sectional area fibrosis as measured by trichrome staining. Data from all age groups, including more mildly affected dogs <6 m, were included. All three groups were highly significantly different ($p < 0.001$), with carriers having greater fibrosis (mean: 9.82 ± 1.01% blue staining) compared to GRMD (7.84 ± 0.25%), while normal dogs (4.35 ± 0.26%) had the lowest percentage. An independent t-test indicated no difference between the sexes in fibrosis.

Additionally, the degree of fibrosis staining differed significantly among GRMD age groups as determined by one-way ANOVA (f score = 15.01, $p < 0.001$). The Tukey post-hoc test revealed that the mean value at 6–12 m (5.38 ± 3.54%) was significantly lower than all other groups ($p < 0.05$) and that the 12–24-m group had the highest degree of fibrosis (9.80 ± 8.31%), being higher than even the >24-m group (8.28 ± 5.23%; $p < 0.05$). Lower values in the oldest dogs could reflect greater fat deposits, which are not detected by this method, with proportionally lower fibrosis.

One-way ANOVA showed a statistically significant difference between groups (f score = 7.64, $p < 0.001$) for the degree of fibrosis staining across the 17 LV and 4 RV sections from GRMD dogs. The Tukey post-hoc test revealed that the RV sections had the highest levels of fibrosis compared to the other sections but were similar among themselves ($p < 0.001$). The mid-LV anterolateral section had significantly lower fibrosis than the other sections.

Localization of Lesions Within the Wall

Previous studies of GRMD (25) and DMD (4) describe a diffuse cardiomyopathy with sometimes prominent sub-epicardial localization of fibrosis and other lesions. We scored the predominant localization in each section as primarily sub-epicardial, mid-myocardial, sub-endocardial, or transmural (even distribution across the myocardial wall) (**Figure 2**). Consistent with the previous observations, degenerative lesions were initially concentrated in the outer half of the myocardium (the sub-epicardium and mid-myocardium or the RV portion of the septum wall). In older dogs, more sections had transmural lesions as might be expected in a progressive disease. In general, the basal LV sections had a greater degree of outer (or sub-epicardial) lesions, while the RV and more apical portions had a more diffuse/transmural distribution overall or, as described above, a prominent mid-myocardial distribution, particularly in the more apical RV.

Correlation With LGE in Cardiac MRI

Correlating specific histologic findings with diagnostic imaging is the ultimate goal to better track cardiomyopathy progression. CMR with late gadolinium enhancement is a common modality for the clinical assessment of cardiomyopathy in GRMD and DMD (44). Eight GRMD dogs in this study were part of our cardiac imaging natural history study (38), and seven of them had sufficient LGE imaging scans within 7 days prior to heart collections, allowing a retrospective comparison with the pathologic results (the preliminary data of one dog was previously reported, including a representative visual comparison of gross, MRI, and histologic images) (38). In order to evaluate the correlation between LGE and the pathologic assessment within each section of the heart across the seven dogs, Spearman's rank-order analysis was performed. Observations without a pair between approaches were removed from analysis. This non-parametric test revealed a highly significant ($p < 0.0001$) monotonic relationship between these two methods, with a moderately positive relationship coefficient of 0.44. The LGE and semi-quantitative pathology scores for each section increased together, showing a consistency between the imaging and pathologic assessments. Fibrosis percentage was also compared to the three LGE categories across the same sections (N = 107) by performing a one-way ANOVA. The one-way ANOVA did not produce statistically significant results ($p = 0.493$). While there was a slight increase in fibrosis percentage in the highest LGE category, this is likely due to an increase in findings within this category compared to other groups. Based on this analysis, there is not a clear correlation between these variables.

Discussion

Myocardial disease in DMD is classically defined as dilated cardiomyopathy with more pronounced LV vs. RV lesions and functional changes (4–6). Prior studies of the GRMD cardiomyopathy have been limited by either the number of dogs studied or the anatomical sections assessed (25, 26). This paper describes the gross and histologic lesions across the heart in a large cohort of GRMD dogs ranging from 3 to 76 m in age. Like the previous more limited studies, we did not see an overall increase in HW/BW ratio typically associated with hypertrophic cardiomyopathy. However, the HW/BW ratios of some GRMD and carrier dogs were 3 to 4 times higher than the normal range (39, 40). While decreased BW due to muscle atrophy in GRMD dogs could contribute to increased HW/BW ratio, there was little difference in BW among the groups. On the other hand, HW increased in the oldest GRMD and carrier dogs. Moreover, HW was not directly correlated with age in the adult dogs. Taken together, these findings suggest that elevated HW/BW ratios in affected and carrier hearts occurred due to eccentric cardiac hypertrophy as previously reported in our dogs (38) and seen in canine dilated cardiomyopathy (45), mdx mice (46), and in some studies of DMD carriers (47) and DMD boys (48, 49).

Fibrosis is the principal pathological change in DMD cardiomyopathy, occurring initially in the posterobasal portion of the left ventricular free wall and extending to the outer third and ultimately the entire left ventricle and septum (4, 22). The right ventricle may be dilated but, generally, is free of fibrosis. The GRMD dogs of this study also had pronounced LV lesions, but in contrast to DMD, the RV was also heavily affected, although often with more fatty than fibrotic changes. The cardiac lesions in DMD are consistently more pronounced in the subepicardium, with sparing of muscle fibers closest to the left ventricular chamber. This was also the case in the GRMD dogs studied here, but we did not detect the distinct posterobasal concentration seen with early DMD lesions, instead finding more diffuse changes. Notably, involvement of

Tabla de contenido:

the papillary muscles and posterobasal area accounts for mitral valve regurgitation in DMD (50). The papillary muscles in GRMD dogs were also highly affected, although we were unable to link this to mitral valve dysfunction.

Similar to other studies (25, 26, 29) that assessed specific histopathologic changes, lesion severity tended to increase with age. Despite this general trend, some older dogs had few, if any, lesions (**Table 3**), in keeping with the marked phenotypic variation seen in the DMD cardiomyopathy (51, 52). Carrier hearts had lower levels of involvement, and normal dogs had the lowest scores. The lack of regional associations in our study may have occurred because the dogs were assessed at a single time point rather than longitudinally. The fact that many of our dogs were older and had lesions in all examined sections and that there were relatively few dogs in the potentially critical 12–24-m age range group may also have prevented the detection of regional differences in lesion development. With that said, our study had a distinct advantage in that hearts from dogs across many ages and stages of disease progression were included, while in DMD, routine cardiac biopsy is not commonly done, and autopsies are also uncommon, potentially causing the lesions outside of chronic fibrosis to be missed.

In quantifying fibrosis using the trichrome stain in adult (>6 m) dogs, those at 6–12 m had significantly less fibrosis than either of the two older groups. Unexpectedly, the dogs >24 m had less quantitative collagen staining than those at 12–24 m, even though half of these younger dogs had relatively mild lesions. The proportionally lower percentage of collagen staining may have occurred because lesions, such as fatty infiltration, non-compact fibrosis, and mineralization, are not stained by the methods used, and fat, in particular, was increased in the older dogs. Importantly, this demonstrates that methods aimed solely at fibrosis detection may underestimate phenotypic severity in older GRMD dogs. Semi-quantitative scoring of total cross-sectional lesion area and the percentages of sections showing various lesions more clearly demonstrated a strong correlation with age and disease progression. This scoring also highlighted the large phenotypic variation of cardiac lesions in GRMD dogs, similar to the variation in skeletal muscle disease (2). In particular, one 17-m-old GRMD male had no cardiac lesions. All semiquantitative scoring tasks were done by a single pathologist in this case. This method would likely have a higher inter-operator variability, making it unreliable for comparing results between studies without more robust agreement on scoring. Having multiple interpreters for each slide with a consensus score would likely improve the result reproducibility.

Even more than fibrosis, fatty infiltration was a feature of cardiomyopathy progression in older GRMD dogs. While some fatty infiltration may be seen with normal aging, this change was particularly pronounced in the GRMD dogs, as is seen with other chronic canine cardiomyopathies (45, 53–56). Lipomatous (fatty) metaplasia is also seen with chronic degenerative conditions in the hearts of dogs and humans, most frequently with chronic ischemic cardiomyopathy and ischemic scar replacement (57, 58), with an associated increased propensity for ventricular tachycardia and arrhythmias (53, 59). Although we cannot rule out a specific response to dystrophin deficiency, the occurrence of a similar fatty change in a variety of diseases suggests it is a general reaction to chronic myocardial degeneration and remodeling.

Interestingly, coagulative necrosis was seen in some GRMD dogs in the absence of vascular thrombosis. The severity of these changes correlated with the degree of vascular thickening. Given that the coronary vascular supply to the ventricles differs between dog and man (60), it is difficult to draw inferences regarding DMD cardiac disease pathogenesis. However, we have previously seen a syndrome of acute

myocardial infarction in GRMD dogs (61) that appears analogous to a condition in DMD (62). This has led to a speculation that dystrophin-deficient cardiomyocytes are operating in a state of functional hypoxia (61, 63, 64) and that a dystrophin-deficient muscle has reduced capacity to compensate for increased metabolic demands (65, 66). Coagulative necrosis is associated with anoxia/hypoxia, occurring often subsequent to ischemia, infarction, or toxicosis. Lesions are detected histologically at ~12–24 h post-event, become infiltrated by sheets of macrophages within 48–72 h, and contain foci of interstitial cell and vascular proliferation by 10 days to 6 weeks (41, 42). We found each of these lesions in all GRMD age groups older than 6 m, in keeping with the full range of cardiac necrosis and healing described by Malvestio et al. (29). Considering that vascular thrombosis is not a feature of DMD/GRMD, these changes more likely occur secondary to non-occlusive hypoxia. Extending the potential significance of vascular/hypoxic disease in GRMD cardiomyopathy, we also found a positive correlation between arteriolar hypertrophy and the most severe semi-quantitative cross-sectional lesion scores. Dystrophin-deficient mdx mice also have enhanced neointimal formation, with wall thickening and narrow lumens due to vascular smooth muscle proliferation (67). In principle, these changes could occur due to chronic degenerative lesions in dystrophin-deficient smooth muscle and might be a factor in the acute myocardial syndrome seen in DMD/GRMD. While increased wall thickness and connective tissue are a reported aging change in the cardiac arterioles of senescent dogs (68), the normal dogs in this study had significantly less smooth muscle hypertrophy than GRMD dogs, indicating that this change is part of disease progression.

Dystrophin deficiency in vascular smooth muscle in both mdx mice and GRMD dogs has been shown to have functional consequences, including altered sympathetic vasoregulation and reduced attenuation of vasoconstriction during contraction (67, 69–72). This is partly due to loss of sarcolemmal nNOS in skeletal and cardiac muscle, leading to decreased nitric oxide-induced vasodilation. However, the selective expression of dystrophin in vascular smooth muscle partially rectified the vasoregulatory responses (72) in mdx mice, suggesting that smooth muscle dystrophin may have a primary functional role in vasoregulation. In combination with the types of degeneration seen in the hearts of GRMD dogs of our study, these vascular changes could support the "two hits" hypothesis for lesions in dystrophin deficiency (73), with functional ischemia related to altered vasoregulation combined with increased susceptibility to metabolic stress leading to impaired cardiomyocyte survival.

Stereotypical ECG abnormalities are common in DMD and GRMD patients. The degenerative changes described in the Purkinje fibers of affected boys (43) and dogs (27) have been proposed as a possible contributing factor. Urasawa et al. (27) described marked abnormal vacuolation in Purkinje fibers associated with ultrastructural degenerative changes in young, crossbred beagles with the GRMD mutation (CXMDJ). We also detected increased Purkinje fiber vacuolation, starting with the youngest GRMD dogs, though this lesion was not present in all GRMD dogs, and normal dogs also had Purkinje fiber vacuolation. Interestingly, the carrier dogs of this study did not have Purkinje fiber vacuolation, even though they also have conduction abnormalities (35). Additionally, the degree of vacuolation did not correlate with cross-sectional lesion severity in our dogs. Due to the retrospective nature of this study, ECG was not available for correlation of vacuolar severity with conduction differences or arrhythmia.

The pattern of CMR LGE changes in DMD patients tends to parallel the distribution of histopathologic changes, beginning in the LV posterior basal and subepicardial wall (44). Although our LGE imaging quality was insufficient to

localize lesions to the subepicardial region, the pathological results were consistent with the LGE findings. Moreover, the semi-quantitative assessments for histopathologic lesion score and LGE severity were strongly correlated, further validating the association between our pathologic and CMR findings. Conversely, quantitative fibrosis percentage was not correlated with LGE. As with the Purkinje fiber changes, we did not have an opportunity to determine whether there was an association between ECG findings, such as the occurrence of deep Q waves, with septal fibrosis. This would require a detailed longitudinal prospective study.

While the data reported here substantially extended prior pathologic studies of GRMD cardiomyopathy, limitations included the inability to perfectly age-match dogs across disease groups, low number of carrier dogs, variation in phenotypic severity, and necessity for using normal control hearts from dogs outside the colony. Heart availability and age across disease groups were limited by the availability of dogs dying for other reasons. Since carrier and normal dogs are infrequently euthanized at young ages, these groups, in particular, lacked exact-age-matched controls. Here, we assessed a separate cohort of hound dogs outside our colony. Although minimal differences would be expected between hearts from normal dogs within and outside the colony, variable housing and management could have altered the cardiac phenotype—for instance, two dogs were excluded due to PCR-confirmed Chagas's disease, suggesting that all the normal dogs may have been exposed to infections not present in our colony. That may also explain the unexpected lymphoplasmacytic inflammation in some hearts from this group.

Like previous studies, cardiac pathology was limited or absent in our GRMD dogs <6 m, and changes would likewise not be expected in normal dogs, so the inability to compare directly likely had a minimal impact. Carrier dogs that are not used for breeding are routinely adopted out of the colony, limiting our access to tissue from this group. The lower numbers hindered our ability to detect significance between this disease group and the GRMD and normal dogs; however, the trends are intriguing, and more studies are warranted.

The conclusions drawn from non-longitudinal studies are also always limited by the phenotypic variation in disease expression among dogs. In our cohort, we had a low number of dogs and a high degree of phenotypic variation in the seemingly critical 6–12-m age range, while the 12–24-m group seemed to have an overall milder severity, including one dog with no lesions. This likely muddled the differences between the age groups. The mild to non-detectable disease in dogs of this age that had not had any cardiac-specific treatments highlights the importance of not relying on a single animal to determine treatment effects.

This study provides the largest comprehensive gross pathologic and histopathologic review of GRMD cardiomyopathy to date. Our findings highlight the differences in disease severity and suggest that semi-quantitative scoring is preferable to fibrosis quantification for assessing the overall lesion severity. The disease is universally progressive, but due to the difficulty in detecting early lesions pre-mortem, there is still debate over the sequence of cardiac lesion progression in GRMD and, by extension, DMD. Based on previously published findings and the results reported here, we suggest that two interacting factors are involved. Underlying metabolic deficiencies in cardiac muscle, such as calcium dysregulation, membrane fragility, poor response to hypoxia, and mitochondrial abnormalities, place the fibers under a constant metabolic strain. Over time, this may lead to individual fiber necrosis, mineralization, and dropout, with fatty transition in some fibers, particularly in areas of strain (i.e., basoinferior LV wall). Additionally, episodic stress in the face of the vascular changes we have described could produce non-throm-

botic infarction and loss of larger foci of myocardium compatible with large acute/subacute lesions in some dogs. Sequential episodes of damage may result in a stairstep cycle of damage, repair, and stabilization, with increasing strain, fatty metaplasia, and decreasing reserve over time.

Data Availability Statement

The raw data supporting the conclusions of this article will be made available by the authors, without undue reservation.

Ethics Statement

The animal study was reviewed and approved by the Institutional Animal Care and Use Committee at Texas A&M University.

Author Contributions

SS, JK, BW, and L-JG contributed to the conception and design of the study including sample collection protocols. SS and BW contributed to the interpretation of histologic changes. SS developed the interpretation categories, collected the hearts and samples, wrote the first draft and major revisions of the paper, and scanned and read the slides. SF developed the Image J macro. SF and SS collected the image J data. L-JG performed the CMR imaging, LGE data collection, and interpretation. GS performed the statistical analysis. SS, JK, GS, and L-JG wrote sections of the paper. All authors contributed to manuscript revision and read and approved the submitted version.

Funding

This work was part of the Ph.D. dissertation of SS, supported by a Zoetis-Morris Animal Foundation fellowship (grant number D14CA-903). The digital scanning of slides was supported through generous equipment sharing by the GI Lab at Texas A&M University. Amanda Bettis and Heather Heath-Barnett provided dedicated care of the dogs and maintenance of the colony.

Conflict of Interest

JK reports personal fees from Solid Biosciences as a paid consultant, outside the submitted work.

The remaining authors declare that the research was conducted in the absence of any commercial or financial relationships that could be construed as a potential conflict of interest.

Publisher's Note

All claims expressed in this article are solely those of the authors and do not necessarily represent those of their affiliated organizations, or those of the publisher, the editors and the reviewers. Any product that may be evaluated in this article, or claim that may be made by its manufacturer, is not guaranteed or endorsed by the publisher.

Supplementary Material

The Supplementary Material for this article can be found online at: https://www.frontiersin.org/articles/10.3389/fvets.2021.759585/full#supplementary-material

References

1. Valentine BA, Winand NJ, Pradhan D, Moise NS, de Lahunta A, Kornegay JN, et al. Canine X-linked muscular dystrophy as an animal model of Duchenne muscular dystrophy: a review. Am J Mol Genet. (1992) 42:352–6. doi: 10.1002/ajmg.1320420320
2. Kornegay JN, Bogan JR, Bogan DJ, Childers MK, Li J, Nghiem P, et al. Canine models of Duchenne muscular dystrophy and their use in therapeutic strategies. Mamm Genome. (2012) 23:85–108. doi: 10.1007/s00335-011-9382-y
3. Hoffman EP, Brown RH, Kunkel LM. Dystrophin: the protein product of the duchenne muscular dystrophy locus. Cell. (1987) 51:919–28. doi: 10.1016/0092-8674(87)90579-4
4. Frankel K, Rosser R. The pathology of the heart in progressive muscular dystrophy: epimyocardial fibrosis. Hum Pathol. (1976) 7:375–86. doi: 10.1016/S0046-8177(76)80053-6

5. Heymsfield SB, McNish T, Perkins JV, Felner JM. Sequence of cardiac changes in Duchenne muscular dystrophy. Am Heart J. (1978) 95:283–94. doi: 10.1016/0002-8703(78)90358-7
6. Spurney CF. Cardiomyopathy of duchenne muscular dystrophy: current understanding and future directions. Muscle Nerve. (2011) 44:8–19. doi: 10.1002/mus.22097
7. Prosser BL, Ward CW, Lederer WJ. X-ROS signaling: rapid mechano-chemo transduction in heart. Science. (2011) 333:1440–5. doi: 10.1126/science.1202768
8. Viola HM, Adams AM, Davies SM, Fletcher S, Filipovska A, Hool LC. Impaired functional communication between the L-type calcium channel and mitochondria contributes to metabolic inhibition in the mdx heart. Proc Natl Acad Sci. (2014) 111:E2905–14. doi: 10.1073/pnas.1402544111
9. Fanchaouy M, Polakova E, Jung C, Ogrodnik J, Shirokova N, Niggli E. Pathways of abnormal stress-induced Ca2+ influx into dystrophic mdx cardiomyocytes. Cell Calcium. (2009) 46:114–21. doi: 10.1016/j.ceca.2009.06.002
10. Markham LW, Brinkmeyer-Langford CL, Soslow JH, Gupte M, Sawyer DB, Kornegay JN, et al. GRMD cardiac and skeletal muscle metabolism gene profiles are distinct. BMC Med Genom. (2017) 10:21. doi: 10.1186/s12920-017-0257-2
11. Klietsch R, Ervasti JM, Arnold W, Campbell KP, Jorgensen AO. Dystrophin-glycoprotein complex and laminin colocalize to the sarcolemma and transverse tubules of cardiac muscle. Circ Res. (1993) 72:349–60. doi: 10.1161/01.RES.72.2.349
12. Iwata Y, Pan Y, Hanada H, Yoshida T, Shigekawa M. Dystrophin–glycoprotein complex purified from hamster cardiac muscle. Comparison of the complexes from cardiac and skeletal muscles of hamster and rabbit. J Mol Cell Cardiol. (1996) 28:2501–9. doi: 10.1006/jmcc.1996.9999
13. Holland A, Ohlendieck K. Proteomic profiling of the dystrophin-deficient mdx phenocopy of dystrophinopathy-associated cardiomyopathy. BioMed Res Int. (2014) 2014:1–15. doi: 10.1155/2014/246195
14. Birnkrant DJ, Ashwath M, Noritz GH, Merrill MC, Shah TA, Crowe CA, et al. Cardiac and pulmonary function variability in Duchenne/Becker muscular dystrophy: an initial report. J Child Neurol. (2010) 25:1110–5. doi: 10.1177/0883073810371003
15. Jin JB, Carter JC, Sheehan DW, Birnkrant DJ. Cardiopulmonary phenotypic discordance is common in Duchenne muscular dystrophy. Pediatr Pulmonol. (2019) 54:186–93. doi: 10.1002/ppul.24205
16. Posner AD, Soslow JH, Burnette WB, Bian A, Shintani A, Sawyer DB, et al. The correlation of skeletal and cardiac muscle dysfunction in Duchenne muscular dystrophy. J Neuromusc Dis. (2016) 3:91–9. doi: 10.3233/JND-150132
17. Hor KN, Mah ML, Johnston P, Cripe TP, Cripe LH. Advances in the diagnosis and management of cardiomyopathy in Duchenne muscular dystrophy. Neuromusc Disord. (2018) 28:711–6. doi: 10.1016/j.nmd.2018.06.014
18. Birnkrant DJ, Bushby K, Bann CM, Alman BA, Apkon SD, Blackwell A, et al. Diagnosis and management of Duchenne muscular dystrophy, part 2: respiratory, cardiac, bone health, and orthopaedic management. Lancet Neurol. (2018) 17:347–61. doi: 10.1016/S1474-4422(18)30025-5
19. Fayssoil A, Nardi O, Orlikowski D, Annane D. Cardiomyopathy in Duchenne muscular dystrophy: pathogenesis and therapeutics. Heart Fail Rev. (2010) 15:103–7. doi: 10.1007/s10741-009-9156-8
20. Bostick B, Yue Y, Long C, Marschalk N, Fine DM, Chen J, et al. Cardiac expression of a mini-dystrophin that normalizes skeletal muscle force only partially restores heart function in aged mdx mice. Mol Ther. (2009) 17:253–61. doi: 10.1038/mt.2008.264
21. Łoboda A, Dulak J. Muscle and cardiac therapeutic strategies for Duchenne muscular dystrophy: past, present, and future. Pharm Reports. (2020) 72:1227–63. doi: 10.1007/s43440-020-00134-x
22. Perloff JK, Roberts WC, de Leon AC, O'Doherty D. The distinctive electrocardiogram of Duchenne's progressive muscular dystrophy. Am J Med. (1967) 42:179–88. doi: 10.1016/0002-9343(67)90017-4
23. Moise SN, Valentine BA, Brown CA, Erb HN, Beck KA, Cooper BJ, et al. Duchenne's cardiomyopathy in a canine model: electrocardiographic and echocardiographic studies. J Am Coll Cardiol. (1991) 17:812–20. doi: 10.1016/S0735-1097(10)80202-5

Tabla de contenido:

24. James J, Kinnett K, Wang Y, Ittenbach RF, Benson WD, Cripe L. Electrocardiographic abnormalities in very young Duchenne muscular dystrophy patients precede the onset of cardiac dysfunction. Neuromuscul Disord. (2011) 21:462–7. doi: 10.1016/j.nmd.2011.04.005

25. Valentine BA, Cummings JF, Cooper BJ. Development of duchenne-type cardiomyopathy: Morphologic studies in a canine model. Am J Pathol. (1989) 135:671–8.

26. Yugeta N, Urasawa N, Fujii Y, Yoshimura M, Yuasa K, Wada MR, et al. Cardiac involvement in Beagle-based canine X-linked muscular dystrophy in Japan (CXMDJ): electrocardiographic, echocardiographic, and morphologic studies. BMC Cardiovascul Disord. (2006) 6:1–13. doi: 10.1186/1471-2261-6-47

27. Urasawa N, Wada MR, Machida N, Yuasa K, Shimatsu Y, Wakao Y, et al. Selective vacuolar degeneration in dystrophin-deficient canine Purkinje fibers despite preservation of dystrophin-associated proteins with overexpression of Dp71. Circulation. (2008) 117:2437–48. doi: 10.1161/CIRCULATIONAHA.107.739326

28. Miyazato LG, Beretta DC, Engracia Filho JR, Moraes FR, Moraes JR. Involvement of organic systems in golden retriever X-linked muscular dystrophy. Braz J Vet Pathol. (2011) 4:87–94. Available online at: http://lareferencia.redclara.net/vufind/Record/BR_625bbab58155f201733038b302714389

29. Malvestio L, Martins I, Moares F, Moares JRE. Histopathologic evolution of cardiomyopathy in a canine model of Duchenne muscular dystrophy. J Adv Vet Res. (2015) 5:121–6. Available online at: http://citeseerx.ist.psu.edu/viewdoc/download?doi=10.1.1.933.1085&rep=rep1&type=pdf

30. Nigro G, Somma S, Comi L, Politano L, Papparella S, Restucci B, et al. Structural basis of cardiomyopathy in Duchenne/Becker carriers. Ann NY Acad Sci. (1995) 752:108–10. doi: 10.1111/j.1749-6632.1995.tb17412.x

31. van Westrum S, Hoogerwaard E, Neurology DL. Cardiac abnormalities in a follow-up study on carriers of Duchenne and Becker muscular dystrophy. Neurol. (2011) 77:62–6. doi: 10.1212/WNL.0b013e318221ad14

32. Holloway S, Wilcox D, Wilcox A, Dean J, Berg J, Goudie D, et al. Life expectancy and death from cardiomyopathy amongst carriers of Duchenne and Becker muscular dystrophy in Scotland. Heart. (2008) 94:633–6. doi: 10.1136/hrt.2007.125948

33. Hoogerwaard EM, Wouw PA, Wilde AAM, Bakker E, Ippel PF, Oosterwijk JC, et al. Cardiac involvement in carriers of Duchenne and Becker muscular dystrophy. Neuromusc Disord. (1999) 9:347–51. doi: 10.1016/S0960-8966(99)00018-8

34. Cooper BJ, Gallagher EA, Smith CA, Valentine BA, Winand NJ. Mosaic expression of dystrophin in carriers of canine X-linked muscular dystrophy. Lab Investig. (1990) 62:171–8.

35. PubMed Abstract | 35. Kane AM, DeFrancesco TC, Boyle MC, Malarkey DE, Ritchey JW, Atkins CE, et al. Cardiac structure and function in female carriers of a canine model of Duchenne muscular dystrophy. Res Vet Sci. (2013) 94:610–7. doi: 10.1016/j.rvsc.2012.09.027

36. Cerqueira MD, Weissman NJ, Dilsizian V, Jacobs AK, Kaul S, Laskey WK, et al. Standardized myocardial segmentation and nomenclature for tomographic imaging of the heart. J Cardiovasc Magn Reson. (2002) 4:203–10. doi: 10.1081/JCMR-120003946

37. Palate BM, Denoël SR, Roba JL. A simple method for performing routine histopathological examination of the cardiac conduction tissue in the dog. Toxicol Pathol. (1995) 23:56–62. doi: 10.1177/019262339502300107

38. Guo L-J, Soslow JH, Bettis AK, Nghiem PP, Cummings KJ, Lenox MW, et al. Natural history of cardiomyopathy in adult dogs with golden retriever muscular dystrophy. J Am Heart Assoc. (2019) 8:e012443. doi: 10.1161/JAHA.119.012443

39. Northup DW, Liere EJ, van Stickney JC. The effect of age, sex, and body size on the heart weight-body weight ratio in the dog. Anat Rec. (1957) 128:411–7. doi: 10.1002/ar.1091280305

40. Bienvenu JG, Drolet R. A quantitative study of cardiac ventricular mass in dogs. Can J Vet Res. (1991) 55:305–9.

41. PubMed Abstract | 41. Dewald O, Ren G, Duerr GD, Zoerlein M, Klemm C, Gersch C, et al. Of mice and dogs: species-specific differences in the inflammatory response following myocardial infarction. Am J Pathol. (2004) 164:665–77. doi: 10.1016/S0002-9440(10)63154-9

42. Grant Maxie M, Robinson WF. Cardiovascular System. In: Jubb, Kennedy & Palmer's Pathology of Domestic Animals. 5th ed.
43. Nomura H, Hizawa K. Histopathological study of the conduction system of the heart in Duchene progressive muscular dystrophy. Pathol Int. (1982) 32:1027–33. doi: 10.1111/j.1440-1827.1982.tb02082.x
44. Bilchick KC, Salerno M, Plitt D, Dori Y, Crawford TO, Drachman D, et al. Prevalence and distribution of regional scar in dysfunctional myocardial segments in Duchenne muscular dystrophy. J Cardiovasc Magn Reson. (2011) 13:1–8. doi: 10.1186/1532-429X-13-20
45. Tidholm A, Jönsson L. Histologic characterization of canine dilated cardiomyopathy. Vet Pathol. (2005) 42:1–8. doi: 10.1354/vp.42-1-1
46. Wagner S, Knipp S, Weber C, Hein S, Schinkel S, Walther A, et al. The heart in Duchenne muscular dystrophy: early detection of contractile performance alteration. J Cell Mol Med. (2012) 16:3028–36. doi: 10.1111/j.1582-4934.2012.01630.x
47. Politano L, Nigro V, Nigro G, Jama PV. Development of cardiomyopathy in female carriers of Duchenne and Becker muscular dystrophies. JAMA. (1996) 275:1335–8. doi: 10.1001/jama.1996.03530410049032
48. Nigro G, Comi LI, Politano L, Bain RJI. The incidence and evolution of cardiomyopathy in Duchenne muscular dystrophy. Int J Cardiol. (1990) 26:271–7. doi: 10.1016/0167-5273(90)90082-G
49. Bornaun H, Muhtar Yilmazer M, Dedeoglu S, Dedeoglu R. An exhaustive echocardiographic analysis of left ventricular structure and functions in children with duchenne muscular dystrophy. Iran J Pediatr. (2018) 28:e62204. doi: 10.5812/ijp.62204
50. CrossRef Full Text | 50. Sanyal SK, Johnson WW, Dische MR, Pitner SE, Beard C. Dystrophic degeneration of papillary muscle and ventricular myocardium. A basis for mitral valve prolapsed in Duchenne's muscular dystrophy. Circulation. (1980) 62:430–8. doi: 10.1161/01.cir.62.2.430
51. Desguerre I, Christov C, Mayer M, Zeller R, Becane H-M, Bastuji-Garin S, et al. Clinical heterogeneity of Duchenne Muscular Dystrophy (DMD): definition of sub-phenotypes and predictive criteria by long-term follow-up. PLoS ONE. (2009) 4:e4347. doi: 10.1371/journal.pone.0004347
52. Pettygrove S, Lu Z, Andrews JG, Meaney FJ, Sheehan DW, Price ET, et al. Sibling concordance for clinical features of Duchenne and Becker muscular dystrophies. Muscle Nerve. (2014) 49:814–21. doi: 10.1002/mus.24078
53. Meurs KM. Boxer dog cardiomyopathy: an update. Vet Clin N Am Small Anim Pract. (2004) 34:1235–44. doi: 10.1016/j.cvsm.2004.05.003
54. Lobo L, Carvalheira J, Canada N, Bussadori C, Gomes J, Faustino A. Histologic characterization of dilated cardiomyopathy in Estrela mountain dogs. Vet Pathol. (2010) 47:637–42. doi: 10.1177/0300985810364511
55. Agudelo C, Svoboda M, Husnik R, Dvir S. Heart lipomatosis in domestic animals: a review. Vet Med. (2013) 58:252–9. doi: 10.17221/6806-VETMED
CrossRef Full Text | 56. Everett RM, McGann J, Wimberly HC, Althoff J. Dilated cardiomyopathy of Doberman Pinschers: Retrospective histomorphologic evaluation of heart from 32 cases. Vet Pathol. (1999) 36:221–7. doi: 10.1354/vp.36-3-221
57. Nucifora G, Aquaro GD, Masci PG, Barison A, Todiere G, Pingitore A, et al. Lipomatous metaplasia in ischemic cardiomyopathy: current knowledge and clinical perspective. Int J Cardiol. (2011) 146:120–2. doi: 10.1016/j.ijcard.2010.09.090
58. Baroldi G, Silver MD, De RM, Parodi O, Pellegrini A. Lipomatous metaplasia in left ventricular scar. Can J Cardiol. (1997) 13:65–71.
59. PubMed Abstract | 59. Samanta R, Pouliopoulos J, Thiagalingam A, Kovoor P. Role of adipose tissue in the pathogenesis of cardiac arrhythmias. Heart Rhythm. (2016) 13:311–20. doi: 10.1016/j.hrthm.2015.08.016
60. Kato T, Yasue T, Shoji Y, Shimabukuro S, Ito Y, Goto S, et al. Angiographic difference in coronary artery of man, dog, pig, and monkey. Path Interntl. (1987) 37:361–73. doi: 10.1111/j.1440-1827.1987.tb00371.x
61. Schneider S, Coleman A, Guo L-J, Tou S, Keene BW, Kornegay JN. Suspected acute myocardial infarction in a dystrophin-deficient dog. Neuromusc Disord. (2016) 26:361–6. doi: 10.1016/j.nmd.2016.02.005
62. Hor KN, Johnston P, Kinnett K, Mah ML, Stiver C, Markham L, et al. Progression of duchenne cardiomyopathy presenting with chest pain and troponin elevation. J Neuromuscul Dis. (2017) 4:307–14. doi: 10.3233/JND-170253

Tabla de contenido:

63. Sander M, Chavoshan B, Harris SA, Iannaccone ST, Stull JT, Thomas GD, et al. Functional muscle ischemia in neuronal nitric oxide synthase-deficient skeletal muscle of children with Duchenne muscular dystrophy. Proc Natl Acad Sci. (2000) 97:13818–23. doi: 10.1073/pnas.250379497

64. Rando TA. Oxidative stress and the pathogenesis of muscular dystrophies. Am J Phys Med Rehab. (2002) 81:S175. doi: 10.1097/00002060-200211001-00018

65. Nghiem PP, Bello L, Stoughton WB, Lopez SM, Vidal AH, Hernandez BV, et al. Changes in muscle metabolism are associated with phenotypic variation in golden retriever muscular dystrophy. Yale J Biol Med. (2017) 90:351–60.

66. Schneider SM, Sridhar V, Bettis AK, Heath-Barnett H, Balog-Alvarez CJ, Guo L-J, et al. Glucose metabolism as a pre-clinical biomarker for the golden retriever model of Duchenne muscular dystrophy. Mol Imaging Biol. (2018) 20:780–8. doi: 10.1007/s11307-018-1174-2

67. Rauch U, Shami A, Zhang F, Carmignac V, Durbeej M, Hultgårdh-Nilsson A. Increased neointimal thickening in dystrophin-deficient mdx mice. PLoS ONE. (2012) 7:e29904. doi: 10.1371/journal.pone.0029904

68. Tomanek RJ, Aydelotte MR, Torry RJ. Remodeling of coronary vessels during aging in purebred beagles. Circ Res. (1991) 69:1068–74. doi: 10.1161/01.RES.69.4.1068

69. Kodippili K, Hakim CH, Yang HT, Pan X, Yang NN, Laughlin MH, et al. Nitric oxide-dependent attenuation of noradrenaline-induced vasoconstriction is impaired in the canine model of Duchenne muscular dystrophy. J Physiol. (2018) 596:5199–216. doi: 10.1113/JP275672

70. Harricane M-C, Fabbrizio E, Lees D, Prades C, Travo P, Mornet D. Dystrophin does not influence regular cytoskeletal architecture but is required for contractile performance in smooth muscle aortic cells. Cell Biol Interntl. (1994) 18:947–58. doi: 10.1006/cbir.1994.1015

71. Dye WW, Gleason RL, Wilson E, Humphrey JD. Altered biomechanical properties of carotid arteries in two mouse models of muscular dystrophy. J Appl Physiol. (2007) 103:664–72. doi: 10.1152/japplphysiol.00118.2007

72. Ito K, Kimura S, Ozasa S, Matsukura M, Ikezawa M, Yoshioka K, et al. Smooth muscle-specific dystrophin expression improves aberrant vasoregulation in mdx mice. Hum Mol Genet. (2006) 15:2266–75. doi: 10.1093/hmg/ddl151

73. Rando TA. Role of nitric oxide in the pathogenesis of muscular dystrophies: A "two hit" hypothesis of the cause of muscle necrosis. Microsc Res Tech. (2001) 55:223–35. doi: 10.1002/jemt.1172

Citation: Schneider SM, Sansom GT, Guo L-J, Furuya S, Weeks BR and Kornegay JN (2022) Natural History of Histopathologic Changes in Cardiomyopathy of Golden Retriever Muscular Dystrophy. Front. Vet. Sci. 8:759585. doi: 10.3389/fvets.2021.759585

Received: 16 August 2021; Accepted: 28 December 2021; Published: 17 February 2022.

Edited by: David Bruyette, Anivive Lifesciences, United States

Reviewed by: José Manuel Verdes, Universidad de la República, Uruguay Inès Barthélémy, Univ Paris-Est Creteil, France

*Correspondence: Sarah M. Schneider, Sarah.Schneider@uga.edu

†Present address: Sarah M. Schneider, Department of Pathology, University of Georgia, Athens, GA, United StatesShinji Furaya, University of Yamanashi, Chuo, Japan

Comparte tu opinión con nosotros

https://axoncomunicacion.net/cambios-histopatologicos-en-la-miocardiopatia-de-la-distrofia-muscular-del-golden-retriever/

(R) evolution

PEQUEÑOS ANIMALES

Tabla de contenido:

Por el bienestar de tu paciente **elige LASERVET**

No invasivo

Sin dolor

Tiempos de recuperación reducidos o nulos

Mas información en:
info@laservet-iberia.com

LASERVET

EL LÁSER PARA EL VETERINARIO

5 FUNCIONES EN 1

1. DESCONTAMINACIÓN BACTERIANA
2. CIRUGÍA CON HEMOSTASIA
3. TERAPIA
4. ENDOSCOPIA
5. ACUPUNTURA

Modelo:
I-VET

Solicita una
DEMOSTRACIÓN
Gratuita y sin compromiso

- **Otohematoma:** (15´ sin anestesia general)
- **Paladar:** (5´ sin sangrado)
- **Gingivitis en gatos:** (sin sedación)
- **Papilomas:** (sin sedación)…

Accede a más de 30 vídeos

Por el bienestar de tu paciente **elige LASERVET**

LASERVET

EL LÁSER PARA EL VETERINARIO

No invasivo

Sin dolor

Tiempos de recuperación reducidos o nulos

Formación:

Accede a más de 30 vídeos:

https://www.youtube.com/playlist?list=PLi-UE7avyz5a0JgTHEMnHFudBr4H9Qn8M

Mas información en:
info@laservet-iberia.com

Hemeroteca

https://axoncomunicacion.net/pequenos-animales-revolution-hemeroteca/

(R) evolution

PEQUEÑOS ANIMALES